© Copyright 2017

Kelly M. Hennessey

Exploring Kinase Function and Drug Targets in *Giardia lamblia*

Kelly M. Hennessey

A dissertation

submitted in partial fulfillment of the

requirements for the degree of

Doctor of Philosophy

University of Washington

2017

Reading Committee:

Alexander R. Paredez, Chair

Ethan R. Merritt

Kayode K. Ojo

Program Authorized to Offer Degree:

Biology

University of Washington

Abstract

Exploring Kinase Function and Drug Targets in *Giardia lamblia*

Kelly M. Hennessey

Chair of the Supervisory Committee:
Alexander R. Paredez
Department of Biology

Giardia lamblia is the most commonly reported intestinal protozoan parasite in the United States and the cause of giardiasis, a gastrointestinal illness resulting in diarrhea, nutrient malabsorption, vomiting, and weight loss [1]. It infects approximately 280 million people worldwide annually [2–4]. *G. lamblia* has a simple life cycle consisting of two forms, the binucleate flagellated trophozoites and the tetranucleate infective cysts. Cysts are the environmentally resistant forms responsible for transmission of the disease[1]. In countries where sanitation is inadequate, waterborne diseases such as giardiasis are common.

Giardiasis contributes to the global health burden of diarrheal diseases that collectively constitute the second-leading cause of death in children under five years old[2,4]. Infection can also cause developmental delays and failure to thrive[5]; as few as 3 occurrences (>2 weeks duration)

of diarrheal disease per year during the first 2 years of life is associated with reduced height (approximately 10 cm) and intelligence quotient score (10 points) by 7 – 9 years of age[6]. First choice therapeutic options are limited to metronidazole and chemically related nitroimidazole drugs. Resistance has been reported for up to 20% of clinical presentations [7,8]. The mechanism of action of these drugs are mediated by their toxic intermediates which cause DNA damage in *G. lamblia* trophozoites[9], and attack protein sulfhydryl groups non-specifically. Even when infection is cleared, pathophysiological changes in the gut may persist, severely impacting quality of life [4,8]. Consequently, emergence of metronidazole-resistance strains and adverse reactions to the treatments suggest that alternative therapies against giardiasis are necessary.

In summary, this dissertation is an investigation to find targets in *G. lamblia* that are druggable. We used genetic and molecular techniques to inform us of the essentiality and biology of putative targets. Chapter 1 consists of the Introduction, which provides a more detailed explanation of why this research is needed.

Chapter 2 of my dissertation focuses on targeting the ATP binding pocket of kinases with small molecule inhibitors. We identified a set of protein kinases in *G. lamblia* that have small amino acid residues in the gatekeeper position; these small gatekeeper kinases are uncommon in the mammalian kinome, creating opportunity for drug targeting by a class of small molecule inhibitors called "bumped" kinase inhibitor (BKIs). In Chapter 2, we profiled two kinases determined to be essential for *Giardia* survival and were found to be sensitive to BKIs.

Based on phenotypic characteristics, Chapter 3 involves investigating the biological role of one of the two kinases identified during the work done in Chapter 2.

Chapter 4 describes the development of a tool that can be used as a high-throughput screening method to assay large drug libraries. This will be essential in screening small-molecule

inhibitors that can be used to target the kinases described in Chapter 2 and 3, as well as other compound libraries with *G. lamblia*. As a proof of concept, we screened the Pathogen Box available through the Medicines for Malaria Venture. Each of the compounds in the Pathogen Box has confirmed activity against at least one of the key pathogens that cause some of the most neglected diseases on the planet. The Pathogen Box has not been screened against *G. lamblia*, to our knowledge.

Chapter 5 describes an entirely different approach towards drug-design against *G. lamblia.* We targeted the Prolyl-tRNA synthetase with compounds designed to stall protein synthesis. Recent work identified *Plasmodium* prolyl-tRNA synthetase (ProRS) as a target of halofuginone[10], a drug derived from a natural product found in traditional herbal treatments for malaria. We evaluated its activity against *Giardia lamblia* and *Trichomonas vaginalis*; neither of which had previously been investigated.

References:

1. Adam RD. Biology of Giardia lamblia. Clin Microbiol Rev. 2001;14(3):447–475.
2. Lalle M. Giardiasis in the post genomic era: treatment, drug resistance and novel therapeutic perspectives. Infectious disorders drug targets. 2010;10(4):283–94.
3. Lane S, Lloyd D. Current trends in research into the waterborne parasite Giardia. Critical reviews in microbiology. 2002;28(2):123–147.
4. Ansell BRE, McConville MJ, Ma'ayeh SY, Dagley MJ, Gasser RB, Svärd SG, Jex AR. Drug resistance in Giardia duodenalis. Biotechnology advances. 2015.
5. Savioli L, Smith H, Thompson A. Giardia and Cryptosporidium join the "Neglected Diseases Initiative." Trends Parasitol. 2006;22(5):203–208.
6. Guerrant RL, DeBoer MD, Moore SR, Scharf RJ, Lima A a M. The impoverished gut--a triple burden of diarrhoea, stunting and chronic disease. Nature reviews. Gastroenterology & hepatology. 2013;10(4):220–9.
7. Farthing MJ. Giardiasis. Gastroenterology clinics of North America. 1996;25(3):493–515.
8. Müller J, Sterk M, Hemphill A, Müller N. Characterization of Giardia lamblia WB C6 clones resistant to nitazoxanide and to metronidazole. The Journal of antimicrobial chemotherapy. 2007;60(2):280–7.
9. Uzlikova M, Nohynkova E. The effect of metronidazole on the cell cycle and DNA in

metronidazole-susceptible and -resistant Giardia cell lines. Molecular and biochemical parasitology. 2014;198(2):75–81.
10. Keller TL, Zocco D, Sundrud MS, Hendrick M, Edenius M, Yum J, Kim Y-J, Lee H-K, Cortese JF, Wirth DF, et al. Halofuginone and other febrifugine derivatives inhibit prolyl-tRNA synthetase. Nature Chemical Biology. 2012;8(3):311–317.

TABLE OF CONTENTS

Title Page…….ii

Abstract……...…iv

Table of Contents…….1

Acknowledgements……..2

Dedication……....4

Chapter 1: Introduction to Exploring Kinase Function and Drug Targets in *Giardia lamblia*

Chapter 2: Identification and Validation of Small-Gatekeeper Kinases in *Giardia lamblia*

Chapter 3: Characterization of NEKxit, a small gatekeeper protein kinase involved in cytokinesis in *Giardia lamblia*

Chapter 4: Screening of the Pathogen Box for inhibitors with dual efficacy against *Giardia lamblia* and *Cryptosporidium parvum*

Chapter 5: Validation of prolyl-tRNA synthetase as a drug target in *Giardia lamblia* and *Trichomonas vaginalis*

ACKNOWLEDGEMENTS

I am thankful for the many faculty, staff, students, friends who have helped me in countless ways while completing this journey called graduate school. I thank each of my committee members, Alex Paredez, Barbara Wakimoto, Kayode Ojo, Ethan Merritt, Marti Bosma and Marilyn Parsons. Thank you to all members of the Paredez lab, Jana Krtkova, Elizabeth Thomas, Han-Wei Shih, Bill Hardin, Melissa Steele-Ogus, Germain Alas, and to all of our undergraduate assistants, Kelsey Kent, Habib Bejhatnia, Elmer Vazquez, Andrew Shelton, Lucy Zhang, Christine Wong, and Brytania Deloza. Thank you to the C.E.R.I.D group and Van Voorhis lab, specifically Wes Van Voorhis, Lynn Barrett, Ryan Choi, Matt Hulverson, Kasey Rivas, Sam Arnold, Hannah Udell, Tess Smith, Fred Buckner, Rob Gillespie, Ranae Ranade and Chetan Seshadri for adopting me into your research group. Thank you for your contribution to this work and to my growth and development as a scientist.

Thank you to the incredible Biology Department staff, Marissa Heringer, Dave Hurley, Ben Wiggins, Sarah O'Hara, Shirley Gretchen-Bellande, Jeannette Takashima and Ron Killman.

To our fabulous faculty, thank you Scott Freeman, Linda Martin-Morris, Ben Kerr, Leslie Zeman, Merrill Hille, Jennifer Nemhauser, Alison Crowe, Billie Swalla, Charles Laird, Estella Leopold, and Toby Bradshaw.

To our wonderful postdocs, thank you Elli Theobold, Angela Katsuyama, Jiae Lee, and Jen Day. Thank you to the special friends I made in graduate school, Shawn Luttrell, Itzue Caviedes, Hannah Jordt, Arida Dhanaswar, Takuo Yamaki, Harry Hunter, Melissa Freyman, Melissa Lacey, Brandon Peecook, Aric Rininger, Josh Swore, Katrina van Raay, Lauren Vandepas, Jared Grummer, Audrey Ragsac, Laura Frost, Mike Dorrity, Myles Feneske, Nan

Jiang and Emily Bain.

To my dear friends and family that have supported me through the years, thank you, Joanne Hennessey, Kathie Hennessey, Renee McDonald, Laura Willett, Becky Lang-Boyd, Gail Fast, Carol Barany, Laurie Moshier, Marilyn Staudinger, the Freeman family (Scott, Susan, Judy, and Hollis), the Ojo family, the Raney family, the Quincy family, the Jeromes, the McDonalds, the Boyds, the Willetts, the Ramirez', and to my Davis H.S. family. Finally, to my sister Stephanie Mudgett and her family, my brother Mike Bauer and his family, and my sister Belinda Hudmon and her family, thank you.

DEDICATION

For my dad (Cal Bauer) and my children Maureen, Matt, Kerry, Colleen and Billy

Nothing I put into words can or will truly express how grateful and blessed

I am to have each of you in my life. You ARE my life! I love you.

CHAPTER 1: INTRODUCTION

Giardiasis is an intestinal disease caused by the eukaryotic protozoan *Giardia lamblia* (synonymous with *Giardia intestinalis* and *Giardia duodenalis.*) Common symptoms of the disease include extreme diarrhea, malabsorption, fatigue, vomiting, and weight loss. Chronic infections can cause developmental delays and, in extreme cases, lead to death. Recent estimates for worldwide incidence are 280 million symptomatic cases per year[1–3]. Front line clinical treatments for giardiasis are metronidazole and tinidazole[4], yet up to 20% of cases are resistant and the medications can have severe side effects [5,6]; consequently, alternative therapies are needed.

G. lamblia is an excavates, which are thought to be one of the earliest diverging eukaryotic lineages. This extreme divergence offers promising opportunity for identifying novel drug targets, which opens up possibilities for new treatments[7,8].

The *Giardia* kinome (strain WB) contains 278 protein kinases, 80 of which constitute the core kinome and 198 of which are classified as Nek kinases. The core kinome of 80 protein kinases is fully conserved between the three sequenced genomes[8]. Sixty-one of the 80 kinases are classified into 49 families, which are highly conserved in many other eukaryotes. The remaining 19 families are unique to *Giardia*[8]. The highly expanded Nek family contains 198 kinases, compared to only 11 in humans and constitutes 71% of its kinome[8]. Universally, eukaryotic Nek kinases are hypothesized to control mitotic entry[9] and flagella length[10].

Protein kinases are enzymes that modify other proteins by adding a phosphate group from ATP to a substrate. They belong to a very extensive family of proteins that share a conserved catalytic domain[11]. They direct the activity, localization and overall function of many proteins, thereby regulating many cellular processes such as the cell cycle. The ATP binding pocket is

highly conserved in all eukaryotic protein kinases[12,13]. However, specific variations within the binding pocket, such as the "gatekeeper" residue exist[14]. This gatekeeper residue severely limits access to the hydrophobic subpocket within the ATP binding pocket, creating the possibility to design small molecule inhibitors that can specifically access the binding pocket and inhibit kinase activity[14,15]. Understanding that the majority of mammalian protein kinases have a large amino acid residue in the gatekeeper position,[14] Bishop *et al.* used a reverse chemical genetic strategy to generate inhibitor-sensitive kinase mutants that were sensitive to rationally designed cell-permeable small molecule inhibitors (bumped kinase inhibitors) based on the pyrazolopyrimidine scaffold. [16,17]. These bumped kinase inhibitors (BKIs) are too large to access a typical large gatekeeper kinase active site[18] but bind with relative specificity to protein kinases with small gatekeeper residues[14,19].

Using targeted phenotypic screening, the Medical Structural Genomics of Pathogenic Protozoa (MSGPP) group and the Structural Genomics Consortium, Toronto, selected *Toxoplasma gondii* Calcium-Dependent Protein Kinase 1 (*Tg*CDPK1) as a protein kinase target because this family of kinases is not present in higher eukaryotes[20,21]. Subsequent research in the Van Voorhis lab, University of Washington, Department of Medicine found that in several apixomplexan parasitic protists there are rare, naturally occurring protein kinases with small gatekeeper residues, many of which are sensitive to BKIs [19,22–29].

The kinase domain amino acid sequence of *Tg*CDPK1 was used as a template to probe *G. lamblia* strain WB using BLASTP. The original BLAST revealed 232 hits, 121 of which had E scores < $2x10^{-4.}$ Within those, eight *G. lamblia* kinases were selected based the presence of a glycine, alanine, serine or threonine gatekeeper residue; each had E scores <$4x10^{-24}$ and, based on the sequence similarity to *Tg*CDPK1, we anticipated the small gatekeeper proteins would

demonstrate sensitivity to BKI compounds. One kinase was determined to be a catalytically inactive NEK kinase[8] and was not pursued further. Our collaborators provided accessibility to a library of BKI compounds designed specifically to target the ATP binding pocket of small gatekeeper kinases in *Toxoplasmosis gondii* [20]; they can access the ATP binding site and inhibit the kinase but do not inhibit most mammalian kinases[20].

The foundation of this dissertation is based on the presence of seven protein kinases in *G. lamblia* with a rare small gatekeeper residue in the ATP binding pocket, four of which are proposed to be part of the Nek kinase family[30].

The research conducted in Chapter 2 focused on seven small gatekeeper kinases in *G. lamblia* to determine whether those kinases are necessary for parasite growth and proliferation, and assess them as molecular targets for development of drugs against giardiasis. Knockdown of each small gatekeeper protein identified two kinases with strong growth, attachment and cytokinesis defects (GL50803_8445 and GL50803_16034); the cells appeared to have completed nuclear division but never completed cytokinesis. As a result of the cytokinesis defect, growth was inhibited and a high percentage of cells were unable to maintain attachment, presumably due to gross morphological defects impeding the function of the ventral adhesive disc - the structure responsible for parasite adhesion to host intestines. This phenotype was mimicked in *G. lamblia* cells treated with the most potent BKI compound, BKI 1213. In particular, exposure to BKI 1213 induced defects in cytokinesis similar to those produced by kinase knockdown, as observed by fluorescence microscopy. Such a severe defect hindered the cells ability to attach, which creates the potential to clear an infection from the intestines. Furthermore, we found that BKIs can inhibit the growth of metronidazole-resistant *G. lamblia* due to their entirely different mechanism of action[30]. Additionally, BKIs are not expected to have the problematic side effects

associated with the free radical production by metronidazole and related drugs. Collectively, these results suggest that *in vivo* use of BKIs may provide an alternative treatment for giardiasis.

In the course of the work targeting small-gatekeeper kinases, a strong defective phenotype was observed when kinase GL50803_8445 had been knocked down. Compared to the morpholino control, there was a distinct increase in the number of cells that had not completed cytokinesis. After repeating knockdown and immunofluorescence assays, results were quantified and we found a six-fold increase in the number of cells that were stuck in cytokinesis[30]. This initial observation prompted an investigation into the role this kinase has in progression through the cell cycle, and specifically, cytokinesis, which is the focus of Chapter 3.

It was recently established that flagella-based force generation is required for cytokinesis in *G. lamblia*, that actin is involved in the progression of cleavage furrow and additional membrane delivery to the cleavage furrow is mediated by GTPase Rab11[31]; all elements are required for cytokinesis. These findings were informing because kinase GL50803_8445 shows similar protein localization patterns around both nuclei, the cell cortex, and enrichment in the spindles during mitosis. In addition, morpholino knockdown of protein kinase 8445 produced severe cytokinesis defects. Based on these observations, we began to describe the role GL50803_8445 played in cytokinesis, and its function in *G. lamblia*, the results of which are discussed in Chapter 3.

The research completed in Chapters 2 and 3 utilized a low throughput screening format that required counting cells with a coulter counter. In order to consider screening large small-molecule inhibitor libraries to target the kinases identified in Chapter 2, it was necessary to create an efficient tool amenable to high throughput screening. To accomplish this, we made an RE9 luciferase-expressing *G. lamblia* strain, which enabled us to rapidly quantify parasites using

a plate reader. Additionally, this red-shifted luciferase has the potential to be used to assay parasite loads in live animals.

As a proof of concept, we screened the Medicines for Malaria Venture (MMV) Pathogen Box. This venture launched an initiative to stimulate the discovery of drugs for neglected diseases. The Pathogen Box contains 400 diverse drug-like compounds with confirmed activity against at least one of the key pathogens that cause some of the most neglected diseases on the planet.

The 400 compounds were selected by experts to provide those with the most promise for drug discovery for neglected diseases such as Chagas disease as well as malaria and tuberculosis.

G. lamblia growth was assayed against each compound, using the validated luciferase strain. EC_{50} assays against the compounds that showed a minimum parasite growth inhibition of 95% were then completed. The results of the assays and implications for targeting both *G. lamblia* and *Cryptosporidia parvum* with compounds that dually hit both pathogens are discussed in Chapter 4.

Chapter 5, "Validation of prolyl-tRNA synthetase as a drug target in *Giardia lamblia* and *Trichomonas vaginalis*", summarized an additional approach to target *G. lamblia.*

Recent work identified prolyl-tRNA synthetase (ProRS) as a target of halofuginone, a drug derived from a natural product found in traditional herbal treatments for malaria[32]. Halofuginone is a nanomolar inhibitor of human cytosolic ProRS and of homologs from apicomplexan parasites *Plasmodium falciparum* and *C. parvum*. Long term inhibition has the effect of stalling protein synthesis by depleting the pool of aminoacylated (or charged) prolyl-tRNA needed for ribosomal integration of proline into a growing polypeptide chain. As part of a collaboration with Dr. Ethan Merritt in the UW Department of Biochemistry, halofuginone and

19 related compounds were evaluated as anti-giardial drugs against *G. lamblia.* Halofuginone was also evaluated against *T. vaginalis*, along with the first 6 compounds the chemists in this collaboration synthesized early on.

References:

1. Ankarklev J, Jerlstrom-Hultqvist J, Ringqvist E, Troell K, Svard SG. Behind the smile: cell biology and disease mechanisms of Giardia species. Nat Rev Microbiol. 2010;8(6):413–422.

2. Baldursson S, Karanis P. Waterborne transmission of protozoan parasites: review of worldwide outbreaks - an update 2004-2010. Water Res. 2011;45(20):6603–6614.

3. Lane S, Lloyd D. Current trends in research into the waterborne parasite Giardia. Critical reviews in microbiology. 2002;28(2):123–147.

4. Lalle M. Giardiasis in the post genomic era: treatment, drug resistance and novel therapeutic perspectives. Infectious disorders drug targets. 2010;10(4):283–94.

5. Farthing MJ. Giardiasis. Gastroenterology clinics of North America. 1996;25(3):493–515.

6. Müller J, Hemphill A MN. Structure-function relationship of thiazolides, a novel class of anti-parasitic drugs, investigated in intracellular and extracellular protozoan parasites and larval-stage cestodes. Antiinf Agents Med Chem. 2007;6:273–282.

7. Hopkins AL, Groom CR. The druggable genome. Nat Rev Drug Discov. 2002;1(9):727–730.

8. Manning G, Reiner DS, Lauwaet T, Dacre M, Smith A, Zhai Y, Svard S, Gillin FD. The minimal kinome of Giardia lamblia illuminates early kinase evolution and unique parasite biology. Genome Biol. 2011;12(7):R66.

9. O'Connell MJ, Krien MJE, Hunter T. Never say never. The NIMA-related protein kinases in mitotic control. Trends in Cell Biology. 2003;13(5):221–228.

10. Bradley BA, Quarmby LM. A NIMA-related kinase, Cnk2p, regulates both flagellar length and cell size in Chlamydomonas. Journal of cell science. 2005;118(Pt 15):3317–3326.

11. Hanks SK, Hunter T. The eukaryotic protein kinase superfamily : kinase (catalytic) domam structure and classification. The FASEB Journal. 1995;9(8):576–596.

12. Hanks SK, Quinn a M, Hunter T. The protein kinase family: conserved features and deduced phylogeny of the catalytic domains. Science (New York, N.Y.). 1988;241(1985):42–52.

13. Johnson LN, Lowe ED, Noble MEM, Owen DJ. The structural basis for substrate recognition and control by protein kinases. In: FEBS Letters. Vol. 430. 1998. p. 1–11.

14. Bishop AC, Ubersax J a, Petsch DT, Matheos DP, Gray NS, Blethrow J, Shimizu E, Tsien JZ, Schultz PG, Rose MD, et al. A chemical switch for inhibitor-sensitive alleles of any protein kinase. Nature. 2000;407(6802):395–401.

15. Bishop AC et al., Bishop a C, Buzko O, Shokat KM. Magic bullets for protein kinases. Trends in cell biology. 2001;11(4):167–172.

16. Bishop AC, Kung C, Shah K, Witucki L, Shokat KM, Liu Y. Generation of Monospecific Nanomolar Tyrosine Kinase Inhibitors via a Chemical Genetic Approach. Journal of the American Chemical Society. 1999;121(4):627–631.

17. Bishop AC. Chemical genetic approaches to highly selective protein kinase inhibitors. 2000. 233-233.

18. Zhang C, Kenski DM, Paulson JL, Bonshtien A, Sessa G, Cross J V, Templeton DJ, Shokat KM. A second-site suppressor strategy for chemical genetic analysis of diverse protein kinases. Nature methods. 2005;2(6):435–41.

19. Keyloun KR, Reid MC, Choi R, Song Y, Fox AM, Hillesland HK, Zhang Z, Vidadala R, Merritt EA, Lau AO, et al. The gatekeeper residue and beyond: homologous calcium-dependent protein kinases as drug development targets for veterinarian Apicomplexa parasites. Parasitology. 2014;141(11):1499–1509.

20. Ojo KK, Larson ET, Keyloun KR, Castaneda LJ, Derocher AE, Inampudi KK, Kim JE, Arakaki TL, Murphy RC, Zhang L, et al. Toxoplasma gondii calcium-dependent protein kinase 1 is a target for selective kinase inhibitors. Nature structural & molecular biology. 2010;17(5):602–607.

21. Wernimont AK, Artz JD, Finerty P, Lin Y-H, Amani M, Allali-Hassani A, Senisterra G, Vedadi M, Tempel W, Mackenzie F, et al. Structures of apicomplexan calcium-dependent protein kinases reveal mechanism of activation by calcium. Nature structural & molecular biology. 2010;17(5):596–601.

22. Castellanos-Gonzalez A, White AC, Ojo KK, Vidadala RSR, Zhang Z, Reid MC, Fox AMW, Keyloun KR, Rivas K, Irani A, et al. A novel calcium-dependent protein kinase inhibitor as a lead compound for treating cryptosporidiosis. Journal of Infectious Diseases. 2013;208(8):1342–1348.

23. Murphy RC, Ojo KK, Larson ET, Castellanos-Gonzalez A, Perera BGK, Keyloun KR, Kim JE, Bhandari JG, Muller NR, Verlinde CLMJ, et al. Discovery of Potent and Selective Inhibitors of Calcium-Dependent Protein Kinase 1 (CDPK1) from C. parvum and T. gondii. ACS medicinal chemistry letters. 2010;1(7):331–335.

24. Lourido S, Zhang C, Lopez MS, Tang K, Barks J, Wang Q, Wildman SA, Shokat KM, Sibley LD. Optimizing small molecule inhibitors of calcium-dependent protein kinase 1 to prevent

infection by toxoplasma gondii. Journal of Medicinal Chemistry. 2013;56(7):3068–3077.
25. Ojo KK, Reid MC, Siddaramaiah LK, Müller J, Winzer P, Zhang Z, Keyloun KR, Vidadala RSR, Merritt EA, Hol WGJ, et al. Neospora caninum calcium-dependent protein kinase 1 is an effective drug target for neosporosis therapy. PLoS ONE. 2014;9(3).

26. Ojo KK, Dangoudoubiyam S, Verma SK, Scheele S, DeRocher AE, Yeargan M, Choi R, Smith TR, Rivas KL, Hulverson MA, et al. Selective inhibition of Sarcocystis neurona calcium-dependent protein kinase 1 for equine protozoal myeloencephalitis therapy. International Journal for Parasitology. 2016;46(13–14):871–880.

27. Hines SA, Ramsay JD, Kappmeyer LS, Lau AO, Ojo KK, Van Voorhis WC, Knowles DP, Mealey RH. Theileria equi isolates vary in susceptibility to imidocarb dipropionate but demonstrate uniform in vitro susceptibility to a bumped kinase inhibitor. Parasites & vectors. 2015;8:33.

28. Ojo KK, Pfander C, Mueller NR, Burstroem C, Larson ET, Bryan CM, Fox AMW, Reid MC, Johnson SM, Murphy RC, et al. Transmission of malaria to mosquitoes blocked by bumped kinase inhibitors. Journal of Clinical Investigation. 2012;122(6):2301–2305.

29. Pedroni MJ, Vidadala RSR, Choi R, Keyloun KR, Reid MC, Murphy RC, Barrett LK, Van Voorhis WC, Maly DJ, Ojo KK, et al. Bumped kinase inhibitor prohibits egression in Babesia bovis. Veterinary Parasitology. 2016;215:22–28.

30. Hennessey KM, Smith TR, Xu JW, Alas GCM, Ojo KK, Merritt EA, Paredez AR. Identification and Validation of Small-Gatekeeper Kinases as Drug Targets in Giardia lamblia. PLOS Neglected Tropical Diseases. 2016;10(11):e0005107.

31. William R. Hardina, Renyu Lia, Jason Xub, Andrew M. Sheltona, Germain C. M. Alasa, Vladimir N. Minina B, and Alexander R. Paredeza 1. Myosin-independent cytokinesis in Giardia utilizes flagella to coordinate force generation and direct membrane trafficking. Proceedings of the National Academy of Sciences of the United States of America. 2017;(July).

32. Keller TL, Zocco D, Sundrud MS, Hendrick M, Edenius M, Yum J, Kim Y-J, Lee H-K, Cortese JF, Wirth DF, et al. Halofuginone and other febrifugine derivatives inhibit prolyl-tRNA synthetase. Nature Chemical Biology. 2012;8(3):311–317.

CHAPTER 2: Identification and Validation of Small-Gatekeeper Kinases as Drug Targets in *Giardia lamblia*

This chapter was published in Public Library of Science, Neglected Tropical Diseases, 2016.

Identification and Validation of Small- Gatekeeper Kinases As Drug Targets in *Giardia lamblia*

Kelly M. Hennessey[1], Tess R. Smith[2], Jennifer W. Xu[1], Germain C. M. Alas[1], Kayode K. Ojo[2], Ethan A. Merritt[3]*, Alexander R. Paredez[1]*

1 Department of Biology, University of Washington,
Seattle, Washington, United States of America,
2 Division of Allergy and Infectious Diseases, Center for Emerging and Re-emerging Infectious Disease (CERID), University of Washington,
Seattle, Washington, United States of America,
3 Department of Biochemistry, University of Washington,
Seattle, Washington, United States of America

* aparedez@uw.edu (ARP); merritt@u.washington.edu (EAM)

PLOS | NEGLECTED TROPICAL DISEASES

RESEARCH ARTICLE

Identification and Validation of Small-Gatekeeper Kinases as Drug Targets in *Giardia lamblia*

Kelly M. Hennessey[1], Tess R. Smith[2], Jennifer W. Xu[1], Germain C. M. Alas[1], Kayode K. Ojo[2], Ethan A. Merritt[3]*, Alexander R. Paredez[1]*

1 Department of Biology, University of Washington, Seattle, Washington, United States of America, **2** Division of Allergy and Infectious Diseases, Center for Emerging and Re-emerging Infectious Disease (CERID), University of Washington, Seattle, Washington, United States of America, **3** Department of Biochemistry, University of Washington, Seattle, Washington, United States of America

* aparedez@uw.edu (ARP); merritt@u.washington.edu (EAM)

CrossMark
click for updates

OPEN ACCESS

Citation: Hennessey KM, Smith TR, Xu JW, Alas GCM, Ojo KK, Merritt EA, et al. (2016) Identification and Validation of Small-Gatekeeper Kinases as Drug Targets in *Giardia lamblia*. PLoS Negl Trop Dis 10(11): e0005107. doi:10.1371/journal.pntd.0005107

Editor: Timothy G. Geary, McGill University, CANADA

Received: June 20, 2016

Accepted: October 12, 2016

Published: November 2, 2016

Copyright: © 2016 Hennessey et al. This is an open access article distributed under the terms of the Creative Commons Attribution License, which permits unrestricted use, distribution, and reproduction in any medium, provided the original author and source are credited.

Data Availability Statement: All relevant data are within the paper and its Supporting Information files.

Funding: This work was supported by the University of Washington Royalty Research Fund (https://www.washington.edu/research/or/?page=rrf) award number A83259 to ARP and Washington Research Fund Benjamin Hall Fellowship (http://www.biology.washington.edu/grad/awards/WRF-Hall-Fellowship) to KMH. The funders had no role in study design, data collection and analysis,

Abstract

Giardiasis is widely acknowledged to be a neglected disease in need of new therapeutics to address toxicity and resistance issues associated with the limited available treatment options. We examined seven protein kinases in the *Giardia lamblia* genome that are predicted to share an unusual structural feature in their active site. This feature, an expanded active site pocket resulting from an atypically small gatekeeper residue, confers sensitivity to "bumped" kinase inhibitors (BKIs), a class of compounds that has previously shown good pharmacological properties and minimal toxicity. An initial phenotypic screen for biological activity using a subset of an in-house BKI library found that 5 of the 36 compounds tested reduced trophozoite growth by at least 50% at a concentration of 5 μM. The cellular localization and the relative expression levels of the seven protein kinases of interest were determined after endogenously tagging the kinases. Essentiality of these kinases for parasite growth and infectivity were evaluated genetically using morpholino knockdown of protein expression to establish those that could be attractive targets for drug design. Two of the kinases were critical for trophozoite growth and attachment. Therefore, recombinant enzymes were expressed, purified and screened against a BKI library of >400 compounds in thermal stability assays in order to identify high affinity compounds. Compounds with substantial thermal stabilization effects on recombinant protein were shown to have good inhibition of cell growth in wild-type *G. lamblia* and metronidazole-resistant strains of *G. lamblia*. Our data suggest that BKIs are a promising starting point for the development of new anti-giardiasis therapeutics that do not overlap in mechanism with current drugs.

Author Summary

The eukaryotic protozoan *Giardia lamblia* is the most commonly reported intestinal parasite worldwide. Current treatments used to treat giardiasis include metronidazole and

decision to publish, or preparation of the manuscript.

Competing Interests: The authors have declared that no competing interests exist.

other nitroimidazole derivatives. However, emergence of metronidazole-resistance strains and adverse reactions to the treatments suggest that alternative therapies against giardiasis are necessary. Here we identify a set of protein kinases in the *Giardia* genome that have an atypically small amino acid residue, called the gatekeeper residue, in the ATP binding pocket. Small gatekeeper residues are rare in mammalian kinases. We investigated whether this subset of kinases is necessary for parasite growth and proliferation and, if so, could they be targeted with a class of compounds called bumped kinase inhibitors (BKIs), designed to exploit the enlarged active site pocket made accessible by the small gatekeeper amino acid. Morpholino knockdown of two of the small gatekeeper kinases produced a distinctive phenotype characterized by defective cytokinesis. This phenotype was mimicked in *Giardia* cells treated with our most potent BKI. These results suggest that BKIs may be developed to selectively target small gatekeeper kinases in *Giardia lamblia* to provide a novel treatment option for giardiasis.

Introduction

Giardia lamblia is the most commonly reported intestinal protozoan parasite and the cause of giardiasis, a gastrointestinal illness resulting in diarrhea, nutrient malabsorption, vomiting, and weight loss [1]. It infects approximately 280 million people worldwide [2,3,4]. This disease contributes to the global health burden of diarrheal diseases that collectively constitute the second-leading cause of death in children under five years old [3,4]. Infection can also cause developmental delays and failure to thrive [5]; as few as 3 occurrences (>2 weeks duration) of diarrheal disease per year during the first 2 years of life is associated with reduced height (approximately 10 cm) and intelligence quotient score (10 points) by 7–9 years of age [6]. *G. lamblia* has a simple life cycle consisting of two forms, the binucleate flagellated trophozoites and the tetranucleate infective cysts. Cysts are the environmentally resistant forms responsible for transmission of the disease [1].

First choice therapeutic options are limited to metronidazole and chemically related nitroimidazole drugs. These compounds are prodrugs whose reduction to reactive radicals is mediated intracellularly by pyruvate: ferredoxin oxidoreductase and other enzymes involved in anaerobic metabolism. Resistance can occur in up to 20% of clinical presentations, primarily due to down-regulation or mutation of these activating enzymes [7,8]. The toxic intermediates cause DNA damage in *Giardia* trophozoites [9], and attack protein sulfhydryl groups non-specifically. Even when infection is cleared, pathophysiological changes in the gut may persist, severely impacting quality of life [3,8]. Consequently, there is an increasing need to develop alternative drugs to treat giardiasis.

To address this need, we have combined a structure-based approach with targeted phenotypic screening to jointly identify and validate a class of potential protein targets in *Giardia* and a corresponding class of drug-like molecules that attack them. This approach takes advantage of an in-house library of protein kinase inhibitors based on a limited number of chemical scaffolds, developed in the course of previous work to optimize potency, pharmacological properties, and selectivity for inhibition of CDPK (Calcium Dependent Protein Kinase) homologs in several apicomplexan pathogens [10,11]. A primary structural determinant of target selectivity in this library is the fortuitous presence of an atypically small gatekeeper residue in the active site of the target CDPKs [12,13]. The presence of a small amino acid at the gatekeeper position creates a much larger effective pocket than is found in the majority of protein kinases [14], allowing inhibition by compounds that are too large to be accommodated in a typical kinase

active site. Compounds from this library have been shown to have minimal cytotoxicity against human cells, consistent with selective activity disfavoring inhibition of human kinases. Several have shown promise in animal trials for anticoccidial efficacy [15,16]. While design of the 400 + compounds in our BKI (bumped kinase inhibitor) library was biased toward optimal selectivity for CDPK homologs, all library compounds are expected to preferentially inhibit small gatekeeper kinases.

Protein kinases in general constitute an attractive class of molecular targets for drug discovery, distinct from the targets of existing anti-giardiasis drugs. Of the 278 protein kinases identified in the *G. lamblia* genome (strain WB), 80 kinases form a core kinome while the remaining 198 constitute a massively expanded family of NEK kinases [17]. The core kinome contains 80 kinases from 49 families that are recognizably also present in higher eukaryotes. It contains 19 families that have no recognized homologs outside of *Giardia* [17]. Where direct homologs can be identified, the average sequence identity between *Giardia* and human homologs is roughly 40% [17]. Thus, individual *Giardia* kinases are in general expected to show extensive sequence and structural differences to their human homologs, if any, facilitating development of selective inhibitors. Furthermore, the greatly reduced number of core kinome classes, each containing no more than three members in the *G. lamblia* genome, suggests that gene loss in these parasites has pared the remaining core kinome down to a near-minimal set of essential proteins.

The huge expansion of NEK kinase sequences in the *Giardia* genome stands in contrast to the reduction in size of the core kinome. Similar, though less extreme, expansions of the NEK kinase group have been found in ciliates and excavates [18,19]. The total of 198 NEK homologs in the *G. lamblia* genome may be compared to a single NEK homolog in yeast and 11 in humans. Many of the *Giardia* NEK sequences are highly variable across strains, and roughly two-thirds are inferred to be catalytically inactive due to the loss of conserved catalytic residues in the canonical active site [17]. Nevertheless, among the catalytically active *Giardia* NEK kinases some are likely to carry out biologically essential phosphorylation and hence to constitute valid drug targets. In other eukaryotes, NEK kinases are involved in cell cycle control [20,21]. Two *Giardia* NEK kinases have been shown to be active in mitosis and excystation [22]. It is worth noting that two trypanosomal NEK kinases, one of them coincidentally possessing a small gatekeeper residue, have been suggested as drug targets in *Trypanosoma brucei* [23].

While the *G. lamblia* kinome contains no CDPK homologs, it does contain multiple genes encoding kinases with small gatekeeper amino acid residues in their ATP binding sites, creating a potential opportunity to design specific ATP-competitive inhibitors that are highly selective for one or more parasite kinases relative to all human kinases. Using reverse genetics, we show that some of these kinases are essential for *Giardia* trophozoite proliferation. In addition to providing insight into the role of these newly described kinases, we also show that they are targets of some BKIs. Our results constitute the first steps toward further development of BKIs into an effective alternative treatment for giardiasis.

Methods

Bioinformatics and target selection

The sequence of the TgCDPK1 kinase domain core was used as a BLASTP probe of *Giardia* strain WB sequences in GiardiaDB. This search returned 232 hits in total. Of these, 121 had E scores $< 2x10^{-4}$ and within this set the initial alignment for eight *Giardia* kinases indicated a glycine, alanine, serine, or threonine gatekeeper residue. These eight, all with E scores $< 4x10^{-24}$, were selected for the initial evaluation presented here, as their substantial sequence

similarity to TgCDPK1 was expected to indicate higher likelihood of sensitivity to the existing BKI library compounds.

Subsequently, ClustalW/HMMER multisequence alignment was used to match all 232 sequences against TgCDPK1 residues 110–133, corresponding to the β-hairpin containing the gatekeeper residue itself and residues contributing to the active site pocket. Four additional putative small-gatekeeper kinases were identified from this search and earmarked for eventual characterization paralleling the work reported here. Finally, we noted that 15 putative kinase ORFs annotated as active in the tabulation by Manning [17] were not recovered by either of our probes. These were matched individually to the nearest homolog with a representative structure in the PDB in order to identify the gatekeeper residues with certainty.

Parasite culture

G. lamblia wild-type strains *WBC6* (ATCC 50803), *713* and metronidazole-resistant *713-M3* cells [24] (supplied by the L. Eckmann lab, UC San Diego School of Medicine), were grown in TYI-S-33 medium supplemented with 10% bovine serum and 0.05 mg/mL bovine bile [25]. Cells were cultured at 37° under hypoxic conditions using 15 mL polystyrene screw-cap tubes (Corning Life Sciences DL).

In vivo compound screen assays

Preliminary phenotypic screening for inhibitory effects of 36 compounds from our focused BKI library [26] against the trophozoite stage of *G. lamblia* was carried out at a final concentration of 5 μM. This library subset was chosen to include multiple chemical scaffolds and both large and small substituents at the R1 and R2 scaffold positions [10,27,28]. Compounds were screened in 48-hour growth assays in 96-well microtiter plates. Each compound (150 μL) was added to 150 μL of well-suspended diluted parasites (~20,000 cells/mL) and incubated in anaerobic BD GasPak Bio-Bags (Becton Dickinson, San Jose, California). After 48 hours, 96-well plates were placed on ice for 30 minutes, fixed with 0.64% paraformaldehyde, and thoroughly resuspended and counted with a MoxiZ Coulter counter (Orflo Technologies, Hailey, ID.)

Vector construction, transfection, and protein expression

To generate endogenously tagged small gatekeeper kinases, the putative kinase-coding genes were amplified from genomic DNA by PCR and cloned into the pKS_3HA_Neo vector [29]. Primer sequences and restriction enzymes are shown in S1 Table. PCR amplifications were performed using iProof DNA polymerase (Bio-Rad). Typically, an amplicon of ~ I kb in length that lacked the start codon was cloned in frame to a C-terminal triple-hemagglutinin epitope tag (3xHA) into the pKS_3HA_Neo plasmid. The plasmids were linearized by the enzyme reported in S1 Table and ~5 μg of DNA was used to transform wild-type *Giardia*. Transformants were selected with G418 at 40 μg/mL.

For protein expression, the complete coding region of each protein kinase was PCR amplified from *Giardia* genomic DNA. PCR amplicons were cloned into the ligation independent cloning (LIC) site of (MBP)-AVA0421 expression vector and validated by sequencing [30]. Recombinant proteins were expressed in *E. coli* BL21 (DE3), Invitrogen, Carlsbad, CA) using Studier auto-induction protocols at 20°C [31]. Recombinant protein purifications were performed as previously described [26].

Western blot analysis

Giardia trophozoites were harvested after chilling cultures on ice for 30 minutes. After detachment, cells were pelleted at 700xg, washed once in HBS (HEPES buffered saline), then resuspended in 300 μL of lysis buffer (50 mM Tris pH 7.5, 150 mM NaCl, 7.5% Glycerol, 0.25 mM $CaCl_2$, 0.25 mM ATP, 0.5 mM DTT, 0.5 mM PMSF, 0.1% Triton X-100, Halt 100X Protease Inhibitor Cocktail (ThermoFisher Scientific), then sonicated. The lysate was cleared by centrifugation at 10,000xg for 10 minutes at 4°C and then boiled in 2x Laemmli Sample Buffer (Bio-Rad). After SDS-PAGE, samples were transferred to PVDF membrane (Immobilon-FL) following the manufacturers' directions. Primary polyclonal rabbit anti-giActin 28PB+1 [32] and monoclonal anti-HA mouse HA7 antibodies (IgG1; Sigma-Aldrich) were diluted 1:2500 in blocking solution (5% dry milk, 0.05% Tween-20 in TBS). Secondary anti-mouse Alexa-555 and anti-rabbit Alexa-647 antibodies were used. Horseradish peroxidase-linked anti-mouse or anti-rabbit antibodies (Bio-Rad) were used at 1:7,000. Multiplexed immunoblots were imaged on a Chemidoc MP (Bio-Rad) and signals were quantitated using ImageJ [33].

Immunofluorescence analysis

G. lamblia cells were pelleted at 500xg at room temperature, the pellet and remaining attached cells were fixed in PME (100 mM Pipes pH 7.0, 5 mM EGTA, 10 mM $MgSO_4$) plus 0.025% Triton X-100, 100 μM MBS, and 100 μM EGS for 30 minutes at 37°C. Cells were again pelleted, washed, resuspended with PME, and adhered to poly-L-lysine (Sigma-Aldrich) coated coverslips. Cells were permeabilized in PME + 0.1% Triton X-100 for 10 minutes then washed 2X with PME + 0.1% Triton X-100 and blocked for 30 minutes in PMEBALG (PME + 1% BSA, 0.1% NaN_3, 100 mM lysine, 0.5% cold water fish skin gelatin (Sigma Aldrich, St. Louis, MO) [32]. Cells were stained with rabbit anti-giActin antibody 28PB+1 [32] and mouse monoclonal anti-HA (Clone HA7, Sigma-Aldrich) both diluted 1:125 in PMEBALG and incubated overnight. After three subsequent washes with PME + 0.05% Triton X-100, cells were incubated in secondary antibodies Alexa-488 goat anti-mouse and Alexa-555 goat anti-α-rabbit (Sigma-Aldrich, St. Louis, MO) (diluted 1:125 in PMEBALG) for 1 hour [32]. Cells were washed three times with PME + 0.05% Triton X-100. The coverslips were mounted with ProLong Gold antifade plus DAPI, (Thermo Fisher Scientific, Rockford, IL). Fluorescence deconvolution microscopy images were collected as described [34]. A minimum of 150 cells were examined and 30 imaged per experiment.

Morpholino knockdown and growth assays

Trophozoites were cultured to confluency, iced for 30 minutes to detach, spun down (500xg for 5 minutes) and media was replaced with 1.0 mL fresh *Giardia* growth medium. Cells and cuvettes were chilled on ice. Lyophilized morpholinos listed in S1 Table (Gene Tools, LLC, Philomath, OR) were resuspended in sterile water and 30 μL of a 100 mM morpholino stock was added to 300 μL of cells in a 4 mm cuvette. We used Gene Tools, LLC standard morpholino as a negative control. Cells were electroporated (375V, 1000 μF, 750 Ohms, GenePulser Xcell, Bio-Rad, Hercules, CA). Cells were transferred to fresh media and incubated 4 hours at 37°C to allow cells to recover. Cells were then iced for 30 minutes, counted and diluted to 20,000 cells/mL. Aliquots were counted every 12 hours over 48 hours. All cell counting was done using a Coulter counter (MoxiZ). Three independent replicates of each cell line and control were analyzed for each time point. Quantification of protein expression was determined at the 24-hour time point by the Western blot assay described above.

Attachment assays

Trophozoites were cultured and treated with morpholinos as described above. After 4 hours of recovery, cells were iced for 30 minutes, counted, and then diluted to 20,000 cells/mL. After 48 hours, the media was decanted into a fresh tube and replaced with 1XPBS (phosphate buffered saline). Both tubes were placed on ice to detach or prevent attachment. The cells from each group were then counted, using a Coulter counter (MoxiZ), as above.

Thermal shift assays

Thermal shift assays on purified *E. coli* expressed Gl50803_8445 and Gl50803_16034 proteins were performed as described previously [35].

EC50 compound screen assays

EC50 assays were performed on wild type *Giardia* trophozoites to determine the potency of each BKI that elicited a temperature shift in the thermal shift assays. *Giardia* trophozoites were harvested after chilling cultures on ice for 30 minutes. Three-fold serial dilutions of compounds from 10 μM to 1.524 nM concentrations were created in fresh *Giardia* growth media and growth assays were set up in 96-well microtiter plates as above. Growth was assayed after 48-hours and EC50 values were determined using gnuplot.

Accession numbers

Genes/proteins

8445: UniProtKB—A8BXP9 (A8BXP9_GIAIC)

9421: UniProtKB—A8BDH0 (A8BDH0_GIAIC)

9665: UniProtKB—A8BZJ9 (A8BZJ9_GIAIC)

11364: UniProtKB—E2RTY0 (E2RTY0_GIAIC)

12148: UniProtKB—A8BW54 (A8BW54_GIAIC)

13215: UniProtKB—A8B2W4 (A8B2W4_GIAIC)

16034: UniProtKB—A8BHW1 (A8BHW1_GIAIC)

17368: UniProtKB—A8BQY4 (A8BQY4_GIAIC)

Results

Basis for BKI selective activity

BKIs originated conceptually with the observation that most protein kinases will not tolerate ATP analogs containing a "bump" on the ATP purine ring. This restriction arises because the sidechain of a specific residue, the gatekeeper, limits the volume available in the active site to accommodate such chemical modification of the substrate. This observation was exploited, notably by the Shokat group [26,36], to probe the function of individual kinases *in vivo* by introducing an engineered variant in which the naturally occurring gatekeeper was replaced by a smaller residue, making the engineered kinase uniquely competent to recognize bumped ATP analogs. The precision of this technique is possible because naturally occurring kinases

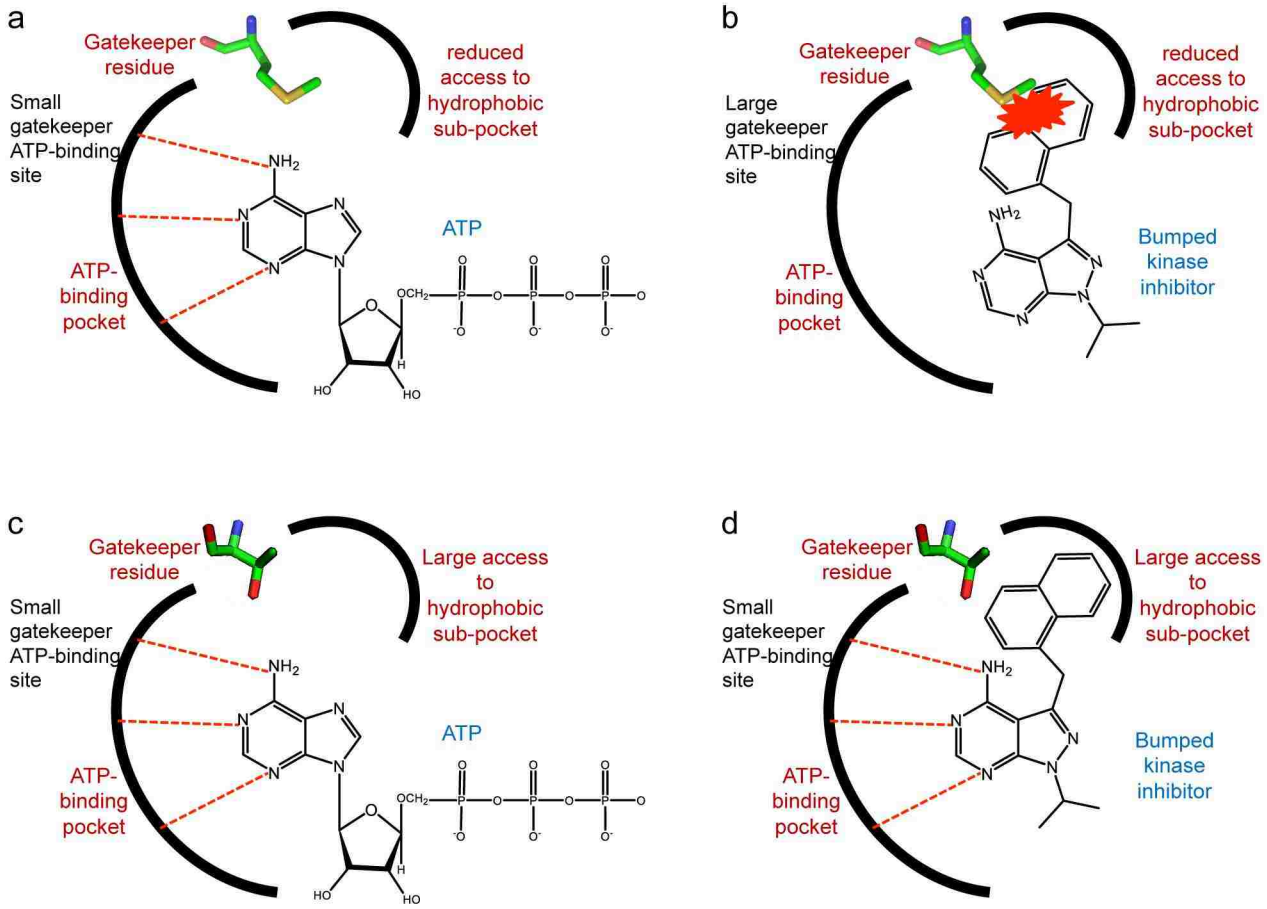

Fig 1. Structural differences between small gatekeeper ATP binding sites and large gatekeeper ATP binding sites. Structural differences form the basis for BKIs to selectively act on the *Giardia* kinases described in this study. **(a)** The ATP binding pocket of protein kinases typically contains a large amino acid gatekeeper residue (e.g. methionine). **(b)** BKIs do not bind to the ATP binding site of typical kinases because of a clash between the "bump" and the side chain of the gatekeeper. **(c)** A small amino acid in the gatekeeper position has no implications for ATP access to the ATP binding site. **(d)** In contrast, the small gatekeeper residue permits the BKI "bump" to extend into the hydrophobic subpocket and outcompete ATP.

doi:10.1371/journal.pntd.0005107.g001

with gatekeepers smaller than threonine (i.e. glycine, serine, alanine) are extremely rare [14]. Threonine is less rare as a gatekeeper residue although still much less common in the human kinome than larger gatekeepers, particularly methionine.

Notwithstanding their rarity in the human kinome, small gatekeeper kinases are found naturally in the genomes of various protozoa. Individual small gatekeeper kinases have been characterized as potential targets for drug development against eukaryotic pathogens such as *T. brucei* [23], *T. gondii* [37], *C. parvum*, and *P. falciparum* [12,26,27]. In the case of apicomplexan targets, BKIs have been designed for high selectivity relative to all human kinases, including human threonine gatekeeper kinases, by simultaneously exploiting the gatekeeper-mediated restriction (Fig 1) and the geometry of the ribose binding pocket in the specific target kinase [38].

Giardia lamblia has multiple small gatekeeper kinases

A genome wide search of the *Giardia lamblia* genome for genes encoding kinases with small amino acid gatekeeper residues was performed using the core kinase domain of *Tg*CDPK1 as

Gene ID	Sequence near gatekeeper		Annotation
TgCDPK1	IMKLYEFFEDKGYFYLV**G**EVYTGGELFDEIISRKR		
GL50803_13215	LVKCYETFQNAA----A**G**EQYVAMELCERSLKDLI	*	NEK GL3 subfamily
GL50803_12148	KYYEILHDEASQILYVV**A**DYFKHSNLSAYCKARRE		NEK (inactive)
GL50803_9421	RCVSATHDEDAMEIRMF**S**EFCSGGDLHAYVQKLEK	*	NEK
GL50803_16034	IVRLLEVIDTPRHIYLV**T**EYVDNGELFNYVVQKQK	*	CAMK (AMPK)
GL50803_9665	IVSYKQSFLENGALNII**T**EYANKGDLQNFMRSSSE		NEK
GL50803_11364	MIKLYHSFQTRTRLFLV**T**TFATGGELFYHLKKIGR	*	AKT family (PKB)
GL50803_17368	TIRFFESFEEDGSVVIV**T**EL-AQSDLHSIFASDGP	*	ULK
GL50803_8445	GYHDVVIDEVEKVIYIF**T**EFCNKGDLF-QLIDKHR		NEK

Fig 2. Initial set of eight putative *Giardia lamblia* small gatekeeper kinases. BLASTP against the *Giardia* genome database using the *T. gondii* CDPK1 core kinase domain as a probe found 8 kinases with substantial sequence similarity ($E < 10^{-24}$) to the probe whose alignment indicated a small gatekeeper residue (threonine or smaller). Sequences near the small gatekeeper are shown with small gatekeeper amino acids in red.

doi:10.1371/journal.pntd.0005107.g002

the sequence template. *Tg*CDPK1 was chosen because it was a primary target guiding the assembly of the BKI library used in this study [13]. BLASTP results identified eight putative kinase-coding sequences with small gatekeeper residues. The gatekeeper residues included a threonine in kinases *Gl50803_8445*, *Gl50803_9665*, *Gl50803_11364*, *Gl50803_16034* and *Gl50803_17368*, a glycine in *Gl50803_13215*, an alanine in *Gl50803_12148* and a serine in *Gl50803_9421*. The Ala-gatekeeper sequence (*Gl50803_12148*) belongs to a catalytically inactive NEK kinase [17] and was not pursued further.

Of the seven small gatekeeper kinases predicted to be sensitive to BKI inhibition, four (*Gl50803_8445*, *Gl50803_9421*, *Gl50803_9665*, and *Gl50803_13215*) are *Giardia*-specific NEK kinases. Based on sequence homology, kinase *Gl50803_17368* is inferred to be a member of the ULK family. *Gl50803_16034* is inferred to be a member of the CAMKL/AMPK family (Fig 2). *Gl50803_11364* is one of the few *G. lamblia* kinases that have been previously investigated. This AKT family kinase is differentially expressed in encystation compared to the trophozoite stage but its regulatory function is unknown [39].

BKIs inhibit *Giardia* growth

Our identification of genes encoding small gatekeeper kinases suggested the possibility that BKIs might affect *Giardia* trophozoites, the stage that colonizes the intestine. As a reference point, we assayed sensitivity of *Giardia* trophozoites to staurosporine, a broad spectrum kinase inhibitor that acts on small and large gatekeeper kinases. As shown in Fig 3, treatment with 5 μM staurosporine in 0.1% DMSO resulted in a 95% reduction in growth compared to vehicle alone or untreated cells. Next, we tested 36 compounds selected from a previously reported BKI library [26], for effects on growth at 5 μM concentration. Five of these compounds reduced growth by at least 50% compared to control cells treated with 0.1% DMSO. Compound 1213 reduced growth by 79% (Fig 3). Although, this BKI library was originally developed to explore selectivity for *Tg*CDPK1 and *Cp*CDPK1 over mammalian kinases [27], these results indicate that this class of compounds can effectively inhibit growth of *Giardia* trophozoites. The presence of multiple kinases with small gatekeeper residues and the ability of BKIs to inhibit *Giardia* growth suggest that BKIs could be developed as an alternative basis for treatment of giardiasis.

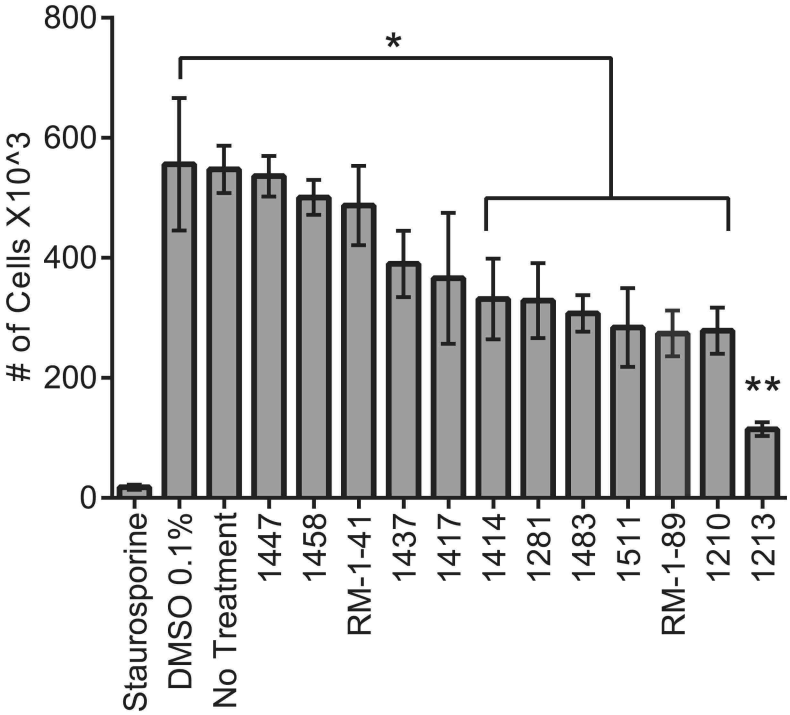

Fig 3. Bumped kinase inhibitors impact *Giardia* trophozoite growth. A subset ~10% of the existing BKI library was screened for impairment of *Giardia* growth at a concentration of 5 μM and results from selected compounds are shown. The general kinase inhibitor staurosporine reduced growth by 95%. Five bumped kinase inhibitors reduced growth by at least 50% (1483, 1511, Rm-1-89, 1210 and 1213.) The results are averaged from 3 biological replicates that were normalized to the control, DMSO 0.1%. Significance was evaluated by t-test, * = $p<0.05$, ** = $p<0.01$.

doi:10.1371/journal.pntd.0005107.g003

Expression and subcellular localization of *Giardia* small gatekeeper kinases

Finding that BKIs can inhibit *Giardia* trophozoite growth established the priority to determine which kinases are critical for trophozoite proliferation and attachment. To accomplish this, we used an epitope tag to facilitate detection of each kinase [29]. We established seven cell lines, each with one specific kinase gene endogenously epitope-tagged with 3xHA [29]. Our integration constructs lack promoters and start codons; therefore, detection of protein products indicated successful integration into the genome with expression driven by the native promoter. Western blot analysis showed that five of the seven lines expressed detectable levels of proteins of the predicted molecular weight (Fig 4a).

Attempts to integrate two of the seven kinase genes (*Gl50803_9665* and *Gl50803_17368*,) in six separate trials, failed to yield lines that expressed detectable levels of the tagged protein as assayed by Western blotting. To assess further whether successful integration had actually occurred, we used PCR to assay the kinase locus for integration. As shown in S1 Fig, successful integration of constructs was achieved for both *Gl50803_9665* and *Gl50803_17368*. The absence of detectable protein expression may be due to low level of endogenous protein expression or more likely developmental regulation; therefore, these two were not carried forward for genetic analyses.

Using the same cell lines that were established for Western blotting, we analyzed cellular localization as a secondary method for detecting relative abundance. Using identical exposure

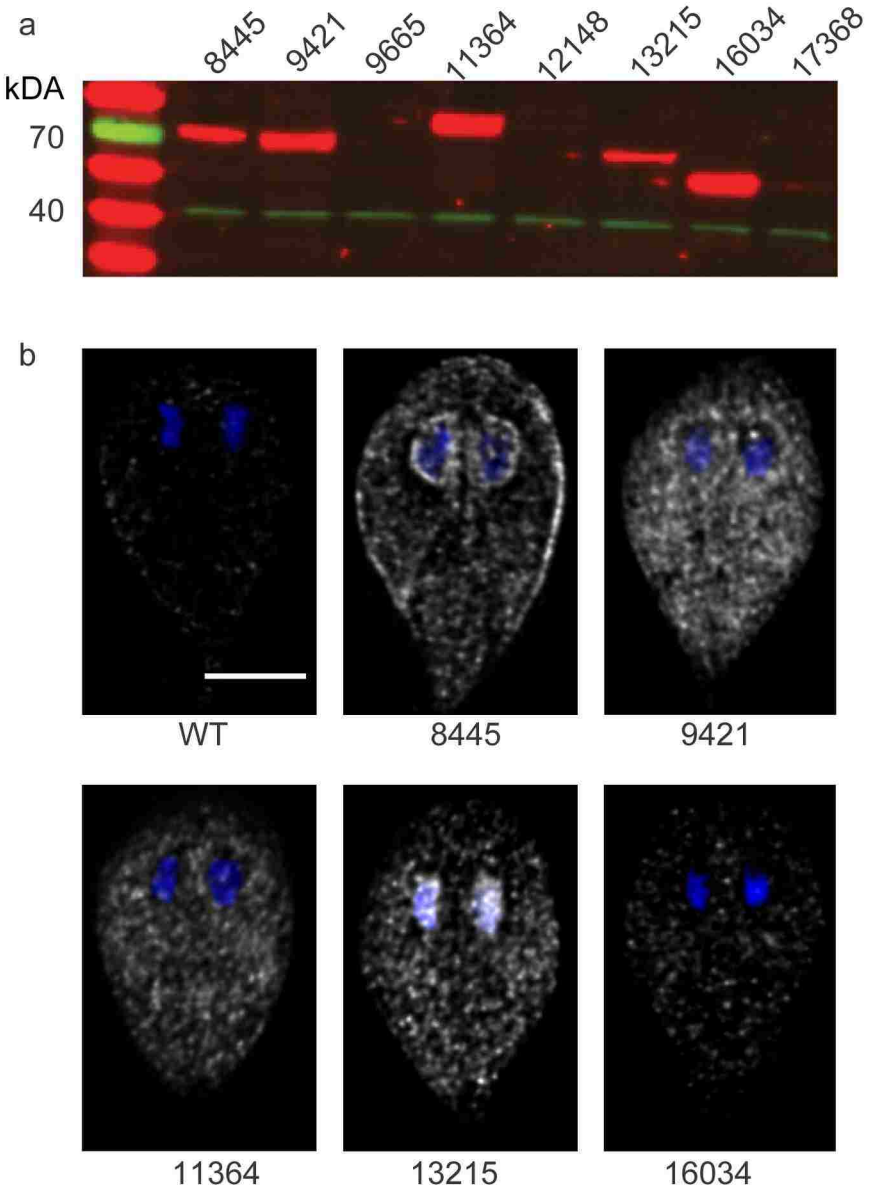

Fig 4. Integration of 3xHA tag allows visualization of protein expression and localization. (a) Western blot analysis showing kinases Gl50803_8445, Gl50803_9421, Gl50803_11364, Gl50803_13215 and Gl50803_16034 are expressed in trophozoites (red). Actin (green) was used as a loading control. **(b)** Immunofluorescence imaging of trophozoites expressing the designated protein: HA (grayscale) and DAPI (blue). Images were acquired and scaled identically. Representative images are shown from a minimum of 150 cells examined for each line. Scale bar = 5 μm.

doi:10.1371/journal.pntd.0005107.g004

and scaling conditions, the five 3xHA-tagged kinases: Gl50803_8445, Gl50803_9421, Gl50803_11364, Gl50803_13215 and Gl50803_16034 were localized by immunofluorescence microscopy. We observed strong signals for kinase Gl50803_8445 around nuclei and the cell perimeter and lower levels distributed throughout the cytosol. Strong signals for kinases Gl50803_9421 and Gl50803_11364 were detected throughout the cytosol. Cytosolic signals for kinase Gl50803_9421 were also observed but were relatively weak. Cytosolic and nuclear signals were enriched for kinase Gl50803_13215. Finally, punctate signals for kinase

Gl50803_16034 were uniformly dispersed throughout the cytosol (Fig 4b). These data document differences in the overall distribution of small gatekeeper kinases, with three distinct patterns resolved by our microscopy thus far. The differences may indicate different cellular roles in the trophozoite stage.

Functional importance of *Giardia* small gatekeeper kinases

Following successful 3xHA integrated tagging of kinases we pursued a reverse genetics approach to test the relative importance of each kinase for trophozoite proliferation. Previous attempts to use RNAi for gene knockdown have been unsuccessful and gene knockouts in *Giardia* are yet to be accomplished due to the tetraploid nature of trophozoites [22]. Therefore, we chose to target the remaining kinases with anti-sense translation blocking morpholino oligomers. Treatment with 100 μM gene specific antisense-morpholino oligomers reduced protein levels by 89%±12 (Gl50803_8445), 42%±9 (Gl50803_9421), 56%±11 (Gl50803_11364), 23%±7 (Gl50803_13215), and 80%±3 (Gl50803_16034) compared to levels observed in cells with control morpholino oligomers (Fig 5a).

For kinases Gl50803_9421 and Gl50803_11364, we did not detect observable changes in growth despite appreciable depletion of protein levels, indicating that they likely may not be essential for trophozoite proliferation (Fig 5b and S2 Fig). Gl50803_13215 showed a significant, yet modest decrease in growth (Fig 5b). In contrast, depleting Gl50803_8445 and

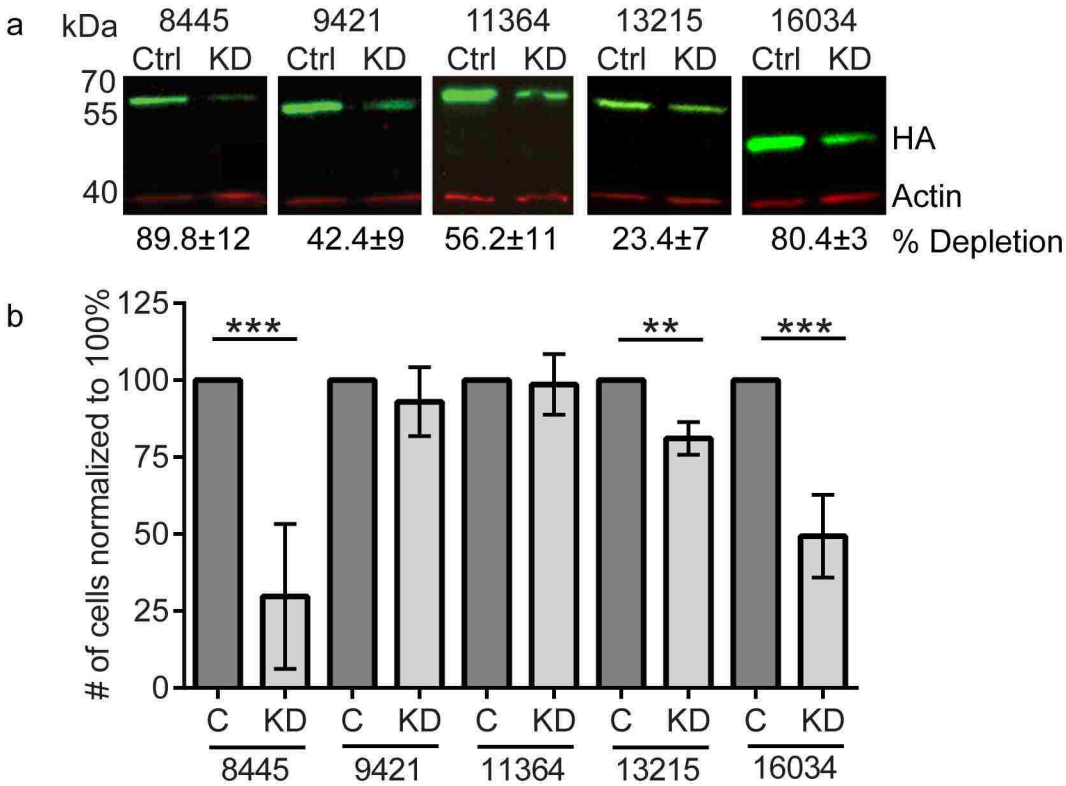

Fig 5. Kinase depletion interferes with growth. The five tagged-kinases shown to express in trophozoites were knocked down using anti-sense morpholinos. **(a)** Knockdown was measured and quantified by Western blot analysis, HA (green) and actin as loading control (red) **(b)** Cell growth was assessed after morpholino knockdown. Experiments were replicated a minimum of three times and significance was evaluated by t-test, * = p<0.05, ** = p<0.01, *** = p<0.001.

doi:10.1371/journal.pntd.0005107.g005

Gl50803_16034 resulted in 70% and 50% reduction in growth, respectively, compared to the control, 48 hours after morpholino treatment (Fig 5b).

Thermal shift assays identify BKIs with high affinity to target kinases

Thermal shift assays (TSAs) quantify the change in the denaturing temperature of a protein due to the stabilizing presence of a bound small molecule, in this case bumped kinase inhibitors bound at the kinase active site. Denaturation is conveniently tracked by following increased fluorescence from a dye that associates with hydrophobic regions that are exposed as the protein denatures [40,41]. For a given protein target, the magnitude of the thermal shift induced by individual small molecules is roughly correlated with the binding affinity of that molecule [35]. This obviates the need to determine activation requirements and suitable substrates for in vitro kinase activity assays of individual target kinases. We used TSAs to rapidly screen the BKI library in order to prioritize a subset of them for individual characterization of anti-giardial activity. After cloning, expressing and purifying both Gl50803_8445 and Gl50803_16034 proteins, we were able to assess ~400 BKIs for interaction with each purified kinase (Fig 6). Two compounds (1264, 1244) induced large shifts ($\Delta Tm > 5°$) in the stability of target Gl50803_16034. No equivalently large shifts were observed for target Gl50803_8445, although several compounds gave $\Delta Tm \approx 3°$. Notably the two compounds with the largest effect on Gl50803_16034 showed minimal effect on GL50803_8445, confirming the expectation that the BKI library compounds can exhibit specificity even among small-gatekeeper kinases. Library compound 1213, previously shown to be potent in suppressing trophozoite growth, induced a moderate ΔTm (2°–3°) in both targets. To see if the implied binding to an essential kinase would translate into *in vivo* activity, we selected 7 compounds with relatively large ΔTm for assessment of their phenotypic suppression of growth or attachment.

Matching cell-active BKIs to their intracellular target kinase[s]

Any or all of the small-gatekeeper kinases we have identified may constitute a target for new drugs against giardiasis. All are likely to be susceptible to bumped kinase inhibitors, and indeed a single compound may act on more than one of these kinases. However, compounds are not expected to be uniformly potent against all of the kinases. While rigorous identification of the specific target kinases for all library compounds found to have anti-*Giardia* activity is beyond the scope of the current report, we performed an initial evaluation of the *in vivo* activity of seven BKIs for which a large thermal shift implied binding to either Gl50803_8445 or Gl50803_16034 (Figs 6d and S3). EC_{50} values for these compounds were determined from dose-response curves for trophozoite growth in culture, based on the total number of cells present 48 hours after introduction of inhibitor. Compound 1264 stands out as having both a submicromolar EC_{50} (0.9 μM) against *Giardia* trophozoites and a large induced thermal shift (6.5°) for kinase Gl50803_16034. We infer that GI50803_16034 is a primary target, although not necessarily the sole target, for 1264. The lower *in vivo* potency (EC_{50} 4.6 μM) for compound 1244, which also shows large ΔTm (5.2°) for this same target kinase, is unexpected but may be due to poor cellular absorption or metabolic degradation.

By contrast, compound 1213 shows somewhat greater *in vivo* activity (EC_{50} 0.80 μM) but shows only modest stabilization of either of the target kinases tested ($\Delta Tm \approx 3°$). This suggests either that the primary target of 1213 is a different kinase or that its potency arises by modest inhibition of multiple targets.

Our initial search for small gatekeeper kinases was focused on identifying kinases most similar to TgCDPK1 due to an available library that could be used for this proof of concept study. Considering the variability of EC50 values relative to thermal shifts, we performed a more

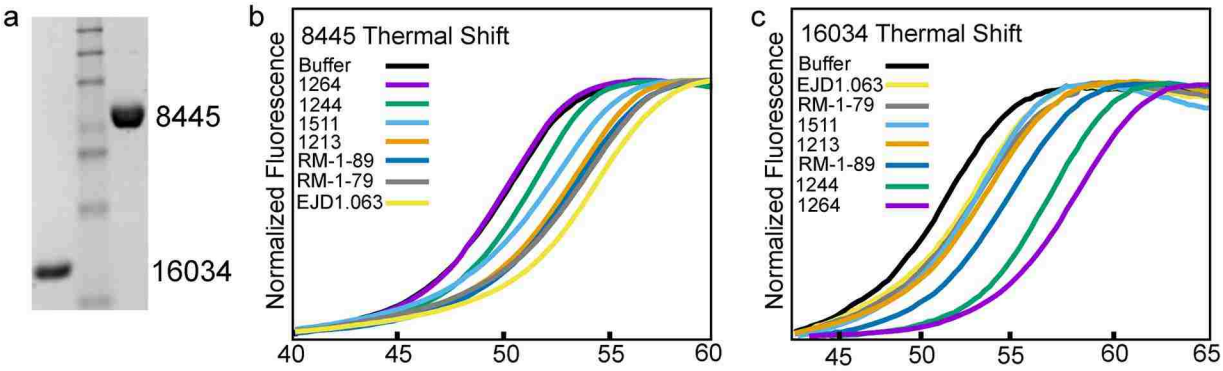

d

Compound	Structure	8445 ΔT_m °C	16034 ΔT_m °C	EC50
1213	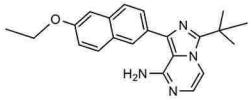	2.8	2.1	0.8 μM
1264	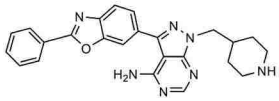	0.0	6.5	0.9 μM
RM-1-79	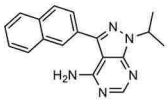	3.3	1.9	3.2 μM
1511	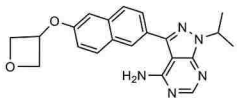	2.1	2.2	3.6 μM
RM-1-89	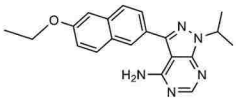	2.9	3.2	3.7 μM
1244	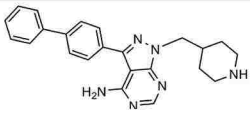	1.1	5.2	4.6 μM
EJDI-063	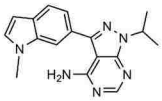	3.6	1.7	5.5 μM

Fig 6. Thermal shift assays identify bumped kinase inhibitors that bind to purified proteins. Kinases Gl50803_8445 and Gl50803_16034 were purified from *E. coli*. **(a)** SDS-PAGE was used to estimate protein purity. Gl50803_8445 was 91% pure and Gl50803_16034 was 98% pure. Note that minor impurities are not expected to affect ΔTm determination. **(b, c)** Melting curves for the BKIS showing the largest ΔTm are shown for Gl50803_8445 (b) and Gl50803_16034 (c). **(d)** The name, chemical structure, ΔTm, and EC_{50} value obtained for 7 BKIs prioritized for phenotypic characterization of anti-growth activity (Also see S3 Fig).

doi:10.1371/journal.pntd.0005107.g006

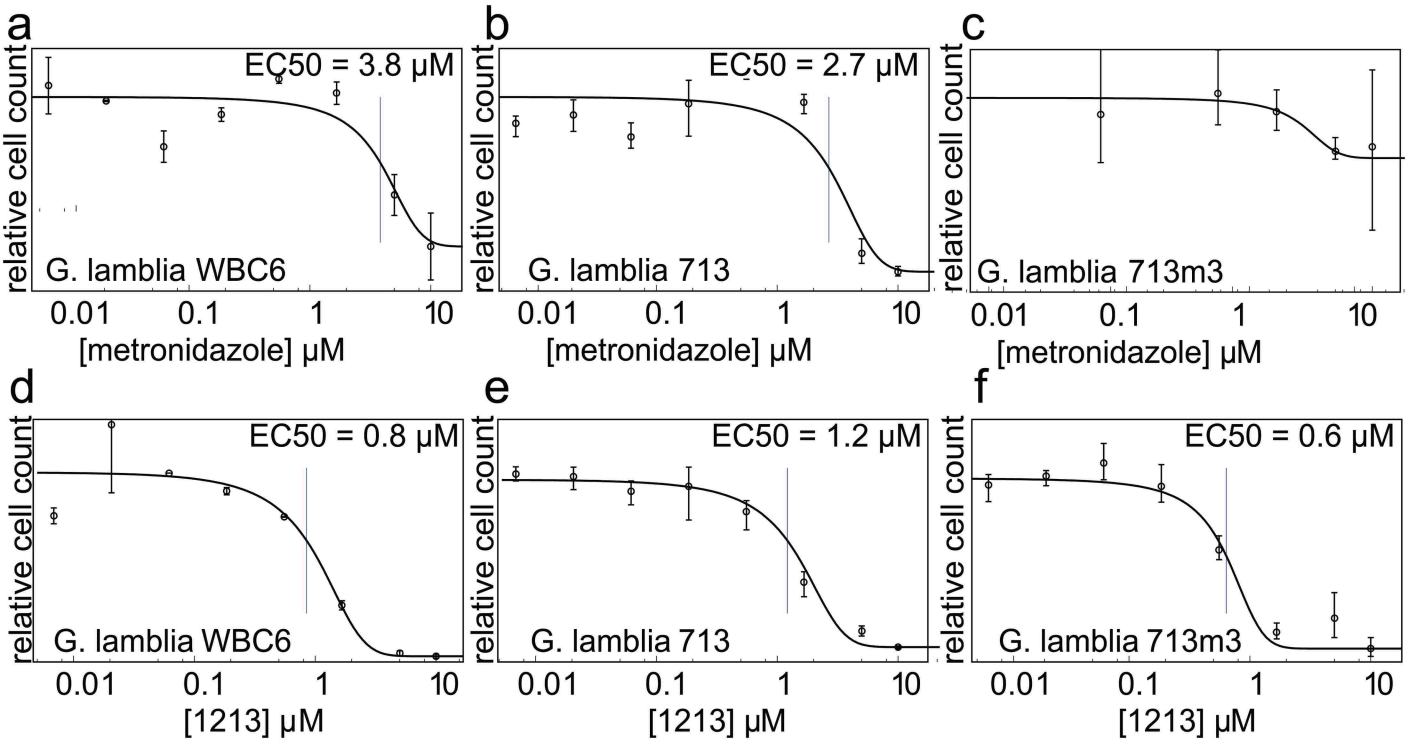

Fig 7. BKIs are effective against metronidazole-resistant *Giardia* cells. (a) Wild-type *G. lamblia* clone *WBC6* and **(b)** clone *713* are inhibited by metronidazole (EC_{50} of 3.8 μM and 2.7μM, respectively), but **(c)** metronidazole-resistant clone *713-M3* is not. Clones **(d)** *WBC6*, **(e)** *713* and **(f)** *713-M3* are each inhibited by BKI 1213 (EC_{50} of 0.8 μM, 1.2 μM, and 0.6 μM, respectively).

doi:10.1371/journal.pntd.0005107.g007

exhaustive search for small gatekeeper kinases, this time setting no threshold on similarity to TgCDPK1. Three additional NEK kinases were identified (GL50803_8152, GL50803_112518, GL50803_40904) and a putative threonine-gatekeeper CDC7 homolog (GL50803_112076). Although initial alignment of active site residues was less certain for sequences in this wider search, we confirmed the identity of the gatekeeper residue in GL50803_112076 by comparison with the known gatekeeper for CDC7 homologs with structures in the PDB. These four hits from the exhaustive search constitute possible additional targets for the activity of BKI compounds reported here.

Note that whether the BKIs act through inhibition of a single target or through inhibition of multiple kinases, this mechanism is distinct from that of the existing anti-giardiasis drug metronidazole and chemically related alternatives. Therefore, cross-resistance is unlikely. This is confirmed by the observed equal potency of compound 1213 against both wild-type and metronidazole-resistant strains of *Giardia* (Fig 7).

Kinase 8445 and 16034 are critical for cytokinesis and attachment

Given the critical role of kinase Gl50803_8445 and Gl50803_16034 in *Giardia* trophozoite growth, we analyzed the terminal phenotype of these kinases and found that depleting either kinase resulted in multinucleate cells indicating a block in cytokinesis (Fig 8). Quantification indicated 68% of l50803_8445 and 70% of Gl50803_16034 cells were blocked in cytokinesis. Compound 1213 induced a similar defective cytokinesis phenotype with slightly higher efficacy than knockdown of either kinase alone. This may reflect incomplete knockdown by morpholino treatment or an additive effect of chemical inhibition acting on multiple kinases.

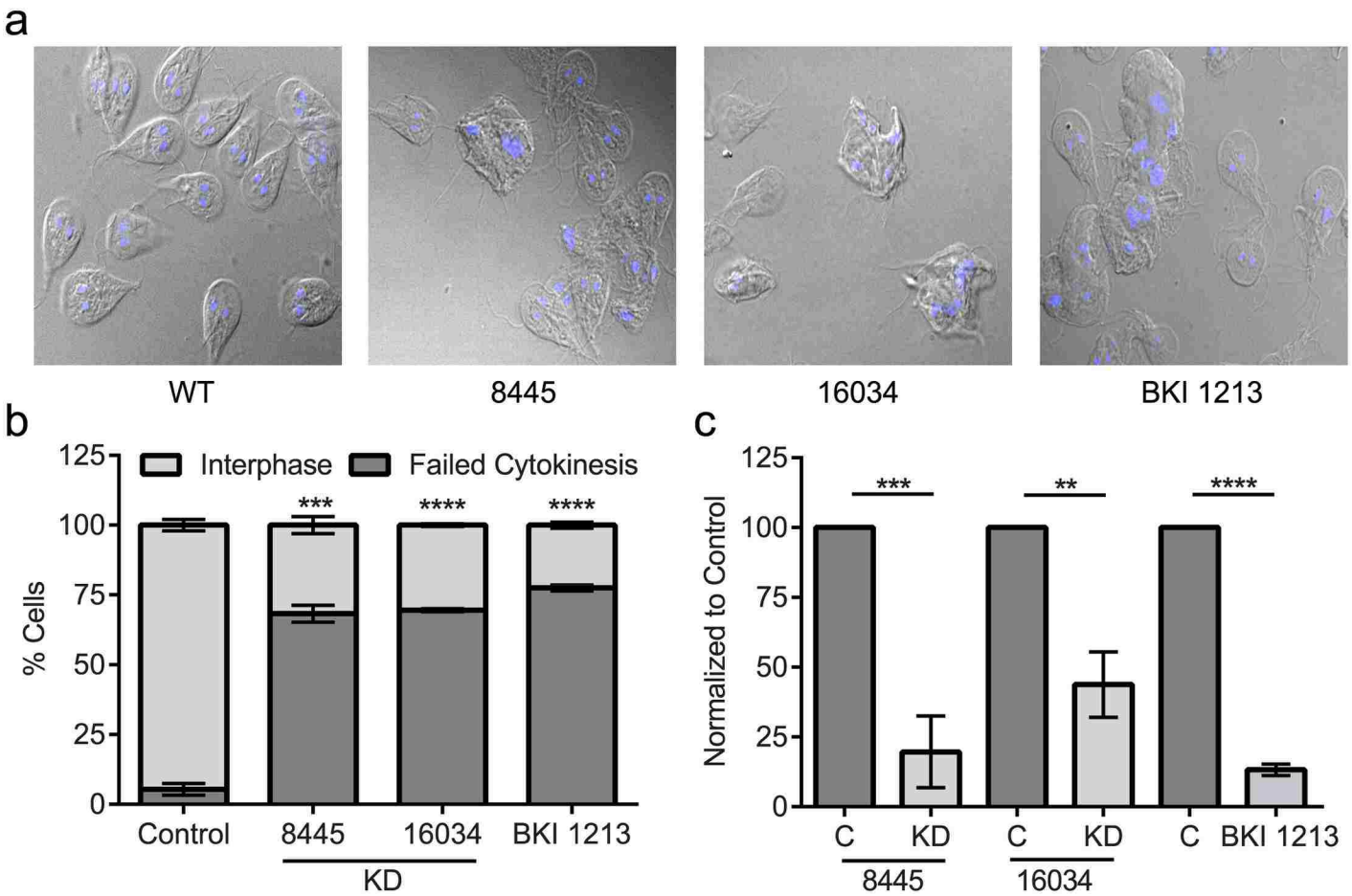

Fig 8. BKI 1213 mimics defects observed in knockdown of kinases GI50803_ 8445 and GI50803_16034. a) Fluorescent microscopy images of cells 48 hours after morpholino knockdown or treatment with BKI 1213 demonstrate a defect in cytokinesis compared to wild type control cells; cells complete nuclear division but not cytokinesis. **b)** Quantification of percent of cells that failed to complete cytokinesis. In each treatment, more than 67% of cells were stuck in cytokinesis; 68% of GI50803_8445, 69.5% of GI50803_16034 and 77.5% of cells treated with BKI 1213 were unable to complete cytokinesis. **c)** Attachment assays confirmed that when protein is depleted or cells are treated with BKI 1213, the ability for cells to attach is greatly reduced. Less than 20% of kinase 50803_8445 cells were able to maintain attachment, 43.8% of kinase 50803_16034 cells were able to maintain attachment and only 13% of cells treated with 5 μM BKI 1213 maintained attachment. Experiments were replicated a minimum of three times and significance was evaluated by t-test, ** = $p<0.01$, *** = $p<0.001$, **** = $p<0.0001$.

doi:10.1371/journal.pntd.0005107.g008

Clinical giardiasis is caused by *Giardia* trophozoites attaching to the intestinal microvilli, colonizing the intestines and creating a barrier against nutrient absorption by the host. Additionally, histological tissue samples have indicated an increased production of mucus by host goblet cells and vacuolated epithelial cells in the mucosa [42,43], that likely reflect an effort to dislodge attached parasites. Therefore, kinases with a role in attachment, even indirectly, would be promising targets, as infection could be cleared without necessarily killing the parasites. An example of this pharmacological strategy is the demonstration that the anti-giardial activity of the isoflavone formononetin occurs by inducing rapid detachment of trophozoites from the intestine of infected mice [44]. In cell culture, *Giardia* attaches to the surface of the culture tube, with a small fraction of cells detached and freely swimming.

Therefore, we assessed the ability of trophozoites to remain attached 48 hours post-knockdown for the two kinases validated to be essential for growth. This was assayed by monitoring the ratio of cells that were free-swimming to those attached to the culture tube. We observed

that the ability of cells to attach to the culture tube was substantially reduced following knockdown of Gl50803_8445 and Gl50803_16034 cells. We observed an 80% and 56% decrease in parasite attachment (Fig 8c) when we knocked down Gl50803_8445 and Gl50803_16034, respectively. In this assay, we simply poured off detached cells; maintaining attachment during intestinal peristalsis would likely present a greater challenge to the cells. These genetic experiments, performed at the population level with incomplete knockdown indicate that targeting kinases Gl50803_8445 and Gl50803_16304 with BKIs could be an effective strategy to clear a *Giardia* infection due to reduced attachment and proliferation. Indeed, treatment of trophozoites with compound 1213 led to an 87% decrease in parasite attachment.

Discussion

Previous phenotypic screening for anti-giardiasis activity

Several efforts to identify potential new anti-giardial therapeutics by phenotypic screening against large libraries of drugs or drug-like molecules have been reported previously. Tejman-Yarden et al [45] screened a library of 910 bioactive compounds including ~750 approved drugs. Of these, 56 compounds exhibited inhibition of *G. lamblia* growth and attachment at 10 μM, including 15 compounds with known anti-giardial activity and most notably the approved anti-arthritis drug auranofin.

Auranofin was reported to be active against *Giardia* trophozoites with an EC_{50} of 4–6 μM. Galkin, et al [46] found the most active compound in the LOPAC^{1280} library of pharmaceutically active compounds to be disulfiram (tetraethylthiuram disulfide), previously used in long-term treatment of alcoholism. They reported an EC_{50} of 0.9 μM against *Giardia* trophozoites. Disulfiram covalently attacks protein sulfhydryls in general, but the primary target in this case is a non-catalytic cysteine near the active site of *G. lamblia* carbamate kinase. Both of these potential leads, disulfiram and auranofin, overlap in part with the chemical action of existing nitroimidazole drugs including metronidazole in attacking protein sulfhydryl groups. Thus, they share a profile of side-effects and potential toxicity, although the specific sets of intracellular targets differ [47].

The use of phenotypic screening is generally viewed in contradistinction to molecular target-based approaches to drug discovery [48]. Identifying off-label activity of an approved drug through phenotypic screening has the obvious benefit of immediate clinical applicability if the compound has sufficient anti-parasite activity. On the other hand, it is not clear that either of the previously reported hits from anti-giardial screening offer much scope for follow-on chemical modification of the existing drug to improve selectivity or anti-giardial potency. This illustrates a common drawback of phenotypic screening, which is further exacerbated if the molecular target of a cell-active compound found by screening is not known, precluding structure-guided optimization of selectivity or potency.

Success of combined structural genomics and targeted phenotypic screening

We have been able to combine the strengths of phenotypic screening and a structural approach to target-based lead discovery. Preliminary examination of the *G. lamblia* genome established that it contained eight coding sequences for kinase homologs with an atypically small (Gly/Ala/Ser/Thr) active site residue at the gatekeeper position. It is important to note that these sequences were not selected on the basis of sequence homology either to each other or to previously characterized drug targets. Instead they were selected because they are predicted to share a specific unusual structural feature at the putative active site. We then conducted an initial

targeted phenotypic screen for anti-giardia activity in a representative subset of compounds drawn from a library designed to target exactly this shared structural feature, confirming that the library was rich in cell-active compounds.

Follow-up TSA screening of the entire library against purified kinases Gl50803_8445 and Gl50803_16034 highlighted specific library compounds with high implied affinity for those targets. Next, we showed that library compounds with high implied affinity for Gl50803_16034 exhibited $EC_{50} \leq 1$ μM against *Giardia* trophozoites, confirming the success of this approach to lead discovery.

It is quite possible that the library compounds selected for high-implied affinity for Gl50803_16034 also bind others of the identified small-gatekeeper kinases not yet individually characterized. This does not diminish their potential as leads for anti-giardia drug design. It is formally possible that they also hit some unknown protein target, but we consider this unlikely based on prior characterization of compounds from this BKI library as being non-cytotoxic to mammalian cell lines and having low activity against a panel of larger gatekeeper kinases [26,31,44].

Concluding remarks

Here we have shown that a set of kinases in *Giardia* possess an unusual structural feature, a small gatekeeper residue, which is a promising target for the development of highly selective inhibitors. Knockdown of target proteins identified two kinases with strong growth, attachment and cytokinesis defects; the cells appear to have completed nuclear division but never completely divided. As a result of the cytokinesis defect, growth is inhibited and a high percentage of cells are unable to maintain attachment presumably due to gross morphological defects impeding the function of the ventral adhesive disc [1,49]. Compounds from a BKI library originally designed to target *T*. *gondii* CDPK1 were able to phenocopy the results observed after kinase knockdown. In particular, exposure to BKI 1213 induced defects in cytokinesis similar to those produced by kinase knockdown as observed by fluorescence microscopy. Such a severe defect hinders the cells ability to attach and creates the potential to clear an infection from the intestines. Collectively, our results suggest that *in vivo* use of BKIs may provide an alternative treatment for giardiasis. Importantly, we have shown that BKIs can inhibit the growth of metronidazole-resistant *Giardia* due to their entirely different mechanism of action. Moreover, BKIs are not expected to have the problematic side effects associated with the free radical production by metronidazole and related drugs. Therefore, BKIs are an attractive starting point to find an alternative treatment for giardiasis.

Supporting Information

S1 Table. PCR primers, morpholino oligo sequences and PCR primers to verify integration of *Gl50803_9665* and *Gl50803_17368*.
(EPS)

S1 Fig. (a) Diagram of vector integration strategy (b) PCR assay to validate integration of 3xHA epitope tag at each kinase, *Gl50803_9665* and *Gl50803_17368*.
(EPS)

S2 Fig. Growth curves of kinases after knockdown vs morpholino standard control.
(EPS)

S3 Fig. EC_{50} of BKI inhibition of *Giardia* trophozoite growth.
(EPS)

Acknowledgments

We thank B. Wakimoto, M. Steele-Ogus, J. Krtkova, and K. Rivas for critical reading of the manuscript. We thank D. Maly for generously sharing the BKI library. We thank the L. Eckmann lab, UC San Diego School of Medicine, for generously providing *Giardia* strains 713 and 713-M3. We thank H. Bejhatnia and M. Nguyen for technical assistance.

Author Contributions

Conceptualization: ARP EAM.

Formal analysis: ARP EAM KKO KMH.

Funding acquisition: ARP KMH.

Investigation: KMH TRS JWX GCMA.

Methodology: ARP KKO.

Project administration: ARP EAM.

Supervision: ARP EAM KKO.

Validation: ARP EAM.

Visualization: KMH EAM GCMA KKO ARP.

Writing – original draft: KMH EAM ARP.

Writing – review & editing: KMH EAM ARP.

References

1. Adam RD. Biology of Giardia lamblia. Clin Microbiol Rev. 2001; 14: 447–475. doi: 10.1128/CMR.14.3.447-475.2001 PMID: 11432808
2. Lane S, Lloyd D. Current trends in research into the waterborne parasite Giardia. Crit Rev Microbiol. 2002; 28: 123–147. doi: 10.1080/1040-840291046713 PMID: 12109771
3. Ansell BRE, McConville MJ, Ma'ayeh SY, Dagley MJ, Gasser RB, Svärd SG, et al. Drug resistance in Giardia duodenalis. Biotechnol Adv. 2015; doi: 10.1016/j.biotechadv.2015.04.009 PMID: 25922317
4. Lalle M. Giardiasis in the post genomic era: treatment, drug resistance and novel therapeutic perspectives. Infect Disord Drug Targets. 2010; 10: 283–94. PMID: 20429863
5. Savioli L, Smith H, Thompson A. Giardia and Cryptosporidium join the "Neglected Diseases Initiative". Trends Parasitol. 2001 Mar 2. 2006; 22: 203–208. doi: 10.1016/j.pt.2006.02.015 PMID: 16545611
6. Guerrant RL, DeBoer MD, Moore SR, Scharf RJ, Lima AAM. The impoverished gut—a triple burden of diarrhoea, stunting and chronic disease. Nat Rev Gastroenterol Hepatol. 2013; 10: 220–9. doi: 10.1038/nrgastro.2012.239 PMID: 23229327
7. Farthing MJ. Giardiasis. Gastroenterol Clin North Am. 1996; 25: 493–515. PMID: 8863037
8. Müller J, Sterk M, Hemphill A, Müller N. Characterization of Giardia lamblia WB C6 clones resistant to nitazoxanide and to metronidazole. J Antimicrob Chemother. 2007; 60: 280–7. doi: 10.1093/jac/dkm205 PMID: 17561498
9. Uzlikova M, Nohynkova E. The effect of metronidazole on the cell cycle and DNA in metronidazole-susceptible and -resistant Giardia cell lines. Mol Biochem Parasitol. 2014; 198: 75–81. doi: 10.1016/j.molbiopara.2015.01.005 PMID: 25681616
10. Johnson SM, Murphy RC, Geiger J a, DeRocher AE, Zhang Z, Ojo KK, et al. Development of Toxoplasma gondii calcium-dependent protein kinase 1 (TgCDPK1) inhibitors with potent anti-toxoplasma activity. J Med Chem. 2012; 55: 2416–26. doi: 10.1021/jm201713h PMID: 22320388
11. Lourido S, Shuman J, Zhang C, Shokat KM, Hui R, Sibley LD. Calcium-dependent protein kinase 1 is an essential regulator of exocytosis in Toxoplasma. Nature. 2010; 465: 359–62. doi: 10.1038/nature09022 PMID: 20485436

12. Castellanos-Gonzalez A, White AC, Ojo KK, Vidadala RSR, Zhang Z, Reid MC, et al. A novel calcium-dependent protein kinase inhibitor as a lead compound for treating cryptosporidiosis. J Infect Dis. 2013; 208: 1342–1348. doi: 10.1093/infdis/jit327 PMID: 23878324

13. Ojo KK, Larson ET, Keyloun KR, Castaneda LJ, Derocher AE, Inampudi KK, et al. Toxoplasma gondii calcium-dependent protein kinase 1 is a target for selective kinase inhibitors. Nat Struct Mol Biol. 2010; 17: 602–607. doi: 10.1038/nsmb.1818 PMID: 20436472

14. Zhang C, Kenski DM, Paulson JL, Bonshtien A, Sessa G, Cross JV, et al. A second-site suppressor strategy for chemical genetic analysis of diverse protein kinases. Nat Methods. 2005; 2: 435–41. doi: 10.1038/nmeth764 PMID: 15908922

15. Doggett JS, Ojo KK, Fan E, Maly DJ, Van Voorhis WC. Bumped kinase inhibitor 1294 treats established toxoplasma gondii infection. Antimicrob Agents Chemother. 2014; 58: 3547–3549. doi: 10.1128/AAC.01823-13 PMID: 24687502

16. Lendner M, Böttcher D, Delling C, Ojo KK, Van Voorhis WC, Daugschies A. A novel CDPK1 inhibitor—a potential treatment for cryptosporidiosis in calves? Parasitol Res. 2015; 114: 335–6. doi: 10.1007/s00436-014-4228-7 PMID: 25398685

17. Manning G, Reiner DS, Lauwaet T, Dacre M, Smith A, Zhai Y, et al. The minimal kinome of Giardia lamblia illuminates early kinase evolution and unique parasite biology. Genome Biol. 2011; 12: R66. doi: 10.1186/gb-2011-12-7-r66 PMID: 21787419

18. Naula C, Parsons M, Mottram JC. Protein kinases as drug targets in trypanosomes and Leishmania. Biochimica et Biophysica Acta—Proteins and Proteomics. 2005. pp. 151–159. doi: 10.1016/j.bbapap.2005.08.018 PMID: 16198642

19. Wloga D, Camba A, Rogowski K, Manning G, Jerka-Dziadosz M, Gaertig J. Members of the NIMA-related Kinase Family Promote Disassembly of Cilia by Multiple Mechanisms. Mol Biol Cell. 2006; 17: 2799–2810. doi: 10.1091/mbc.E05-05-0450 PMID: 16611747

20. Moniz L, Dutt P, Haider N, Stambolic V. Nek family of kinases in cell cycle, checkpoint control and cancer. Cell Div. 2011; 6: 18. doi: 10.1186/1747-1028-6-18 PMID: 22040655

21. Fry AM, O'Regan L, Sabir SR, Bayliss R. Cell cycle regulation by the NEK family of protein kinases. J Cell Sci. 2012; 125: 4423–4433. doi: 10.1242/jcs.111195 PMID: 23132929

22. Smith AJ, Lauwaet T, Davids BJ, Gillin FD. Giardia lamblia Nek1 and Nek2 kinases affect mitosis and excystation. Int J Parasitol. 2012; 42: 411–419. doi: 10.1016/j.ijpara.2012.03.001 PMID: 22429767

23. Jones NG, Thomas EB, Brown E, Dickens NJ, Hammarton TC, Mottram JC. Regulators of Trypanosoma brucei Cell Cycle Progression and Differentiation Identified Using a Kinome-Wide RNAi Screen. PLoS Pathog. 2014; 10. doi: 10.1371/journal.ppat.1003886 PMID: 24453978

24. Townson SM, Laqua H, Upcroft P, Boreham PF, Upcroft JA. Induction of metronidazole and furazolidone resistance in Giardia. Trans R Soc Trop Med Hyg. 1992; 86: 521–2. PMID: 1475822

25. Keister D. Axenic culture of Giardia lamblia in TYI-S-33 medium supplemented with bile. Trans R Soc Trop Med Hyg. 1983; 77: 487–88. PMID: 6636276

26. Keyloun KR, Reid MC, Choi R, Song Y, Fox AM, Hillesland HK, et al. The gatekeeper residue and beyond: homologous calcium-dependent protein kinases as drug development targets for veterinarian Apicomplexa parasites. Parasitology. 2014; 141: 1499–1509. doi: 10.1017/S0031182014000857 PMID: 24927073

27. Murphy RC, Ojo KK, Larson ET, Castellanos-Gonzalez A, Perera BGK, Keyloun KR, et al. Discovery of Potent and Selective Inhibitors of Calcium-Dependent Protein Kinase 1 (CDPK1) from C. parvum and T. gondii. ACS Med Chem Lett. 2010; 1: 331–335. doi: 10.1021/ml100096t PMID: 21116453

28. Zhang Z, Ojo KK, Johnson SM, Larson ET, He P, Geiger JA, et al. Benzoylbenzimidazole-based selective inhibitors targeting Cryptosporidium parvum and Toxoplasma gondii calcium-dependent protein kinase-1. Bioorganic Med Chem Lett. 2012; 22: 5264–5267. doi: 10.1016/j.bmcl.2012.06.050 PMID: 22795629

29. Gourguechon S, Cande WZ. Rapid tagging and integration of genes in Giardia intestinalis. Eukaryotic Cell. 2011. pp. 142–145. doi: 10.1128/EC.00190-10 PMID: 21115739

30. Hewitt SN, Choi R, Kelley A, Crowther GJ, Napuli AJ, Van Voorhis WC. Expression of proteins in Escherichia coli as fusions with maltose-binding protein to rescue non-expressed targets in a high-throughput protein-expression and purification pipeline. Acta Crystallogr Sect F Struct Biol Cryst Commun. 2011; 67: 1006–9. doi: 10.1107/S1744309111022159 PMID: 21904041

31. Studier FW. Protein production by auto-induction in high density shaking cultures. Protein Expr Purif. 2005; 41: 207–234. doi: 10.1016/j.pep.2005.01.016 PMID: 15915565

32. Paredez AR, Assaf ZJ, Sept D, Timofejeva L, Dawson SC, Wang C-JR, et al. An actin cytoskeleton with evolutionarily conserved functions in the absence of canonical actin-binding proteins. Proc Natl Acad Sci U S A. 2011; 108: 6151–6156. doi: 10.1073/pnas.1018593108 PMID: 21444821

33. Schneider C a, Rasband WS, Eliceiri KW. NIH Image to ImageJ: 25 years of image analysis. Nat Methods. 2012; 9: 671–675. doi: 10.1038/nmeth.2089 PMID: 22930834

34. Paredez AR, Nayeri A, Xu JW, Krtkova J, Cande WZ. Identification of obscure yet conserved actin-associated proteins in Giardia lamblia. Eukaryot Cell. 2014; 13: 776–784. doi: 10.1128/EC.00041-14 PMID: 24728194

35. Crowther GJ, He P, Rodenbough PP, Thomas AP, Kovzun KV., Leibly DJ, et al. Use of thermal melt curves to assess the quality of enzyme preparations. Anal Biochem. 2010; 399: 268–275. doi: 10.1016/j.ab.2009.12.018 PMID: 20018159

36. Bishop AC, Ubersax JA, Petsch DT, Matheos DP, Gray NS, Blethrow J, et al. A chemical switch for inhibitor-sensitive alleles of any protein kinase. Nature. 2000; 407: 395–401. doi: 10.1038/35030148 PMID: 11014197

37. Lourido S, Zhang C, Lopez MS, Tang K, Barks J, Wang Q, et al. Optimizing small molecule inhibitors of calcium-dependent protein kinase 1 to prevent infection by toxoplasma gondii. J Med Chem. 2013; 56: 3068–3077. doi: 10.1021/jm4001314 PMID: 23470217

38. Johnson SM, Murphy RC, Geiger J a, DeRocher AE, Zhang Z, Ojo KK, et al. Development of Toxoplasma gondii calcium-dependent protein kinase 1 (TgCDPK1) inhibitors with potent anti-toxoplasma activity. J Med Chem. 2012; 55: 2416–26. doi: 10.1021/jm201713h PMID: 22320388

39. Kim KT, Mok MT, Edwards MR. Protein kinase B from Giardia intestinalis. Biochem Biophys Res Commun. 2005; 334: 333–341. doi: 10.1016/j.bbrc.2005.06.106 PMID: 16018966

40. Pantoliano MW, Petrella EC, Kwasnoski JD, Lobanov VS, Myslik J, Graf E, et al. High-density miniaturized thermal shift assays as a general strategy for drug discovery. J Biomol Screen Off J Soc Biomol Screen. 2001; 6: 429–440. doi: 10.1177/108705710100600609

41. Niesen FH, Berglund H, Vedadi M. The use of differential scanning fluorimetry to detect ligand interactions that promote protein stability. Nat Protoc. 2007; 2: 2212–21. doi: 10.1038/nprot.2007.321 PMID: 17853878

42. Williamson a L, O'Donoghue PJ, Upcroft JA, Upcroft P. Immune and pathophysiological responses to different strains of Giardia duodenalis in neonatal mice. Int J Parasitol. 2000; 30: 129–36. PMID: 10704595

43. Chávez B, González-Mariscal L, Cedillo-Rivera R, Martínez-Palomo A. Giardia lamblia: in vitro cytopathic effect of human isolates. Exp Parasitol. 1995; 80: 133–8. PMID: 7821402

44. Lauwaet T, Andersen Y, van de Ven L, Eckmann L, Gillin FD. Rapid detachment of Giardia lamblia trophozoites as a mechanism of antimicrobial action of the isoflavone formononetin. J Antimicrob Chemother. 2010; 65: 531–534. doi: 10.1093/jac/dkp501 PMID: 20067984

45. Tejman-Yarden N, Miyamoto Y, Leitsch D, Santini J, Debnath A, Gut J, et al. A reprofiled drug, auranofin, is effective against metronidazole-resistant Giardia lamblia. Antimicrob Agents Chemother. 2013; 57: 2029–2035. doi: 10.1128/AAC.01675-12 PMID: 23403423

46. Galkin A, Kulakova L, Lim K, Chen CZ, Zheng W, Turko IV, et al. Structural basis for inactivation of Giardia lamblia carbamate kinase by disulfiram. J Biol Chem. 2014; 289: 10502–10509. doi: 10.1074/jbc.M114.553123 PMID: 24558036

47. Karamanakos PN, Pappas P, Boumba VA, Thomas C, Malamas M, Vougiouklakis T, et al. Pharmaceutical Agents Known to Produce Disulfiram-Like Reaction: Effects on Hepatic Ethanol Metabolism and Brain Monoamines. Int J Toxicol. 2007; 26: 423–432. doi: 10.1080/10915810701583010 PMID: 17963129

48. Zheng W, Thorne N, McKew JC. Phenotypic screens as a renewed approach for drug discovery. Drug Discovery Today. 2013. pp. 1067–1073. doi: 10.1016/j.drudis.2013.07.001 PMID: 23850704

49. Woessner DJ, Dawson SC. The giardia median body protein is a ventral disc protein that is critical for maintaining a domed disc conformation during attachment. Eukaryot Cell. 2012; 11: 292–301. doi: 10.1128/EC.05262-11 PMID: 22247266

CHAPTER 3: Characterization of NEKxit, a small gatekeeper protein kinase involved in cytokinesis in *Giardia lamblia.*

Introduction

The protozoan parasite *G. lamblia* belongs to the excavates, which is thought to be one of the earliest group of protists to branch from other eukaryotes. Its genome is small and many cellular pathways appear to be comprised of fewer components than in later emerging eukaryotes[1], which is evident in the correspondingly small kinome of *Giardia.* This suggests that each individual kinase is more likely to perform an essential function in the cell. The *Giardia* kinome (strain WB) contains 278 protein kinases, 80 of which constitute the core kinome and 198 that are classified as Nek kinases[1]. The core kinome of 80 protein kinases is fully conserved between three sequenced genomes[1]. Sixty-one of the 80 kinases are classified into 49 families that are also present in many other eukaryotes. The remaining 19 families are unique to *Giardia*[1]. The highly expanded *Giardia* Nek family contains 198 kinases, compared to only 11 in humans and constitutes 71% of its kinome[1]. Many eukaryotic Nek kinases are hypothesized to control mitotic entry[2] and flagella length[3].

Protein kinases are known as key players in eukaryotic signal transduction, regulating important cellular processes including protein synthesis, gene expression and subcellular localization of proteins. Furthermore the divergence of a specific protein kinase in protists from their homologs, if any, in humans has been identified as an opportunity for its development of new drugs for disease caused by parasitic protozoa[4]. In particular, most mammalian protein kinases have a large gatekeeper residue, which limits accessibility to a hydrophobic pocket in the active site by certain inhibitor molecules. A class of cell-permeable small molecule inhibitors

called bumped kinase inhibitors (BKIs) have been shown to selectively and effectively block kinase-associated key processes in the life cycle of parasites such as *Toxoplasma gondii, Cryptosporidium parvum* and *Plasmodium flaciparum*[5]

Prior research identified seven protein kinases in *G. lamblia* that have small amino acid residues in their ATP binding sites. Results from chemical and genetic experiments found that two of the *G. lamblia* protein kinases were essential for growth, attachment and progression through cytokinesis; both were also sensitive to several BKIs[6]

Based on the observed severe growth defect associated with morpholino knock down of GL50803_8445 expression, this kinase was identified as an promising drug target. Initial phenotypic characterization suggested that this kinase is required for cytokinesis in *Giardia*. Unlike other eukaryotes that use an actomysin contractile ring, *Giardia* utilizes its flagella to both coordinate membrane trafficking into the furrow and propel daughter cells apart[7]. Here we examine the role of Gl50803_8445 in *Giardia's* unique mode of cytokinesis. This functional analysis adds to the incomplete but growing body of knowledge about cell cycle events and cytokinesis in *G. lamblia.*

GL50803_8445 is hereafter referred to as NEKxit because it is thought to be a Nek kinase involved with flagella exit. Initial characterization of NEKxit suggested that the protein is localized to the cell cortex and perinuclear region corresponding to areas around the nuclei (or possibly the ER) hence may have a role in cytokinesis. Knocking down the expression of NEKxit showed a clear increase in the number of cells that had not completed cytokinesis compared to the control cells. Presence of multinucleated cell masses with no separation of cells was observed, which indicated that nuclear division had taken place but cells had not completed cytokinesis.

Quantitative analysis of the knockdown reaction found a six-fold increase in the number of cells that appeared to be stalled at this stage of the cell cycle. Localization of NEKxit around both nuclei and the phenotypic effect of its knock down are evidence that, it likely has an important role in progression of cells through cytokinesis. This initial observation spurred investigation into the role this kinase has in progression through the cell cycle, and specifically, cytokinesis.

Previous studies show that the onset of cytokinesis begins with the progress of the cleavage furrow between the nascent daughter ventral discs and runs parallel to caudal flagella internal axonemes. Just prior to scission, the dividing cell becomes oriented tail-to-tail and the daughter cells swim apart using flagella-mediated swimming[8].

A recent study demonstrated that flagella-based force generation, membrane delivery to the furrow by GTPase Rab11, and actin involvement in scission are all required elements for cytokinesis[7]. NEKxit exhibits similar localization patterns during mitosis as seen in 3HA-tagged Rab11 cells, suggesting that NEKxit may have a similar role in caudal flagellar positioning, and/or actin regulation as cells progress through cytokinesis.

Methods & Materials

Parasite culture

G. lamblia wild-type strains *WBC6* (ATCC 50803) cells were grown in TYI-S-33 medium supplemented with 10% bovine serum and 0.05 mg/mL bovine bile[9]. Cells were cultured at 37° under hypoxic conditions using 15 mL polystyrene screw-cap tubes (Corning Life Sciences DL).

Vector construction and transfection

To generate endogenously tagged small gatekeeper kinases, the putative kinase-coding genes

were amplified from genomic DNA by PCR and cloned into the pKS_3HA_Neo vector[10]. Primer sequences and restriction enzymes are shown in S1 Table. PCR amplifications were performed using iProof DNA polymerase (Bio-Rad).

Typically, an amplicon of ~ 1 kb in length that lacked the start codon was cloned in frame to a C-terminal triple-hemagglutinin epitope tag (3xHA) into the pKS_3HA_Neo or puromycin plasmid. The plasmids were linearized by the enzyme reported in S1 Table and ~5 µg of DNA was used to transform wild-type *Giardia*. Transformants were selected with G418 at 40 µg/mL or puromycin at 45 µg/mL.

To construct the NEKxit$_{vsvg}$Rabll_3HA cell line, pKS_3HA_Rab11_Pac was used as a template as described by Hardin *et al.* (2017). Gl50803_8445 gene was amplified from genomic DNA by PCR and cloned into the pKS_vsvg_Neo vector, then transfected into Rab11_3HA cells. Transformants were selected with both G418 at 440 µg/mL and puromycin at 45 µg/mL.

Construction of pKS_3HA_8855_Neo was performed as above.

Live cell imaging (with agarose overlay)

To follow NEKxit localization throughout mitosis and cytokinesis, the C terminus of Gl50803_8445 was tagged with an 18-aa flexible linker and the bright fluorescent protein mNeonGreen [11], creating the 8445_mNG_Neo construct (NEKxit_mNG). Cells were imaged as previously described in Hardin *et al*. (2017).

Immunofluorescence microscopy analysis

Fixed cell imaging was performed as described previously[12] after 3.5h starve/release to increase number of mitotic cells[13]. *G. lamblia* cells were pelleted at 500xg at room temperature, the pellet and remaining attached cells were fixed in PME (100 mM Pipes pH 7.0, 5 mM EGTA, 10 mM MgSO4) plus 0.025% Triton X-100, 100 µM MBS, and 100 µM EGS for 30 minutes at 37°C. Cells

were again pelleted, washed, resuspended with PME, and adhered to poly-L-lysine (Sigma-Aldrich) coated cover- slips. Cells were permeabilized in PME + 0.1% Triton X-100 for 10 minutes then washed 2X with PME + 0.1% Triton X-100 and blocked for 30 minutes in PMEBALG (PME + 1% BSA, 0.1% NaN3, 100 mM lysine, 0.5% cold water fish skin gelatin (Sigma Aldrich, St. Louis, MO) [14].

Cells were stained with rabbit anti-giActin antibody 28PB+1[14] and mouse monoclonal anti-HA (Clone HA7, Sigma-Aldrich) both diluted 1:125 in PMEBALG and incubated over-night. After three subsequent washes with PME + 0.05% Triton X-100, cells were incubated in secondary antibodies Alexa-488 goat anti-mouse and Alexa-555 goat anti-α-rabbit (Sigma-Aldrich, St. Louis, MO) (diluted 1:125 in PMEBALG) for 1h[14]. Cells were washed three times with PME + 0.05% Triton X-100. The coverslips were mounted with ProLong Gold anti-fade plus DAPI, (Thermo Fisher Scientific, Rockford, IL). Fluorescence deconvolution microscopy images were collected as described[15]. A minimum of 200 cells were examined and 30 imaged per experiment.

Morpholino knockdown and growth assays

Trophozoites were cultured to confluency, iced for 30 minutes to detach, spun down (500xg for 5 minutes) and media was replaced with 1.0 mL fresh *Giardia* growth medium. Cells and cuvettes were chilled on ice. Lyophilized morpholinos listed in S1 Table (Gene Tools, LLC, Philomath, OR) were resuspended in sterile water and 30 µL of a 100 mM morpholino stock was added to 300 µL of cells in a 4 mm cuvette. We used Gene Tools, LLC standard morpholino as a negative control. Cells were electroporated (375V, 1000 µF, 750 Ohms, GenePulser Xcell, Bio-Rad, Hercules, CA).

Cells were transferred to fresh media and incubated 4h at 37°C to allow cells to recover.

Cells were then iced for 30 minutes, counted and diluted to 20,000 cells/mL. Aliquots were counted every 12h over 48h. Cell counting was done using a Coulter counter (MoxiZ). Three independent replicates of each cell line and control were analyzed for each time point. Quantification of protein expression was determined at the 24-h time point by the Western blot assay described below.

Western blot analysis

Giardia trophozoites were harvested after chilling cultures on ice for 30 minutes. After detachment, cells were pelleted at 700xg, washed once in HBS (HEPES buffered saline), then resuspended in 300 µL of lysis buffer (50 mM Tris pH 7.5, 150 mM NaCl, 7.5% Glycerol, 0.25 mM $CaCl_2$, 0.25 mM ATP, 0.5 mM DTT, 0.5 mM PMSF, 0.1% Triton X-100, Halt 100X Protease Inhibitor Cocktail (ThermoFisher Scientific), then sonicated. The lysate was cleared by centrifugation at 10,000xg for 10 minutes at 4°C and then boiled in 2x Laemmli Sample Buffer (Bio- Rad). After SDS-PAGE, samples were transferred to PVDF membrane (Immobilon-FL) following the manufacturers' directions. Primary polyclonal rabbit anti-giActin 28PB+1[14] and monoclonal anti-HA mouse HA7 antibodies (IgG1; Sigma-Aldrich) were diluted 1:2500 in blocking solution (5% dry milk, 0.05% Tween-20 in TBS). Secondary anti-mouse Alexa-555 and anti-rabbit Alexa-647 antibodies were used. Horseradish peroxidase-linked anti-mouse or anti-rabbit antibodies (Bio-Rad) were used at 1:7,000. Multiplexed immunoblots were imaged on a Chemidoc MP (Bio-Rad) and signals were quantitated using ImageJ[16].

Scanning Electron Microscopy

For scanning electron microscopy (SEM) analysis, trophozoites were pelleted at 700xg for 7 minutes, fixed with 2.5% glutaraldehyde in 0.1 M phosphate buffered saline (PBS), pH 7.4 and incubated for 1 h[17]. After fixation, cells were pelleted again at 700xg for 7 minutes and washed

twice and resuspended in PBS. Cells were adhered to poly-L-lysine (Sigma-Aldrich) coated coverslips for 15 minutes then washed three times for 5 minutes with PBS and post-fixed in 1% OsO_4 for 1 h. Cells were washed three times 5 minutes each with dH_2O, dehydrated in alcohol, dried to critical point with CO_2, sputter coated with gold and analyzed on JEOL JSM-840A SEM.

Accession numbers

Genes/proteins

ORF Gl50803_8445 (NEKxit): UniProtKB—A8BXP9 (A8BXP9_GIAIC)

Results

Cytokinesis defect observed in cells 12h post knockdown

The initial observation that NEKxit had a role in cytokinesis was based on the phenotype of NEKxit depleted cells 48h after treatment with translation blocking antisense morpholinos. To begin characterizing the underlying defect that led to failed cytokinesis, NEKxit depleted cells were filmed from 24 – 26h after morpholino treatment. Remarkably, the majority of these cells already had strong phenotypic defects indicating the need to film the cells at an earlier time point. Cells imaged in time-lapse 4D DIC movies from 12 – 14h after knockdown appeared essentially indistinguishable from control cells yet morpholino treatment had reduced NEKxit levels by 41%. Upon initiation of cytokinesis the cleavage furrow often failed to progress (Supplemental Figure S1). Quantification of the number of cells that did not complete cytokinesis is shown (Figure 1).

Dynamic localization of NEKxit during mitosis and cytokinesis

To visualize protein localization throughout the cell cycle, NEKxit was tagged with the green fluorescent protein mNeonGreen generating NEKxit_mNeon Green (NEKxit-mNG) construct. In

NEKxit-mNG interphase cells, the protein localizes around both nuclei and the cortical region of the cell. As the cell begins mitosis, cortical localization moves inward and the protein can be visualized as it moves from the flagella and spindles to what appears to be only two flagella (Figure 2, T = 5.9) then back to the nuclei and cortex in the later stages. NEKxit's localization is dynamic as the cell cycle progresses.

Fixed cell immunofluorescence confirms localization of NEKxit through mitosis and cytokinesis

To confirm the localization patterns observed during live cell imaging of NEKxit_mNG cells and to further validate where NEKxit localizes throughout the cell cycle, fixed cell immunofluorescent microscopy was used. NEKxit localized in fixed cells as observed in live cell imaging (Figure 3), establishing a baseline of typical NEKxit protein localization throughout the cell cycle and cytokinesis (and eliminating the possibility that the presence of a tag affects localization).

Flagella defect identified in fixed cells using immunofluorescence microscopy

To examine whether proteins required for cell division might be regulated by NEKxit; actin, Rab11, and tubulin were localized in NEKxit depleted cells. Fixed cell images show many cells stuck in cytokinesis as early as 12h post-knockdown, cells were imaged 8h post-knockdown (Figure 4). Because the *G. lamblia* cell cycle is typically 8h, we anticipated very few, if any cells stuck in cytokinesis 8h post-knockdown compared to 12h post-knockdown. Interestingly, defects in the posterior end of cells along with atypical caudal flagellar positioning were observed very early at 8h. It is currently thought that flagella force generation is necessary for cells to complete cytokinesis[7]. A defect in flagellar positioning early in the cell cycle could introduce a downstream effect in cytokinesis. NEKxit depleted cells had blunted posterior ends and rounded

cell shape compared to the typical teardrop shape of control trophozoites; caudal flagella appeared to be tucked under or folded within the cell, however, it was not possible to determine by immunofluorescence microscopy analysis if the caudal flagella actually exited the cell body or if they were inside the cell, unable to exit.

Flagella defect characterized through scanning electron microscopy

In order to determine whether flagella exited the body of the cell, Scanning Electron Microscopy (SEM) was used to examine NEKxit cells 12h post knockdown. Two distinct defective phenotypes were observed (Figure 5).

NEKxit depleted cells were rounder than normal wild-type cells and lacked caudal flagella, similar to what was observed by immunofluorescence microscopy. It is possible that the flagella are retained within the cell body, not able to exit. Cells with the second defective phenotype still retained a recognizable pear shape with tapering of the caudal end of the cell. However, instead of fully formed caudal flagella, knob-shape structures were visible. In both phenotypes, caudal flagella are absent.

Rab11 and actin levels reduced in NEKxit cells after knockdown

Earlier studies established that Rab11 is required for cytokinesis and contributes to membrane delivery throughout cytokinesis[7]. A recent report by Hardin *et al*., (2017) also showed that Rab11_3HA and Rab11_mNG localized to perinuclear regions and the cell cortex. Interestingly, this localization pattern resembles the localization pattern observed in NEKxit cells.

To analyze the effect of NEKxit knockdown on Rab11_3HA expression, NEKxit depleted cells were observed 12h post knockdown using immunofluorescence microscopy; Rab11_3HA protein expression was reduced. Next, to determine if actin expression was affected by NEKxit knockdown, knockdown was repeated. Similar to the results obtained in NEKxit

depleted Rab11_3HA cells, actin levels were also reduced (Figure 6).

Flagella exit point protein Gl50803_8855 levels reduced at caudal exit sites with NEKxit knockdown

We observed that caudal flagella do not exit in NEKxit KD cells but questioned if the defect involves specifying the exit sites. The Hehl lab, University of Zurich, identified distinct localization of protein GL50803_8855 at the flagellar exit sites (2009, unpublished); this prompted examination of NEKxit knockdown on protein 8855. NEKxit depleted cells were imaged 12 h post knockdown using immunofluorescence microscopy. We were able to replicate the localization pattern observed by the Hehl lab in the control cells. However, in NEKxit KD cells, the protein marking the caudal flagella exit site was greatly reduced or absent (Figure 7). Quantification of knockdown was validated by western blot analysis.

Discussion

The understanding of mitosis and cytokinesis in *Giardia lamblia* is still in its infancy. Recent advances in live cell imaging have improved the ability to visualize cellular processes, such as cytokinesis, with greater spatial-temporal resolution[7]. Actin and Rab11are major players in cytokinesis; nascent flagella guide Rab11 vesicles to the furrow, flexion of intracytoplasmic caudal axonemes pushes daughters apart, flagella beating causes cells to swim apart creating membrane tension, and actin and Rab11 work together for abscission[7].

Characterization of NEKxit knockdown phenotypes reported here adds additional pieces to this puzzle. Initial observations of cells imaged 48h showed a high percentage of multinucleated cell masses. The defect was so severe that it was not possible to determine the root cause. Reducing knockdown time from 48h to 24h, 12h, and ultimately 8h, provided the

opportunity to analyze the onset of the defect, which led to the evidence that NEKxit has a role in caudal flagella positioning, development, and exit. The data suggests that NEKxit is involved in cytokinesis; specifically, it affects caudal flagella exit from the cell. However, the complete pathway(s) and other proteins involved in regulating this process are yet to be identified. Nevertheless, the cytokinesis defect associated with NEKxit depletion highlights the importance of the flagella for *Giardia* cytokinesis. Cytokinesis in NEKxit knockdown cells likely fails because caudal axonemes are not able to push daughter cells apart. Cells continue to undergo nuclear division but do not separate, which, after several cell cycles resulted in the multinucleated, shapeless cell masses seen 48h post knockdown.

Interestingly, initial results showed that NEKxit protein localization was visibly similar to Rab11 localization. When NEKxit was knocked down, reduced levels of Rab11 and actin was observed. The relationship between NEKxit, Rab11 or actin remains to be determined.

With the detection of the flagella exit site protein GL50803_8844, another intriguing observation was made. When NEKxit was knocked down in GL50803_8844 cells, protein 8844 marking the caudal flagella exit sites was reduced, adding support that NEKxit is needed for cells to properly position flagella during cytokinesis.

References

1. Manning G, Reiner DS, Lauwaet T, Dacre M, Smith A, Zhai Y, Svard S, Gillin FD. The minimal kinome of Giardia lamblia illuminates early kinase evolution and unique parasite biology. Genome Biol. 2011;12(7):R66.

2. O'Connell MJ, Krien MJE, Hunter T. Never say never. The NIMA-related protein kinases in mitotic control. Trends in Cell Biology. 2003;13(5):221–228.

3. Bradley BA, Quarmby LM. A NIMA-related kinase, Cnk2p, regulates both flagellar length and cell size in Chlamydomonas. Journal of cell science. 2005;118(Pt 15):3317–3326.

4. Ojo Merritt, E A, Maly D J, Van Voorhis, W C KK, Selzer PM. Part IV Drug Discovery. Christian Doerig Martin Wiese, Paul M. Selzer GS, editor. Germany: Wiley-Blackwell; 2014. 456 p.

5. Keyloun KR, Reid MC, Choi R, Song Y, Fox AM, Hillesland HK, Zhang Z, Vidadala R, Merritt EA, Lau AO, et al. The gatekeeper residue and beyond: homologous calcium-dependent protein kinases as drug development targets for veterinarian Apicomplexa parasites. Parasitology. 2014;141(11):1499–1509.

6. Hennessey KM, Smith TR, Xu JW, Alas GCM, Ojo KK, Merritt EA, Paredez AR. Identification and Validation of Small-Gatekeeper Kinases as Drug Targets in Giardia lamblia. PLOS Neglected Tropical Diseases. 2016;10(11):e0005107.

7. William R. Hardina, Renyu Lia, Jason Xub, Andrew M. Sheltona, Germain C. M. Alasa, Vladimir N. Minina B, and Alexander R. Paredeza 1. Myosin-independent cytokinesis in Giardia utilizes flagella to coordinate force generation and direct membrane trafficking. Proceedings of the National Academy of Sciences of the United States of America. 2017;(July).

8. Tůmová P, Kulda J, Nohýnková E. Cell division of Giardia intestinalis: Assembly and disassembly of the adhesive disc, and the cytokinesis. Cell Motility and the Cytoskeleton. 2007;64(4):288–298.

9. Keister D. Axenic culture of Giardia lamblia in TYI-S-33 medium supplemented with bile. Transactions of the Royal Society of Tropical Medicine and Hygiene. 1983;77(4):487–88.

10. Gourguechon S, Cande WZ. Rapid tagging and integration of genes in Giardia intestinalis. Eukaryotic Cell. 2011;10(1):142–145.

11. Shaner NC, Lambert GG, Chammas A, Ni Y, Cranfill PJ, Baird M a, Sell BR, Allen JR, Day RN, Israelsson M, et al. A bright monomeric green fluorescent protein derived from Branchiostoma lanceolatum. Nature methods. 2013;10(5):407–409.

12. Sagolla MS, Dawson SC, Mancuso JJ, Cande WZ. Three-dimensional analysis of mitosis and cytokinesis in the binucleate parasite Giardia intestinalis. Journal of cell science. 2006;119(Pt 23):4889–4900.

13. Krtková J, Thomas EB, Alas GCM, Schraner EM, Behjatnia HR, Hehl AB, Paredez AR. Rac regulates Giardia lamblia encystation by coordinating cyst wall protein trafficking and secretion. mBio. 2016;7(4).

14. Paredez AR, Assaf ZJ, Sept D, Timofejeva L, Dawson SC, Wang C-JR, Cande WZ. An actin cytoskeleton with evolutionarily conserved functions in the absence of canonical actin-binding proteins. Proceedings of the National Academy of Sciences of the United States of America. 2011;108(15):6151–6156.

15. Paredez AR, Nayeri A, Xu JW, Krtkova J, Cande WZ. Identification of obscure yet conserved actin-associated proteins in Giardia lamblia. Eukaryot Cell. 2014;13(6):776–784.

16. Schneider C a, Rasband WS, Eliceiri KW. NIH Image to ImageJ: 25 years of image analysis. Nature Methods. 2012;9(7):671–675.

17. Castillo-Romero A, Leon-Avila G, Rangel AP, Zarate RC, Tovar CG, Hernandez JM. Participation of actin on Giardia lamblia growth and encystation. PLoS ONE. 2009;4(9).

Figure 1

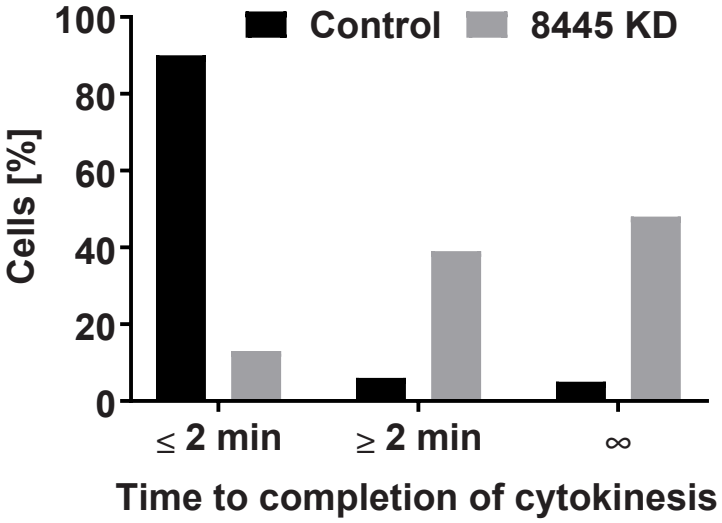
Control
8445 KD
100
80
60
40
20
0
Cells [%]
≤ 2 min
≥ 2 min
∞
Time to completion of cytokinesis

Figure 2

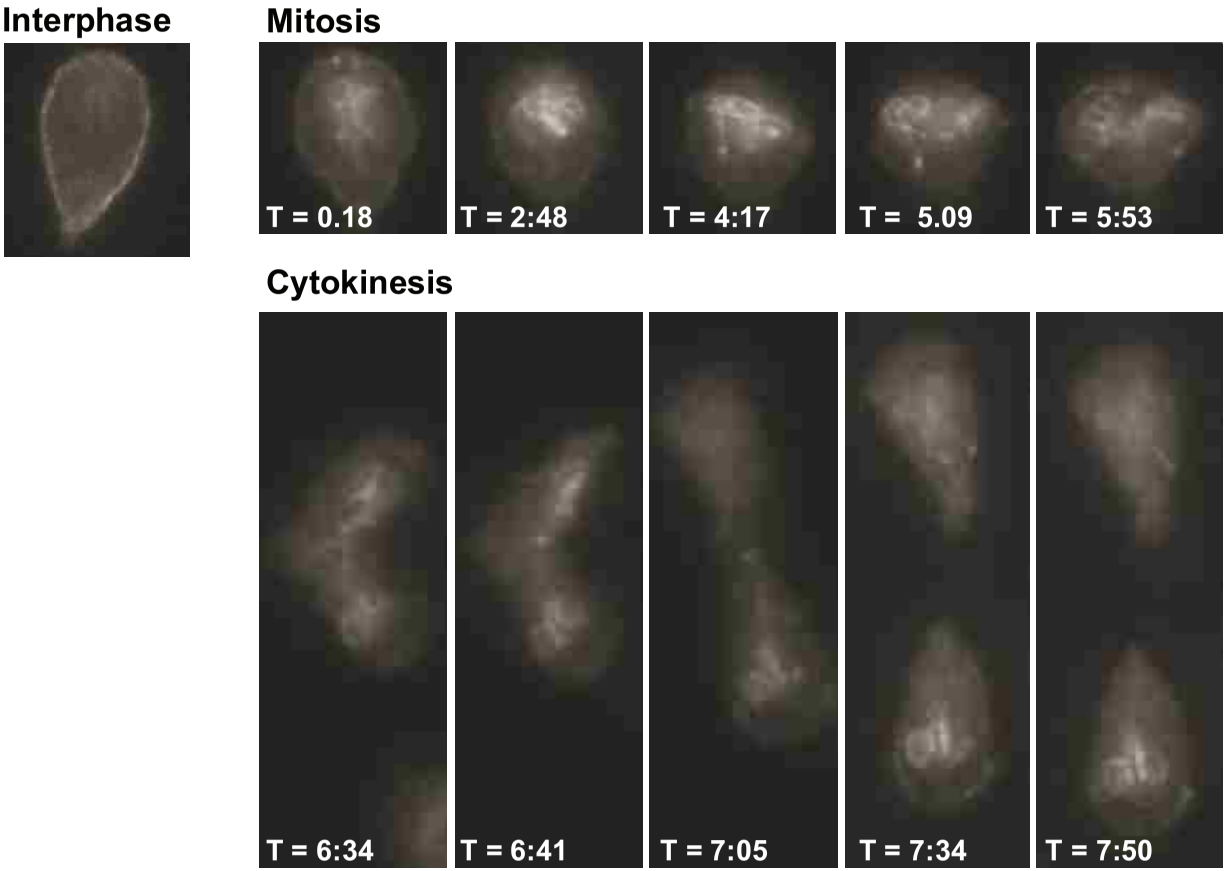
Interphase
Mitosis
T = 0.18
T = 2:48
T = 4:17
T = 5.09
T = 5:53
Cytokinesis
T = 6:34
T = 6:41
T = 7:05
T = 7:34
T = 7:50

Figure 3

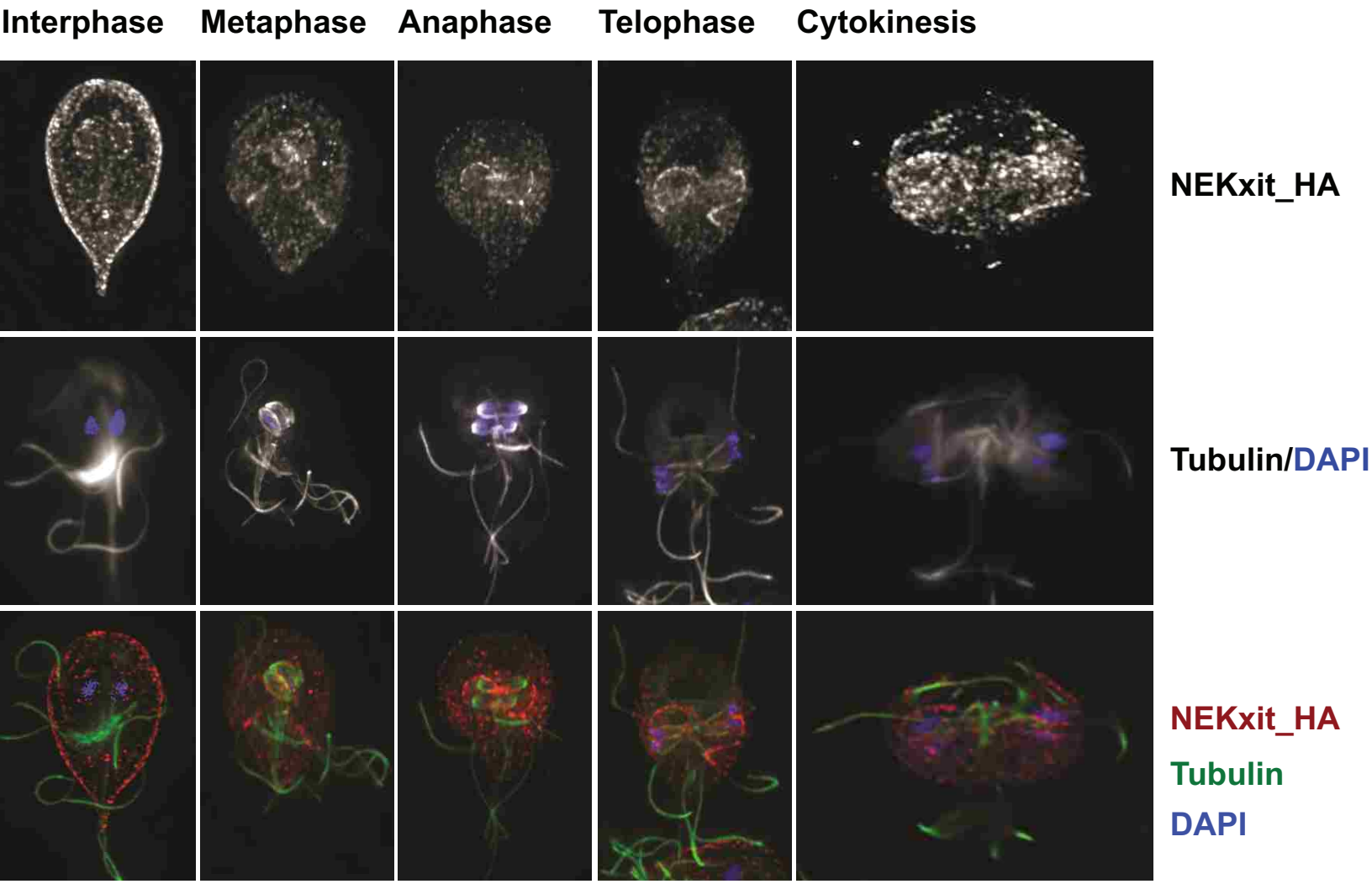
Interphase
Metaphase
Anaphase
Telophase
Cytokinesis
NEKxit_HA
Tubulin/DAPI
NEKxit_HA
Tubulin
DAPI

Figure 4

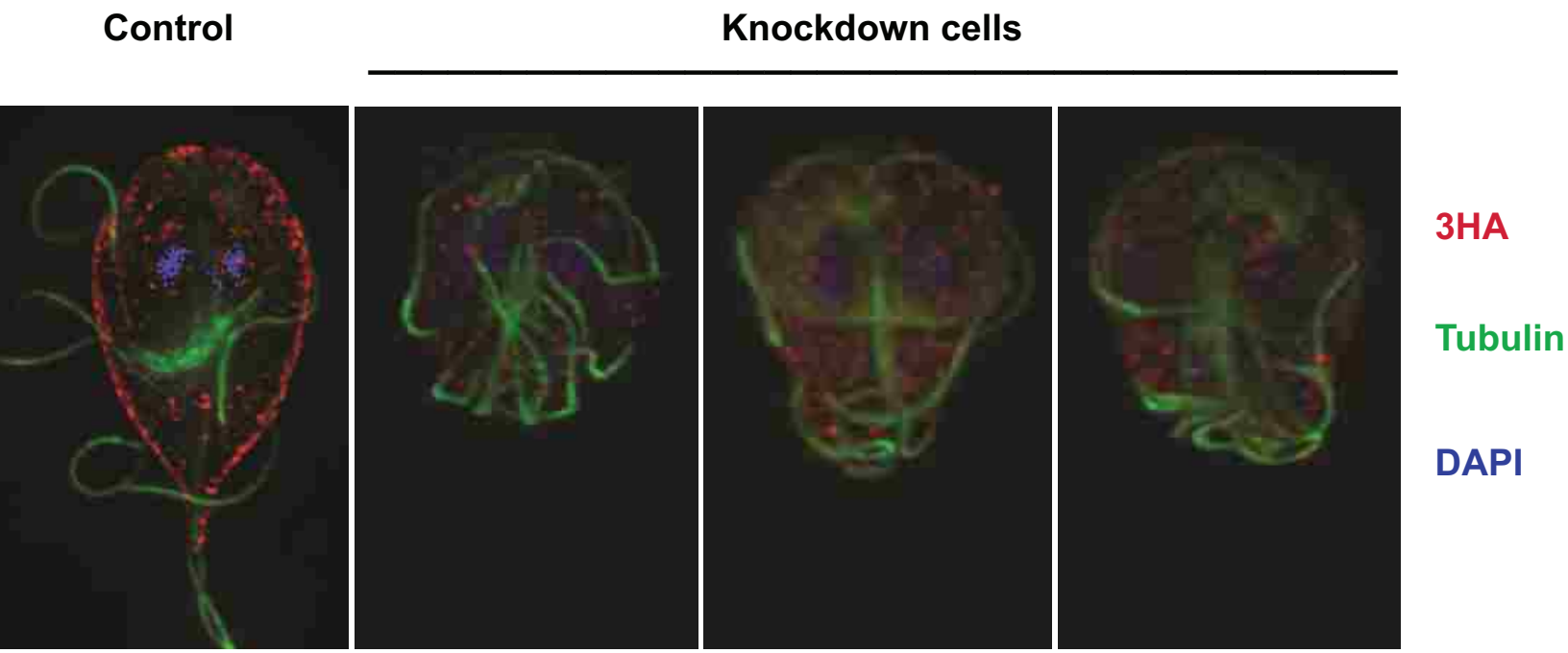

Figure 5

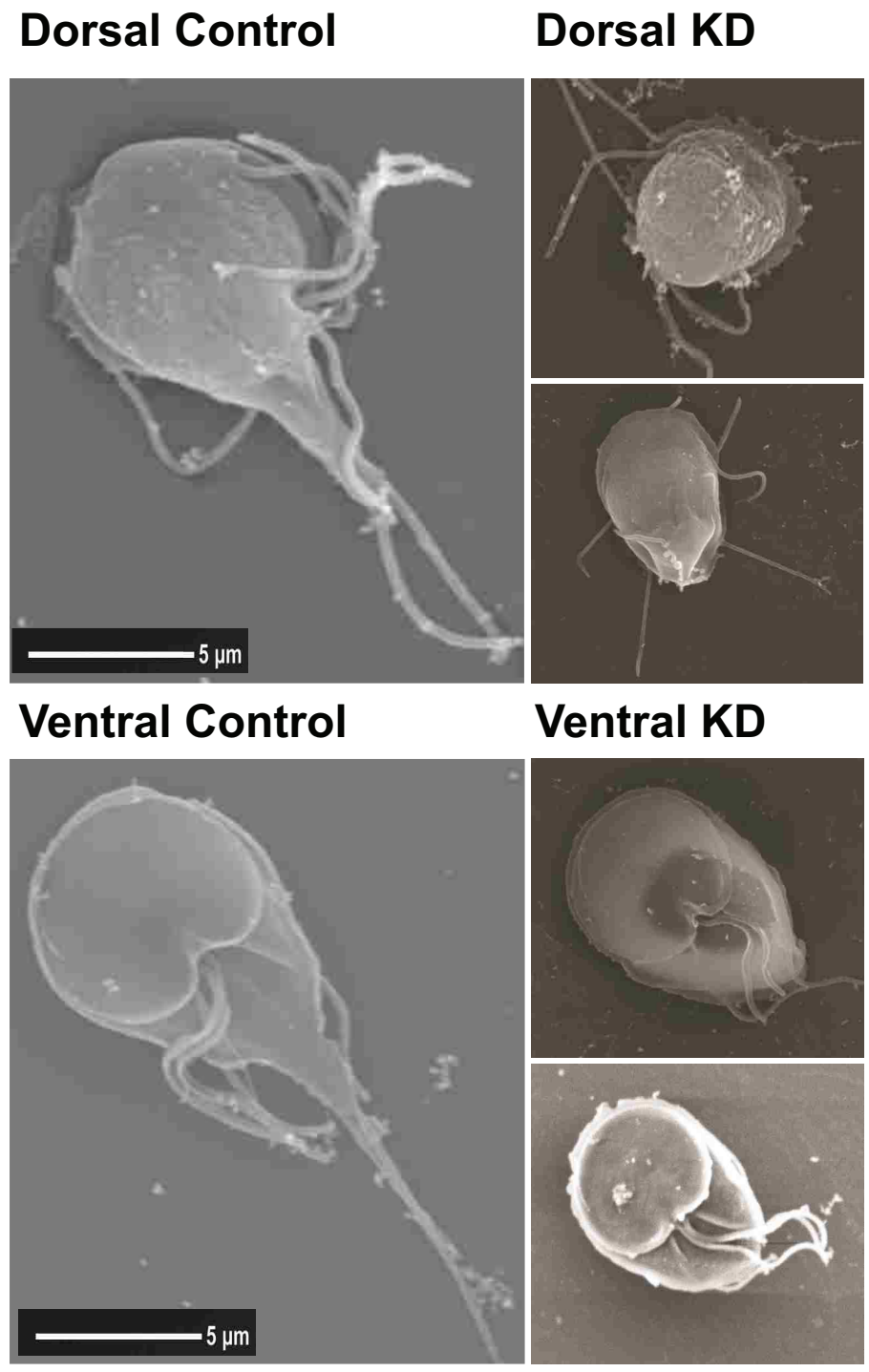
Dorsal Control
Dorsal KD
5 µm
Ventral Control
Ventral KD
5 µm

Figure 6

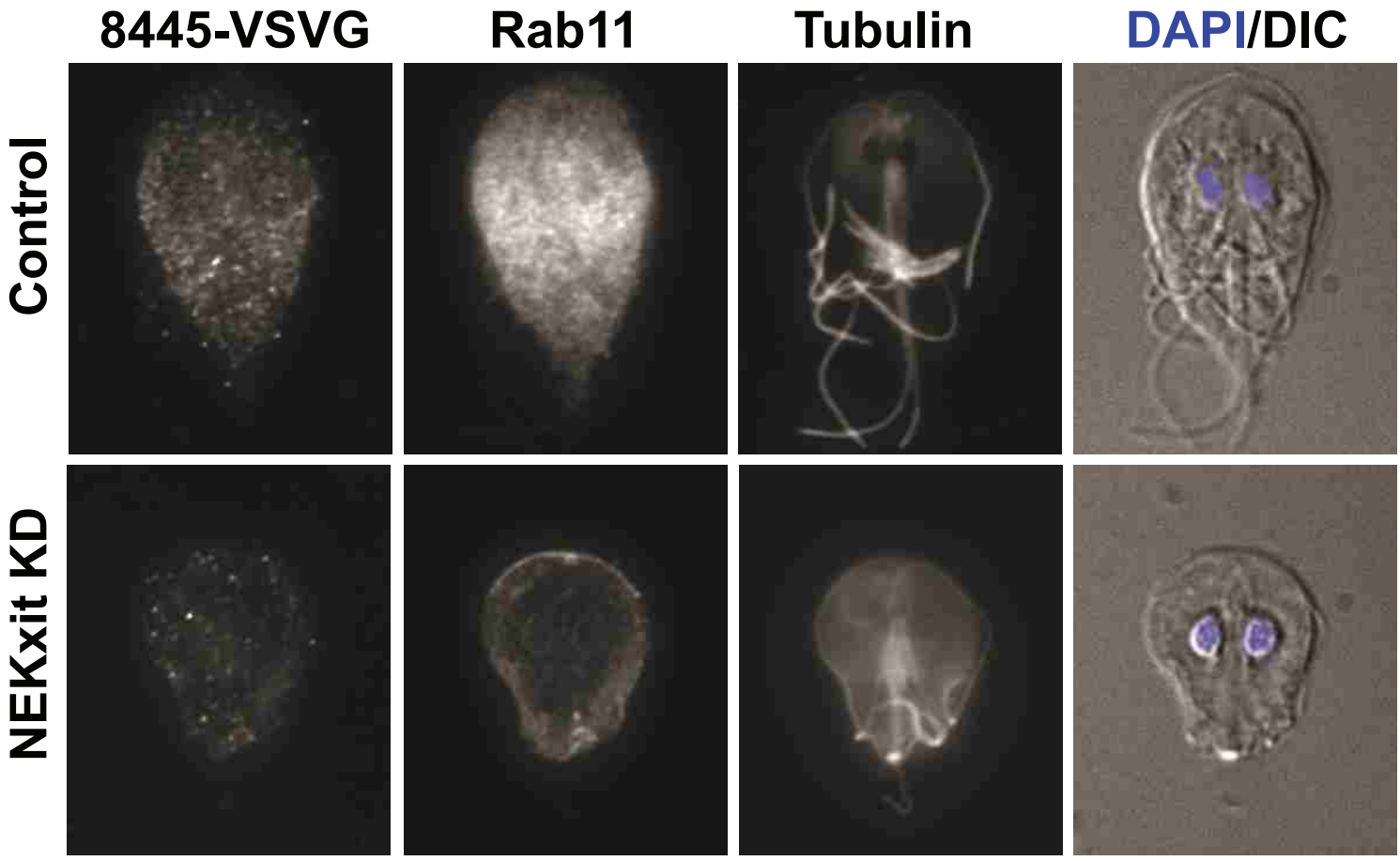
8445-VSVG
Rab11
Tubulin
DAPI/DIC
Control
NEKxit KD

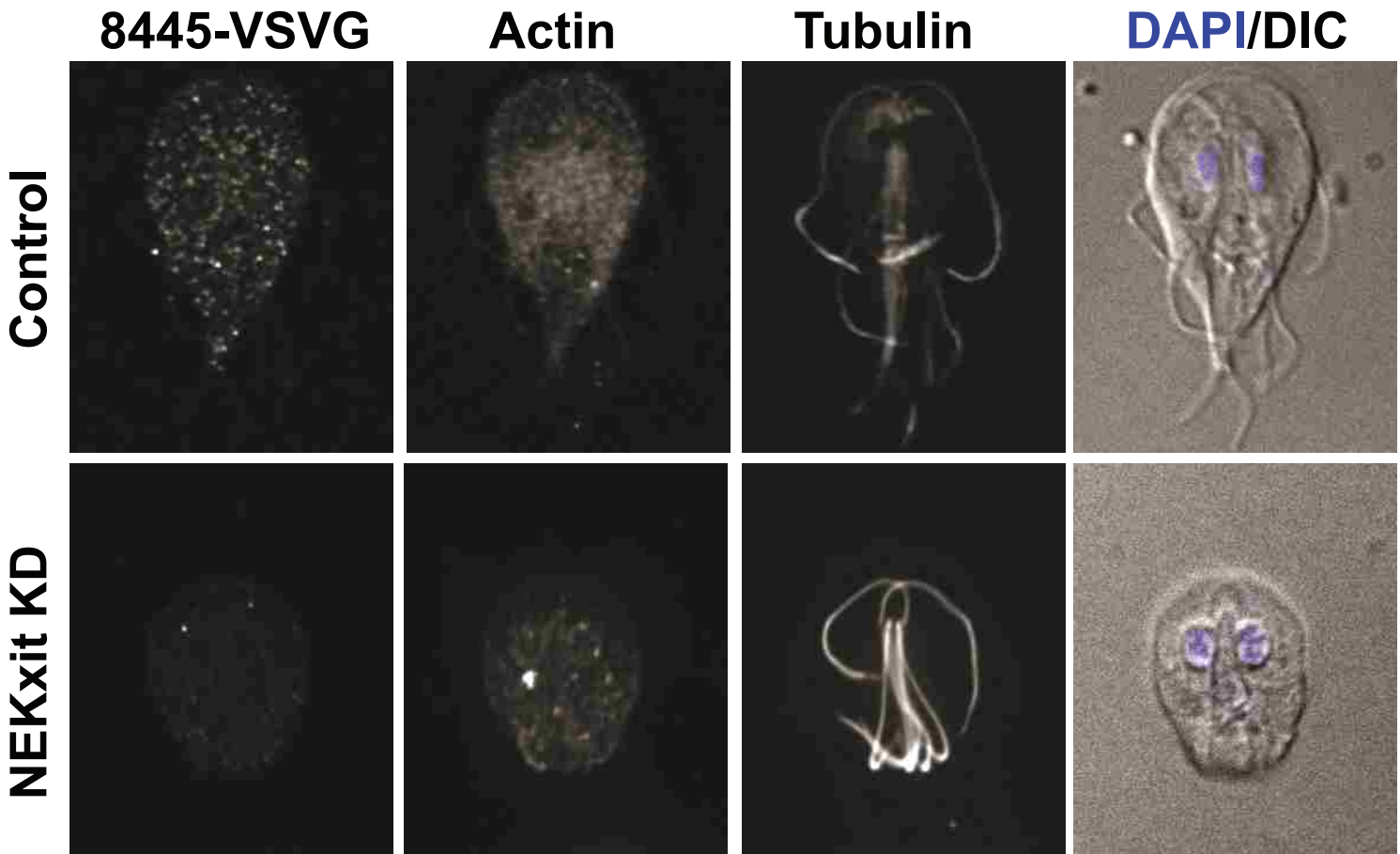
8445-VSVG
Actin
Tubulin
DAPI/DIC
Control
NEKxit KD

Figure 7

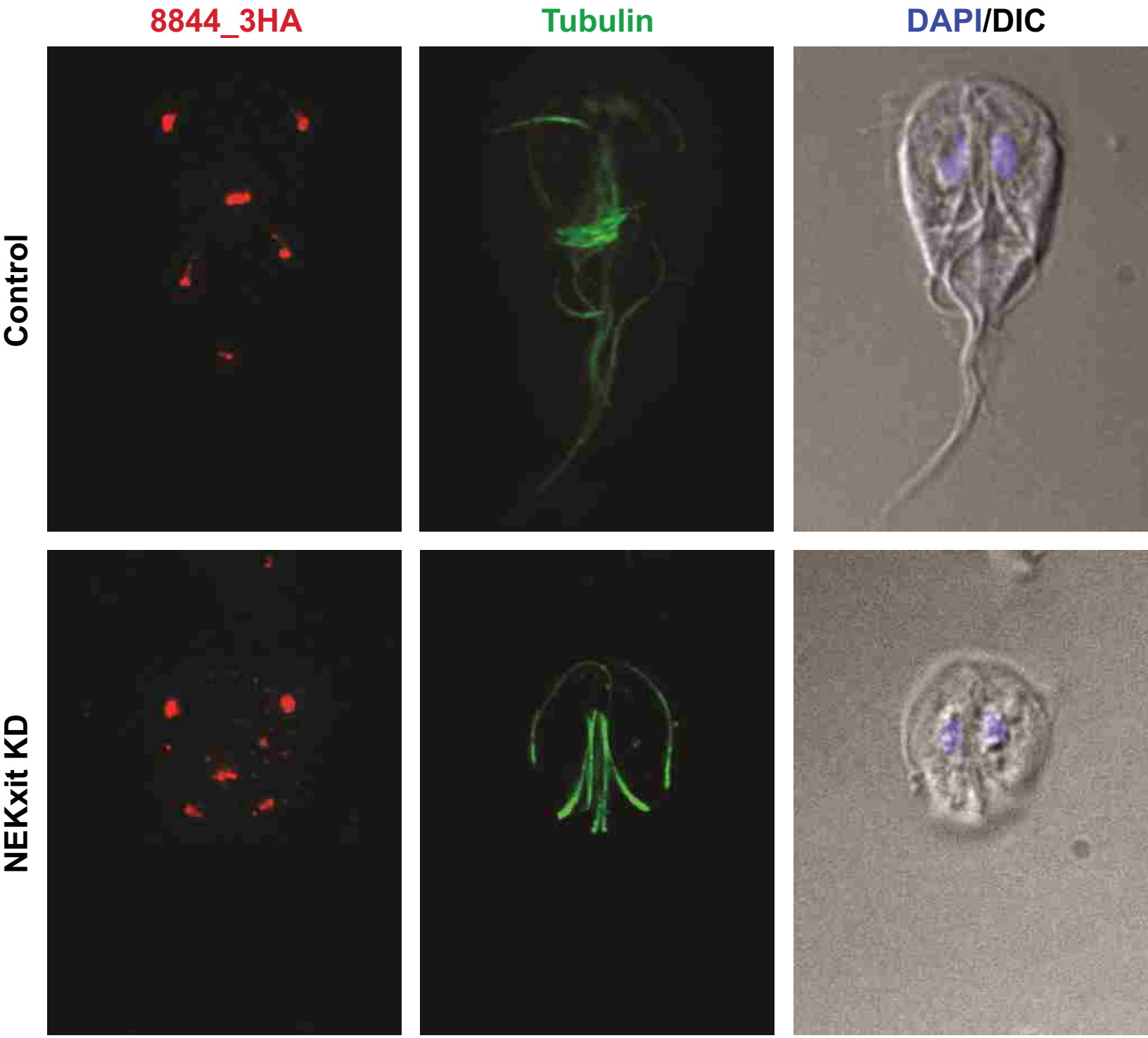

CHAPTER 4: Screening of the Pathogen Box for inhibitors with dual efficacy against *Giardia lamblia* and *Cryptosporidium parvum*

Screening of the Pathogen Box for inhibitors with dual efficacy against *Giardia lamblia* and *Cryptosporidium parvum*

Kelly M. Hennessey[a], Ilse C. Rogiers[b,c], Han-Wei Shih[a], Matthew A. Hulverson[b], Ryan Choi[b], Molly C. McCloskey[b], Grant R. Whitman[b], Lynn K. Barrett[b], Ethan A. Merritt[d], Alexander R. Paredez[a*] and Kayode K. Ojo[b*]

[a]Department of Biology, University of Washington,
Seattle, Washington, 98195 United States of America
[b]Department of Medicine, Division of Allergy and Infectious Disease,
Center for Emerging and Re-emerging Infectious Disease (CERID),
University of Washington, Seattle, Washington 98109 United States of America
[c] Faculty of Pharmaceutical, Biomedical and Veterinary Sciences,
University of Antwerp, Antwerp, Belgium
[d]Department of Biochemistry, University of Washington,
Seattle, Washington, 98195 United States of America

[*]ojo67kk@u.washington.edu (KKO); aparedez@uw.edu (ARP)

***Keywords*:** Pathogen box; *Cryptosporidium* spp*; Giardia lamblia;* bioluminescent assay; high-throughput screening

Abstract

There is a need for efficient cell-based assays amenable to high-throughput drug screening (HTS) against *Giardia lamblia*. Here, we report the development of a screening method utilizing *G. lamblia* engineered to express red-shifted firefly luciferase. Parasite growth and replication were quantified using D-luciferin as a substrate in a bioluminescent read-out platform. This HTS assay was validated for reproducibility and reliability against the Medicines for Malaria (MMV) Pathogen Box compounds. For *G. lamblia,* 43 compounds (10.75 %) were identified with ≥75% inhibition of cell growth at 16 μM, of which 15 (3.75%) showed ≥95% inhibition and were selected for experimental analysis to determine effective concentrations causing 50% growth inhibition (EC_{50}). The Pathogen Box was also screened against Nanoluciferase expressing (Nluc) *C. parvum*, yielding 85 compounds (21.25 %) that had ≥75% cell growth inhibition at 10 μM, from which 6 (1.5%) with ≥95% inhibition were selected for EC_{50} determination. Compounds with EC_{50} ≤5 μM and no discernible cytotoxicity on mammalian HepG2 cells were deemed potent hits. Sixteen compounds are dual hits with ≥75% initial growth inhibition against both parasites, with 13 further analyzed to determine the EC_{50}s against both parasites and mammalian HepG2 cells. Seven of the thirteen compounds (1.75%) inhibited both parasites at ≤5 μM. Three of the 7 dual hit molecules shared no obvious chemical similarity with any previously characterized anti-parasite drugs and offer new medicinal chemistry opportunities for therapeutic development. Our results suggest that the bioluminescent assay is suitable for large-scale screening of chemical libraries against both *C. parvum* and *G. lamblia*. Moreover, this screen found molecules with dual-specificity, which may provide opportunities to treat both giardiasis and cryptosporidiosis in co-infections.

Introduction

Cryptosporidium and *Giardia* are widely acknowledged as significant waterborne pathogens, as both are major contributors to global health burden of diarrheal diseases in children under the age of five[1,2]. The parasites replicate in the small intestines of vertebrate hosts and divide to colonize the intestines, which could result in loss of intestinal surface area with an impairment of the host's ability to effectively absorb necessary nutrients[3–5]. Young children can suffer physical stunting and wasting, cognitive impairment and fine motor movement problems[6].

Cryptosporidium infections become chronic and fatal in AIDS and immune compromised patients[7–10]. Infection is caused by ingestion of environmentally resistant infective stages, called cysts (*G. lamblia*) or oocysts (*C. parvum*), upon passage in the feces[11]. Ingestion of as few as 10 cysts or oocysts can lead to clinical episodes[12–14]. Current treatments for giardiasis include metronidazole and chemically related nitroimidazole drugs. However, up to 20% of clinical presentations are resistant to these treatments[15,16]. Nitazoxanide is the only FDA-approved therapy for cryptosporidiosis. However, nitazoxanide has shown little efficacy in immunocompromised patients[17] and is not approved for use in children under the age of 1[18]. Consequently, there is an increasing need to develop alternative drugs for cryptosporidiosis and giardiasis[5].

Methods to accelerate drug discovery by high-throughput screening of large chemical libraries will require development of robust new assay platforms that provides reliability, sensitivity, easily observable readouts and are both cost and time efficient. A bioluminescent assay that fits these criteria for high-throughput drug screening of inhibitors against *C. parvum* was recently described[19,20]. Screening of molecules against *G. lamblia* parasites previously involved microscopic counting of parasites[21], or utilizing a coulter counter[22] both of which

required manual counting of each well in an assay plate. A semi high-throughput assay based on automated image analysis by cell stained-DAPI signal read-out has also been explored[23]. Most recently, a digital phase-contrast microscopy morphology-based assay method with enumeration by software was developed, which has no need for any cell staining[24]. The morphology-based assay is comparable to the previously reported DAPI stain method, but it relies solely on expensive software to identify and count parasites based on size and morphology[23,24]. Stable expression of Escherichia coli *b*-glucuronidase A (GusA) as a reporter gene for *Giardia lamblia* growth measurement was earlier described as suitable for high throughput drug screening[25]. Other methods such as qRT-PCR or ELISA are less amenable for high-throughput analysis.

The development of an efficient bioluminescent assay used to measure growth inhibition of *G. lamblia* trophozoites for drug screening assays is described here. This bioluminescent assay signal was achieved by engineering a *G. lamblia* strain to express a firefly red-shifted luciferase PpyRE9h gene integrated into an intergenic region flanked by GL50803_17200 and GL50803_93938 on chromosome 5. Expression of PpyRE9h gene was driven using the β-Tubulin promoter.

The Pathogen Box (www.pathogenbox.org; MMV, Geneva, Switzerland) was screened against the transfected *G. lamblia* cells to show the value of the new bioluminescent assay for high-throughput screening. The Pathogen Box is a set of 400 molecules directed to a variety of "neglected disease" pathogens, including malaria, tuberculosis, helminths, kinetoplastids, *Cryptosporidium*, *Toxoplasma*, and dengue, as well as 26 reference molecules that are known bioactives against the aforementioned pathogens. These molecules are generally not characterized fully by molecular target, but rather represent reconfirmed hits with at least a 5X safety index between the pathogen EC_{50} and mammalian cells CC_{50}.

The power of the Pathogen Box is that the molecules are expected to be screened biochemically and phenotypically by hundreds of labs and the information made available to the entire scientific community. Recently, a major screening paper based on MMV's Malaria Box compared data available from over 60 laboratories[26]. This open source science helps investigators select molecules with the best biological activity, safety, and pharmacokinetic properties for further investigation. The Pathogen Box has not been screened against *G. lamblia*, nor have all the compounds been screened against *C. parvum,* to date. Pathogen Box screening was done in parallel for both *G. lamblia* and *C. parvum*, in an attempt to find potential dual pathogen-inhibiting molecules.

Materials and methods

Chemical inhibitors

The Pathogen Box (MMV), molecules were obtained as 10 mM DMSO stocks and stored at -20 °C. Metronidazole, a commercially available drug, was included in the study as a preliminary control of the assay while quinacrine was used in cytotoxicity screening.

G. lamblia parasite culture

Giardia lamblia (WBC6, ATCC 50803) trophozoites were grown in TYI-S-33 medium supplemented with 10% bovine serum and 0.05 mg/mL bovine bile[27]. Cultures were incubated at 37°C.

G. lamblia expression construct, electroporation and selection of luciferase expressing parasite strains

Primers used to generate the *Giardia* transfection construct are listed in Table 1. The expression plasmid (pBetaTubulinPro::PpyRE9h::BetaTubulin3'UTR/pPAC-integ) was constructed by

cloning the PpyRE9h luciferase gene downstream of a *β*-Tubulin promoter.

First, the entire open reading frame of the RE9hum (thermostable red-shifted firefly luciferase *PpyRE9h*) was digested from the parent plasmid vector pTRIX2-RE9h using XbaI and BamHI. The RE9hum fragment, representing the 2.8 kb region, was amplified and subcloned into mNeonGreen-C18-β-tubulin[28] after excising the tubulin gene and mNeonGreen with NcoI and BamHI and digesting the amplicon with the same enzymes forming pβTub::PpyRE9h::βTub3'UTR. The pβTub::PpyRE9h::βTub3'UTR fragment was amplified using Phusion High-fidelity DNA polymerase (Thermo Fisher Scientific, Rockford, IL); and cloned into pPacV-integ digested with EcoRI and PmlI, using Gibson cloning. The vector pβTub::PpyRE9h::βTub3'UTR/pPacV-integ was used to integrate into chromosome 5 by homologous recombination[29].

For integration, 30 µg of pβTub::PpyRE9h::βTub3'UTR/pPacV-integ was linearized with SwaI overnight, precipitated with ethanol and incubated with 300 µL of chilled *G. lamblia* cells (~$13x10^6$/ml) for 30 minutes before electroporation (Bio-Rad GenePulser X at 375 V, 1000 uF, 750 ohms). After electroporation, cells were incubated on ice for 10 minutes before being transferred to fresh media at 37 °C. Transfectants were selected with puromycin after overnight recovery, as previously described[30].

Assay parameters determination for *G. lamblia*

To determine optimal D-luciferin (Gold BioTechnology Inc., St. Louis, MO) concentration, substrate was serially diluted 1:2 in PBS from 100 mg/mL to 0.052 mg/mL. Parasite numbers were kept constant at 50,000 cells/mL in a volume of 250 µL per well. Plates were incubated for 30 minutes at 37 °C on a plate shaker. Wild-type *G. lamblia* (non-luciferase expressing) was used as a control.

To determine the optimal parasite concentration, an initial cell concentration of ~$1x10^6$ cells/mL was serially diluted 1:2, to a minimum concentration of ~500 cells/mL. Luminescence was measured at 20, 30 and 40 minutes in white, polystyrene, flat bottom 96-well plates (Corning Incorporated, Kennebunk, ME) on an EnVision plate reader (PerkinElmer, Waltham, MA).

EC_{50} preliminary- and in vitro compound screening assay for *G. lamblia*

Preliminary EC_{50} assays were performed on the luciferase expressing and wild-type (control) *G. lamblia* cells to establish a correlation between manually counted cells and the bioluminescent signal read out. Trophozoites were harvested by chilling cultures on ice for 30 minutes and plated by adding 150 µL per well at a concentration of 250,000 cell/mL. Metronidazole was used as a control and was serially diluted 1:2 from 10 µM to 0.009 µM and 150 µL was added to the 150 µL of the *G. lamblia* trophozoites. Plates were covered in plastic low-evaporation lids, sealed in individual anaerobic BD GasPak Bio-Bags (Becton Dickinson, San Jose, CA) and incubated at 37 °C for 24 hours. Plates were then iced for 30 minutes before 250 µL of thoroughly resuspended cells were transferred to a 96-well plate and 50 µL of 10 mg/mL D-luciferin was added to a final reaction concentration of 1.67 mg/mL. Plates were incubated on a plate shaker at 37 °C for 30 minutes and read on an EnVision Plate Reader. A duplicate plate was concurrently set up and assayed using a MOXI Z Mini Automated Cell Counter Kit (Orflo, Ketchum, ID). Results obtained from the bioluminescence assay and the MOXI counter data were compared to evaluate their correlation to one another.

Pathogen Box molecule screening

The 400 compounds in the Pathogen Box were initially screened against the bioluminescent

strain of *G. lamblia* in duplicate at 16 μM as described in section 2.5. Further experiments were carried out to determine the EC_{50} values of molecules that were found to have >95% inhibition of *G. lamblia* cell growth after the initial screen. Compounds were serially diluted 1:2 starting at an initial concentration of 8 μM to a final 0.015 μM. *C. parvum* screening against the Pathogen Box compounds was performed as previously described using a concentration of 10 μM[20]. *C. parvum* EC_{50} assays were performed against compounds found to be hits against both *G. lamblia* and *C. parvum* in the initial screens and compounds that were found to have >95% inhibition against *C. parvum* at 10 μM. Mammalian cell cytotoxicity assays were performed on HepG2 cells as previously described[31].

Statistical analysis

The data was analysed in Microsoft Excel and Prism 7 software (GraphPad Software, San Diego, CA). A nonlinear regression sigmoidal dose-response curve fit was applied to dose-response data for both half maximal effective concentration and half maximal cytotoxic concentrations.

Results

***G. lamblia* assay optimization**

Wild-type *G. lamblia* cells were transfected with pβTub::PpyRE9h::βTub3'UTR/pPacV-integ (Fig. 1), selected clones express red-shifted firefly luciferase *PpyRE9h* as validated by detectable bioluminescence signals when incubated with serial concentrations of D-luciferin in parallel to the wild-type strain (Fig. 2a). Optimum luminescence was achieved after 30 minutes of incubation with D-luciferin (Fig. 2b). The optimal concentration of D-luciferin was determined to be 1.67 mg/mL, as bioluminescence signals plateaued at this concentration within 30 minutes (Fig. 2b) demonstrating no reasonable need for higher concentrations. The bioluminescence

signal saturation was not abated nor augmented with either ATP or magnesium supplementation of the reaction (data not shown). The amount of red-shifted firefly luciferase-driven bioluminescence activity was proportional to the number of viable transfected *G. lamblia* parasites per well, as determined by a comparative analysis with direct cell count of both the wild type and transfectant strains (Fig. 2c). Considering *G. lamblia's* doubling time of 8 hours[28], the optimal starting concentration of cells to achieve the highest bioluminescent signal was determined to be ~250,000 cells/mL, as this would result in an ending concentration of $>10^6$ cells/mL after 24-hours of growth (Fig. 2d).

Assay condition validation with metronidazole

A preliminary experiment to determine the reliability of the bioluminescence-based *G. lamblia* assay for drug inhibitory activities was performed using metronidazole. The metronidazole EC_{50} values obtained bycell counting (EC_{50} = 1.06 μM, SE = 0.06) and the luciferase-based assay (EC_{50} = 1.09, SE = 0.07) are within the acceptable range for experimental errors. These EC_{50} values confirmed the reliability of the luminescence signal-based assay as compared to previous cell counting methods. Furthermore, the experimentally derived EC_{50} value for metronidazole using this new assay tracts with previously documented literature values 1.5 μM[32] and 1.227 μM[33].

Initial screening hits and EC_{50} against *Giardia* and *Cryptosporidium*

The screening of the Pathogen Box against *G. lamblia* led to the identification of 43 compounds (10.75%) with ≥75% inhibition of cell growth, among which 22 (5.5%) showed ≥90% and 15 (3.75%) compounds showed ≥95% inhibition at 16 μM (Supplemental Table S1 and Table 2). Of the 400 molecules, 104 (30.75%) showed ≥50% inhibition at 16 μM against *Giardia* and were considered as hits (Supplementary Table S1). EC_{50}s values were determined for the 15 molecules

with ≥95% inhibition at 16 μM, and ranged from 0.5 to >10μM (Table 2).

The Pathogen Box screening yielded 184 compounds (46%) with >50% inhibition at 10 μM, against *C. parvum* and 85 compounds (16.25%) with ≥75% cell growth inhibition at 10 μM (Supplementary Table S1). Twenty-five (6.25%) of these showed ≥90% inhibition and 19 (4.75%) showed between 90 and 95% inhibition. Six compounds (1.5%) with cell growth inhibition ≥95% were tested to determine their EC_{50} values against *C. parvum* (Table 3).

Of the 400 Pathogen Box molecules, there were 16 (4%) molecules with activity against both parasites at the ≥75% inhibition (Table 4). Three molecules were dropped from further consideration due to HepG2 cytoxicity data from MMV. EC_{50} analysis was performed for the remaining 13 compounds. Seven molecules with EC_{50} values of ≤5 μM and no discernible cytotoxicity (in HepG2 > 10-fold of the observed EC_{50} value) were deemed potent dual hits. Previously described anti-giardia and/or anti-cryptosporidiosis drugs auranofin[23,34], nitazoxanide[35], nifurtimox[36], and clofazimine[35]were found as hits in the screen. EC_{50} values for *C. parvum* Pathogen Box hits range from 0.31 μM to >10 μM (Table 4).

Discussion

Despite the significant health impact of giardiasis and cryptosporidiosis, research into new drug treatments is just slowly beginning to move ahead promising strategies and new drug leads[37]. The potential for devastating consequences of giardiasis and cryptosporidiosis in immunocompromised patients and malnourished children emphasizes the need for an effective therapy that could potentially cure a dual pathogen infection or be used syndromically. An important step towards this goal is the use of HTS to identify compounds as potential hits to develop as leads. A recently described bioluminescence assay[19,20] effectively solved this problem

for *C. parvum*. However, challenges for giardiasis drug development have included the lack of an effective HTS method that provides reliable and reproducible results.

ATP-based screening in *G. lamblia* was previously described[36]. This assay employed ATP lite; a Luminescence ATP Detection System (Perkin Elmer) that requires a cell lysis step and exogenous supplementation of the reaction mixture with luciferase protein and D-luciferin in a well-controlled pH environment, to ensure no endogenous ATP degrading enzyme activity. The engineered luciferase expressing *G. lamblia* strain described here employs the same principle. However, it has the additional advantage of neither requiring a lysis step nor exogenous luciferase supplementation since this *G. lamblia* strain constitutively expresses the luciferase needed for the read out, thereby reducing the resources needed for screening.

We have shown here that the engineered *Giardia* strain PpyRE9h-Tub is an effective tool for phenotypic screening of compounds with potential anti-giardia activity. The bioluminescence measurement provided by this strain offer similar efficiency when adapted HTS as the previously described GusA *G. lamblia*[25]. It however has additional benefit for a broader range of assays, in particular for non-invasive imaging of parasite load in *Giardia*-infected animals[19,20,38]. For the broader applicability, additional properties of the reporter strain are desirable. In particular the luciferin signal efficiency should remain constant over the time course of infection both in *in vitro* and animal models of infection, ideally without concurrent administration of a second compound such as puromycin to maintain selective pressure. Evidence of stable expression of the luciferase reporter over the course of 3 weeks without puromycin selection is presented in Figure ABCD. Our on-going work to address this in animal model of infection will be reported separately. Nonetheless, comparative analysis showed that the luciferase-based assay described here has a high level of reliability and reproducibility based on the assay of a known standard

drug, metronidazole, and determination of EC_{50} values for selected hits from the Pathogen Box screening. Furthermore, EC_{50} values obtained using the new assay platform are very similar to that obtained for the wild-type *G. lamblia* strain and available literature-based comparisons (Table 3). This assay also overcomes the limitation of drug screening platforms that rely on assessment of parasite numbers, but disregard viability of the cells[5,23,24] since only viable cells can produce the ATP required for the D-luciferin reaction.

However, a limitation of the luminescence screening platform includes less efficient parasite growth in volumes lower than 300 µL per well, due to *G. lamblia*'s surface area to volume requirement. Lower reaction volume seems to result in higher oxygen exposure during handling that prevent optimum cell replication[32]. The luciferase assay is further constrained by only detecting the bioluminescent signal, while the digitalized methods, using DAPI or phenotypical recognition, both have potential for retrospective analysis of cytology[24]. However, this could be more appropriately re-evaluated further downstream during drug development. Conversely, the set-up of the assay as described here includes a relatively high inoculum size incubated for a day. This may have the disadvantage of missing compounds with a slower mode of action which may explain that reference compounds with known efficacies against *G. lamblia* such as mebendazole (MMV003152) and pentamidine (MMV000062) do not show up in the screening with the luciferase staining. This can be remedied with a set-up using lower inoculum sizes for a longer incubation time. The bioluminescent assay is precise, efficient, less time-consuming and inexpensive method for high-throughput screening that does not require counting, staining, nor lysis and can be further used to study efficacy with *in vivo* models of infection[38,39].

The top hits from screening against *G. lamblia* trophozoites (Table 2) include two drugs,

nitazoxanide and nifurtimox, which share the same free-radical mediated mode of action as the current front-line anti-giardiasis drug metronidazole. Both have been previously noted for potential anti-giardiasis use[35,40] (and nitazoxanide has been used against *C. parvum* demonstrating clinical efficacy including a significantly lower mortality rate in one trial (Amadi et al., Lancet 2002). Because these compounds shared their mechanism of action with metronidazole there is a strong potential for cross resistance[35,37].

Delamanid could not be included as a candidate for dual use due to *in vitro* efficacy against *G. lamblia* but not *C. parvum.* Delaminid was developed as an anti-tuberculosis agent that inhibits synthesis of mycolic acid[41]. This target has no reported effect in either gram-negative or gram-positive bacteria nor does it explain any effect on *G. lamblia* [39]. However, its action against *G. lamblia* is likely due to free radicals generated by reduction of the nitroimidazole group[42,43].

Another known drug identified in the screen, iodoquinol, is primarily used for anti-amoebiasis but is also used as an anti-giardial drug, in combination with metronidazole[44]. Iodoquinol appears to have the most potent anti-proliferative effect to the HepG2 cells tested, perhaps reflecting the common side effects seen during treatment. To the best of our knowledge, it had not been used for treatment of cryptosporidiosis, but can be included as a candidate for dual use. Iodoquinol chelates ferrous ions that are essential for metabolism in amoeba. Although Iodoquinol has cytocidal effects, the mechanism of action is not known[45]. Further investigation into the targets of delaminid and iodoquinol in these parasites could show promising leads for new drug discovery program against these pathogens.

The FDA-approved drug auranofin has gained interest with regards to a possible repurposing strategy due to its anti-parasitic activities in *S. mansoni*[46], *T. brucei*[47], *E. histolytica*[48]

and *G. lamblia*[23]. Auranofin is highlighted as a potent hit against *G. lamblia* and *C. parvum* (Table 3), in agreement with literature results (*G. lamblia* EC_{50} = 4-6 μM in[23]; *C. parvum* EC_{50} = 2 μM in[34]).

Auranofin was previously identified as potent against *C. parvum* [34] in screens of potentially re-purposed drugs. The mechanism of action of auranofin mainly consists of inhibiting reduction/oxidation enzymes, thereby damaging pathogens by oxidative stress. However, this is accompanied by the potentially adverse effects of loose stools, abdominal cramping, watery diarrhea, skin irritations, stomatitis, mouth ulcerations and conjunctivitis[49]. Although auranofin showed high cytotoxicity levels (Table 3), it has already entered clinical trials as a possible anti-giardial[50].

Clofazimine is a promising dual treatment option to further explore. Good clinical out-come in experimental models has increased enthusiasm for clofazimine as a potential drug repurposing candidate for the treatment of human cryptosporidiosis[35]. Nonetheless, GI adverse effects for clofazimine[51] have been reported, mainly after long term use[52]. It would be of scientific interest to further study clofazimine's efficacy and safety for treatment of both pathogens, as it is a regulatory approved drug that has been used for over 50 years for leprosy and more recently for the therapy of multi-drug resistant tuberculosis.

The remaining most potent hits (Table 3) share no obvious chemistry with these previously characterized anti-parasitic drugs. Some of them have detectable cytostatic effects on mammalian cells at high concentrations (Table 3). However, three of these have a reasonable safety index (EC_{50} of both parasites/CC_{50} against mammalian cells) for further exploration. Together with three similarly uncharacterized hits retrieved from recent screening of the Malaria Box[24], these constitute a valuable starting point for the development of dual anti-giardiasis and

anti-cryptosporidiosis drugs.

Conclusion

The described bioluminescent assay was optimized and found to be comparable to assays performed with automated cell counters. Reproducibility was validated by comparing known literature EC_{50} values of metronidazole, auranofin, nitazoxanide and nifurtimox, finding all to be within a two-fold difference of our results. This suggests that the described bioluminescent assay can efficiently be used for semi high-throughput drug screening. Furthermore, the found dual-inhibiting compounds are of great public health importance since these could be suitable for co-infections or in situations where the precise diarrheal-causing pathogens cannot be determined. The luciferase-expressing *G. lamblia* strain could also be adapted for *in vivo* experimentation, advancing drug development and screening for *G. lambia* similar to the way that Nluc expressing *C. parvum* has for *Cryptosporidium* [19,20].

Acknowledgement

We wish to thank Evotec and MMV for providing us the Pathogen Box compound library. The authors will like to thank Dr. Wesley C. Van Voorhis for helpful discussions. The PpyRE9h gene plasmid vector pTRIX2-RE9h was a kind gift from Dr. Bruce Branchini of Connecticut University (USA). The study was supported by the National Institute of Allergy and Infectious Diseases (USA) and National Institute of Child Health and Human Development of the National Institutes of Health (USA) under the award numbers R01AI089441, R01AI111341, R01GM086858 and R01HD080670.

Figure legends

Fig. 1: Schematic of targeting vector and homologous recombination. The expression cassette contains pGDH::Puro Res and pβTub::PpyRE9h:: β3'TubUTR was used for homologous recombination to target a genomic intergenic region which is flanked with GL50803_17200 and GL50803_93938. After electroporation, puromycin was used to select for transfected cells. LB=left border, pGDH=Promoter of glutamate dehydrogenase (GL50803_21942), Puro Res= puromycin N-acetyltransferase, pβTub=β tubulin promoter, PpyRE9h= red-shifted luciferase coding sequence, β3'Tub UTR= β tubulin 3'UTR, RB= right border.

Fig. 2: Assay parameters determination. A. D-luciferin concentration in relation to RLU. Serial concentration of D-luciferin relative to the wild-type strain to determine the optimal concentration of D-luciferin to use in assays. The reaction was carried out for 30 min. The line shows the RLU data-points at 10 mg/ml of D-luciferin. (RLU: relative light units). **B.** Optimization of incubation time. D-luciferin concentration in relation to relative light units (RLU) was measured at different time points. **C.** Linear regression of Parasite Concentration and RLU percentage values. The plot showed bioluminescence read out from the wild type strain and the transfectant strain correlating number of cells to RLU. The values of both the luciferase strain and wild-type strain are shown with respective RLU at 30 min. (P-value of luciferase strain < 0.001: Wild-type p = 0.854). **D**. Ideal maximal parasite end concentration determination**.** Comparison of RLU to parasite concentration in WT and transfected *G.lamblia* cells to determine starting concentration of cells. RLU versus parasite concentration helps to determine

the ideal maximal end concentration without overgrowth carrying out the reaction for 30 min. The RLU line shows the data-point at 1,000,000 cells/mL.

Tables

Table 1: Primers used in this study

Primer Name	Nucleotide sequences 5'-3'
RE9-forward	AccatggaatctagaATGGAGGACGCCAAGAACAT
RE9-reverse	TGGATCCtcTTAATTAATCAGATCTTGCCGCCCTTCTTGGCC
pBetaTub-Gib-forward	tctgcaagttaatttttggccCCTAGGTCGGATCAAGACTTCAAATTAGAAA
BetaTubUTR-Gib-reverse	TTATTTGACCATCGTACTTGCAactagtGAGCTCGGTACCAGCTGATCGGCGC

Table 2: Pathogen Box compounds that inhibit growth in *G.lamblia* ≥95% (15)

Common name	MMV Compound ID	*G. lamblia* EC_{50} (µM)	HepG2 (% inhibition at 40 µM)
Nifurtimox	MMV001499	0.64	0
	MMV022478	2.41	0
	MMV028694	3.88	71
	MMV153413	>10	ND*
	MMV495543	2.77	41
	MMV676395	1.57	11
Clofazimine	MMV687800	1.79	83
	MMV687807	0.51	100
	MMV687812	1.25	90
Delamanid	MMV688262	0.55	ND*
	MMV688283	>10	ND*
	MMV688755	1.57	34

	MMV688844	2.3	40
Auranofin	MMV688978	3.74	95
Nitazoxanide	MMV688991	0.8	71

*ND - Not Done

Table 3: High inhibiting molecules with EC_{50} and cytotoxicity information. Shown are compounds that produced ≥95% inhibition of *Cryptosporidium* replication in the initial screen.

Common name	MMV Compound ID	*C. parvum* EC_{50}	HepG2
		(µM)	(% inhibition at 40 µM)
Iodoquinol	MMV676477	0.22	0
	MMV688853	>10	0
	MMV002817	0.48	69
	MMV085499	1.93	0
	MMV019189	2.52	ND*
	MMV102872	0.14	ND*

*ND - Not Done

Table 4: Dual hits against *Giardia* and *Cryptosporidium* above 75% inhibition. EC_{50}: 50% excitatory concentration, CC_{50}: 50% cytotoxicity concentration, % inh: percentage inhibition. **.

Common name	MMV Compound ID	*G. lamblia* EC_{50}	*C. parvum* EC_{50}	HepG2
		(µM)	(µM)	(% inhibition at 40 µM)
Iodoquinol	MMV002817**	2.5	0.5	69
	MMV010576**	1.9	3	69
	MMV024114	>10	>10	ND*
	MMV024406	2	>10	ND*
	MMV028694**	3.9	1.6	71
	MMV675968	>10	2.1	ND*
	MMV676395	1.6	>10	11
	MMV676501**	1.4	5	ND*
	MMV676602	>10	0.3	ND*
	MMV676604	>10	2.9	ND*

Clofazimine	MMV687800**	1.8	3.3	83
	MMV687807	0.5	ND*	100
	MMV688283	>10	2	ND*
Auranofin	MMV688978 **	3.7	3.3	95
Nitazoxanide	MMV688991**	0.8	3.1	71

*ND - Notdone; **dual hits

References

1. Donowitz JR, Alam M, Kabir M, Ma JZ, Nazib F, Platts-Mills JA, Bartelt LA, Haque R, Petri WA. A Prospective Longitudinal Cohort to Investigate the Effects of Early Life Giardiasis on Growth and All Cause Diarrhea. Clinical Infectious Diseases. 2016;63(6):792–797.

2. Platts-Mills JA, Babji S, Bodhidatta L, Gratz J, Haque R, Havt A, McCormick BJJ, McGrath M, Olortegui MP, Samie A, et al. Pathogen-specific burdens of community diarrhoea in developing countries: A multisite birth cohort study (MAL-ED). The Lancet Global Health. 2015;3(9).

3. Halliez MCM, Buret AG. Extra-intestinal and long term consequences of Giardia duodenalis infections. World Journal of Gastroenterology. 2013;19(47):8974–8985.

4. Fletcher SM, Stark D, Harkness J, Ellis J. Enteric protozoa in the developed world: a public health perspective. Clinical microbiology reviews. 2012;25(3):420–49.

5. Checkley W, White AC, Jaganath D, Arrowood MJ, Chalmers RM, Chen X-M, Fayer R, Griffiths JK, Guerrant RL, Hedstrom L, et al. A review of the global burden, novel diagnostics, therapeutics, and vaccine targets for cryptosporidium. The Lancet Infectious Diseases. 2015;15(1):85–94.

6. Bogitsch BJ. Visceral Protozoa II: Flagellates. In: Human parasitology. 2013.

7. Thompson RCA, Olson ME, Zhu G, Enomoto S, Abrahamsen MS, Hijjawi NS. Cryptosporidium and Cryptosporidiosis. In: Advances in parasitology. Vol. 59. 2005. p. 77–158.

8. Feasey NA, Healey P, Gordon MA. Review article: the aetiology, investigation and management of diarrhoea in the HIV-positive patient. Alimentary Pharmacology & Therapeutics. 2011;34(6):587–603.

9. Shirley D-AT, Moonah SN, Kotloff KL. Burden of disease from cryptosporidiosis. Current Opinion in Infectious Diseases. 2012;25(5):555–563.

10. O'Connor R M, Shaffie R KG et al. Cryptosporidiosis in patients with HIV/AIDS. AIDS. 2011;25(5):549–560.

11. Kirkpatrick CE. Feline giardiasis: a review. Journal of Small Animal Practice. 1986;27(2):69–80.

12. DuPont HL, Chappell CL, Sterling CR, Okhuysen PC, Rose JB, Jakubowski W. The Infectivity of *Cryptosporidium parvum* in Healthy Volunteers. New England Journal of Medicine. 1995;332(13):855–859.

13. Okhuysen PC, Chappell CL, Crabb JH, Sterling CR, DuPont HL. Virulence of Three Distinct *Cryptosporidium parvum* Isolates for Healthy Adults. The Journal of Infectious Diseases. 1999;180(4):1275–1281.

14. Busatti HG, Santos JF, Gomes M a. The old and new therapeutic approaches to the treatment of giardiasis: Where are we? Biologics targets therapy. 2009;3:273–287.

15. Farthing MJ. Giardiasis. Gastroenterology clinics of North America. 1996;25(3):493–515.

16. Nabarro LEB, Lever RA, Armstrong M, Chiodini PL. Increased incidence of nitroimidazole-refractory giardiasis at the Hospital for Tropical Diseases, London: 2008-2013. Clinical Microbiology and Infection. 2015;21(8):791–796.

17. Zhang H, Zhu G. Quantitative RT-PCR assay for high-throughput screening (HTS) of drugs against the growth of Cryptosporidium parvum in vitro. Frontiers in Microbiology. 2015;6:991.

18. Fox LM, Saravolatz LD. Nitazoxanide: a new thiazolide antiparasitic agent. Clinical infectious diseases. 2005;40:1173–1180.

19. Vinayak S, Pawlowic MC, Sateriale A, Brooks CF, Studstill CJ, Bar-Peled Y, Cipriano MJ, Striepen B. Genetic modification of the diarrhoeal pathogen Cryptosporidium parvum. Nature. 2015;523(7561):477–80.

20. Hulverson MA, Vinayak S, Choi R, Schaefer DA, Castellanos-Gonzalez A, R Vidadala RS, Brooks CF, Herbert GT, Betzer DP, Whitman GR, et al. Bumped-Kinase Inhibitors for Therapy of Cryptosporidiosis. J Infect Dis. 2017.

21. Fisher BS, Estraño CE, Cole JA. Modeling long-term host cell-Giardia lamblia interactions in an in vitro co-culture system. PLoS ONE. 2013;8(12).

22. Hennessey KM, Smith TR, Xu JW, Alas GCM, Ojo KK, Merritt EA, Paredez AR. Identification and Validation of Small-Gatekeeper Kinases as Drug Targets in Giardia lamblia. PLOS Neglected Tropical Diseases. 2016;10(11):e0005107.

23. Tejman-Yarden N, Miyamoto Y, Leitsch D, Santini J, Debnath A, Gut J, McKerrow JH, Reed SL, Eckmann L. A reprofiled drug, auranofin, is effective against metronidazole-resistant Giardia lamblia. Antimicrob Agents Chemother. 2013;57(5):2029–2035.

24. Hart CJS, Munro T, Andrews KT, Ryan JH, Riches AG, Skinner-Adams TS. A novel in vitro image-based assay identifies new drug leads for giardiasis. International Journal for Parasitology: Drugs and Drug Resistance. 2017.

25. Müller J, Nillius D, Hehl A, Hemphill A, Müller N. Stable expression of Escherichia coli beta-glucuronidase A (GusA) in Giardia lamblia: application to high-throughput drug susceptibility testing. The Journal of antimicrobial chemotherapy. 2009;64(6):1187–91.

26. Van Voorhis WC, Adams JH, Adelfio R, Ahyong V, Akabas MH, Alano P, Alday A, Alemán Resto Y, Alsibaee A, Alzualde A, et al. Open Source Drug Discovery with the Malaria Box Compound Collection for Neglected Diseases and Beyond. PLoS Pathogens. 2016;12(7).

27. Keister D. Axenic culture of Giardia lamblia in TYI-S-33 medium supplemented with bile. Transactions of the Royal Society of Tropical Medicine and Hygiene. 1983;77(4):487–88.

28. William R. Hardina, Renyu Lia, Jason Xub, Andrew M. Sheltona, Germain C. M. Alasa, Vladimir N. Minina B, and Alexander R. Paredeza 1. Myosin-independent cytokinesis in Giardia utilizes flagella to coordinate force generation and direct membrane trafficking. Proceedings of the National Academy of Sciences of the United States of America. 2017;(July).

29. Stefanic S, Morf L, Kulangara C, Regös A, Sonda S, Schraner E, Spycher C, Wild P, Hehl AB. Neogenesis and maturation of transient Golgi-like cisternae in a simple eukaryote. Journal of Cell Science. 2009;122(16):2846–2856.

30. Krtková J, Thomas EB, Alas GCM, Schraner EM, Behjatnia HR, Hehl AB, Paredez AR. Rac regulates Giardia lamblia encystation by coordinating cyst wall protein trafficking and secretion. mBio. 2016;7(4).

31. Huang W, Hulverson MA, Zhang Z, Choi R, Hart KJ, Kennedy M, Vidadala RSR, Maly DJ, Van Voorhis WC, Lindner SE, et al. 5-Aminopyrazole-4-carboxamide analogues are selective inhibitors of Plasmodium falciparum microgametocyte exflagellation and potential malaria transmission blocking agents. Bioorganic and Medicinal Chemistry Letters. 2016;26(22):5487–5491.

32. Gut J, Ang KKH, Legac J, Arkin MR, Rosenthal PJ, McKerrow JH. An image-based assay for high throughput screening of Giardia lamblia. Journal of Microbiological Methods. 2011;84(3):398–405.

33. Cedillo-Rivera R, Munoz O. In-vitro susceptibility of Giardia lamblia to albendazole, mebendazole and other chemotherapeutic agents. Journal of Medical Microbiology. 1992;37(3):221–224.

34. Debnath A, Ndao M, Reed SL. Reprofiled drug targets ancient protozoans: drug discovery for parasitic diarrheal diseases. Gut microbes. 2013;4(1):66–71.

35. Love MS, Beasley FC, Jumani RS, Wright TM, Chatterjee AK, Huston CD, Schultz PG, McNamara CW. A high-throughput phenotypic screen identifies clofazimine as a potential treatment for cryptosporidiosis. PLOS Neglected Tropical Diseases. 2017;11(2):e0005373.

36. Chen CZ, Kulakova L, Southall N, Marugan JJ, Galkin A, Austin CP, Herzberg O, Zheng W. High-throughput Giardia lamblia viability assay using bioluminescent ATP content measurements. Antimicrob Agents Chemother. 2011;55(2):667–675.

37. Miyamoto Y, Eckmann L. Drug development against the major diarrhea-causing parasites of the small intestine, Cryptosporidium and Giardia. Frontiers in Microbiology. 2015;6(NOV):1–17.

38. Pham, J.K., Nosala, C., Scott, E.Y., Nguyen, K.F., Hagen, K.D., Starcevich, H.N., Dawson

SC. Transcriptomic Profiling of High-Density Giardia Foci Encysting in the Murine Proximal Intestine. Front Cell Infect Microbiol. 2017;7(227).

39. Lewis JM, Sloan DJ. The role of delamanid in the treatment of drug-resistant tuberculosis. Therapeutics and Clinical Risk Management. 2015;11:779–791.

40. Nava-Zuazo C, Ch??vez-Silva F, Moo-Puc R, Chan-Bacab MJ, Ortega-Morales BO, Moreno-D??az H, D??az-Couti??o D, Hern??ndez-N????ez E, Navarrete-V??zquez G. 2-Acylamino-5-nitro-1,3-thiazoles: Preparation and in vitro bioevaluation against four neglected protozoan parasites. Bioorganic and Medicinal Chemistry. 2014.

41. Makoto Matsumoto , Hiroyuki Hashizume, Tatsuo Tomishige, Masanori Kawasaki, Hidetsugu Tsubouchi, Hirofumi Sasaki, Yoshihiko Shimokawa MK. OPC-67683, a Nitro-Dihydro-Imidazooxazole Derivative with Promising Action against Tuberculosis In Vitro and In Mice. PLOS Medicine. 2006;3(11):e466.

42. Müller M. Mode of action of metronidazole on anaerobic bacteria and protozoa. Surgery. 1983;93(1 Pt 2):165–71.

43. Edwards DI. Nitroimidazole druge - action and resistance mechanisms I. Mechanisms of Action. Journal of Antimicrobial Chemotherapy. 1993;31(1):9–20.

44. Stark D, Barratt J, Roberts T, Marriott D, Harkness J, Ellis J. A review of the clinical presentation of dientamoebiasis. The American journal of tropical medicine and hygiene. 2010;82(4):614–9.

45. Knight R. The chemotherapy of amoebiasis. Journal of Antimicrobial Chemotherapy. 1980;6(5):577–593.

46. Angelucci F, Sayed AA, Williams DL, Boumis G, Brunori M, Dimastrogiovanni D, Miele AE, Pauly F, Bellelli A. Inhibition of schistosoma mansoni thioredoxin-glutathione reductase by Auranofin. Structural and kinetic aspects. Journal of Biological Chemistry. 2009;284(42):28977–28985.

47. Lobanov A V., Gromer S, Salinas G, Gladyshev VN. Selenium metabolism in Trypanosoma: Characterization of selenoproteomes and identification of a Kinetoplastida-specific selenoprotein. Nucleic Acids Research. 2006;34(14):4012–4024.

48. Debnath A, Parsonage D, Andrade RM, He C, Cobo ER, Hirata K, Chen S, García-Rivera G, Orozco E, Martínez MB, et al. A high-throughput drug screen for Entamoeba histolytica identifies a new lead and target. Nature medicine. 2012;18(6):956–60.

49. Roder C, Thomson MJ. Auranofin: Repurposing an Old Drug for a Golden New Age. Drugs in R and D. 2015;15(1):13–20.

50. Capparelli EV, Bricker-Ford R, Rogers MJ, McKerrow JH RS. Phase I clinical trial results of auranofin, a novel antiparasitic agent. Antimicrob Agents Chemother. 2017;61(e01947-16).

51. Török, E., Cooke, F.J., Moran E. Oxford handbook of infectious diseases and microbiology. 2017;(Second edition).

52. Queiroz RHC, De Souza AM, Sampaio SV, Melchior E. Biochemical and hematological side effects of clofazimine in leprosy patients. Pharmacological Research. 2002;46(2):191–194.

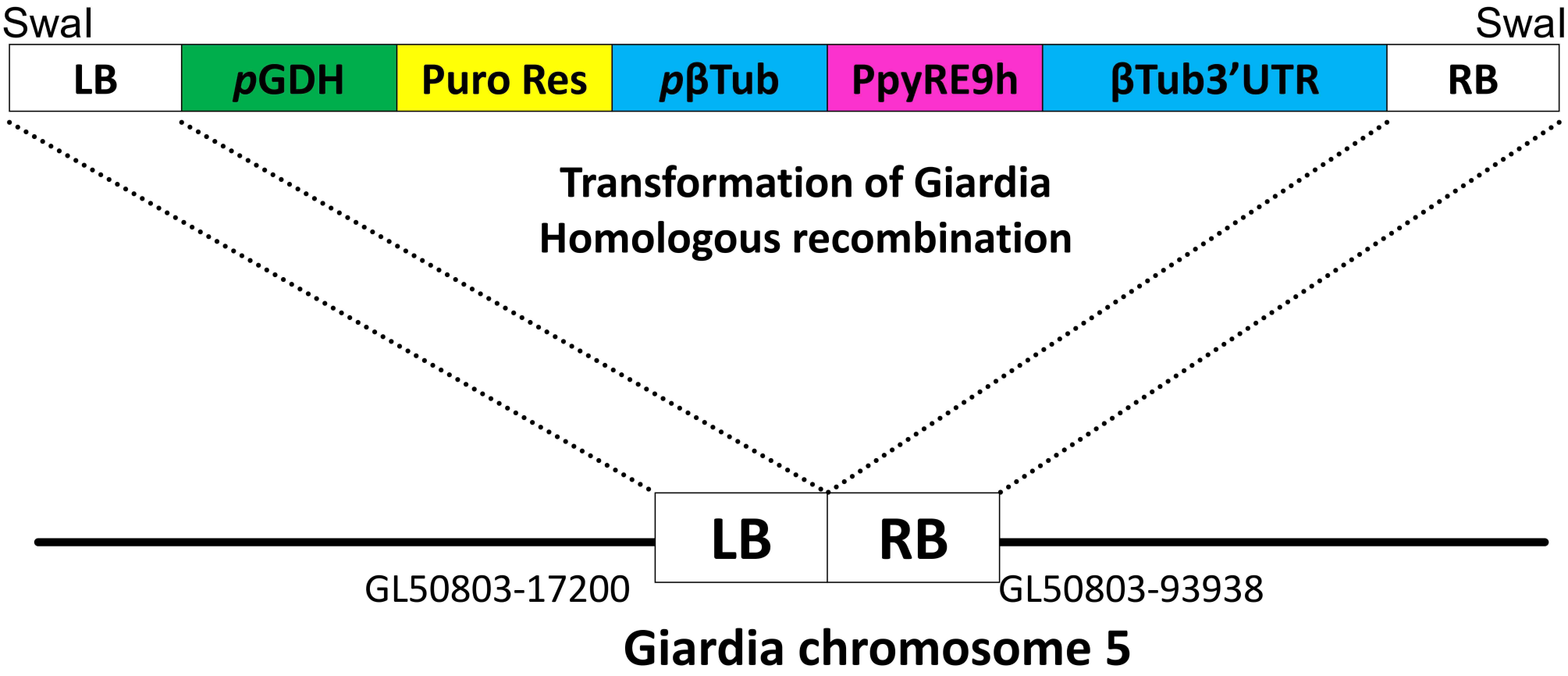
SwaI
SwaI
LB
pGDH
Puro Res
pβTub
PpyRE9h
βTub3'UTR
RB
Transformation of Giardia
Homologous recombination
LB
RB
GL50803-17200
GL50803-93938
Giardia chromosome 5

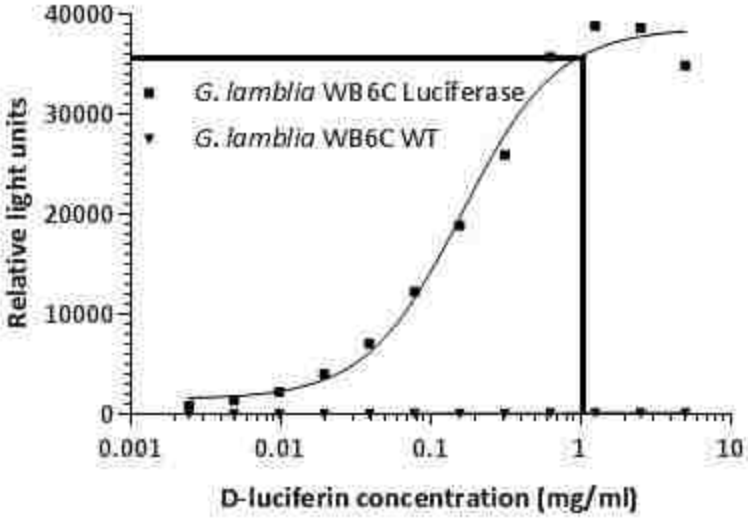
40000
30000
20000
10000
0
Relative light units
G. lamblia WB6C Luciferase
G. lamblia WB6C WT
0.001
0.01
0.1
1
10
D-luciferin concentration (mg/ml)

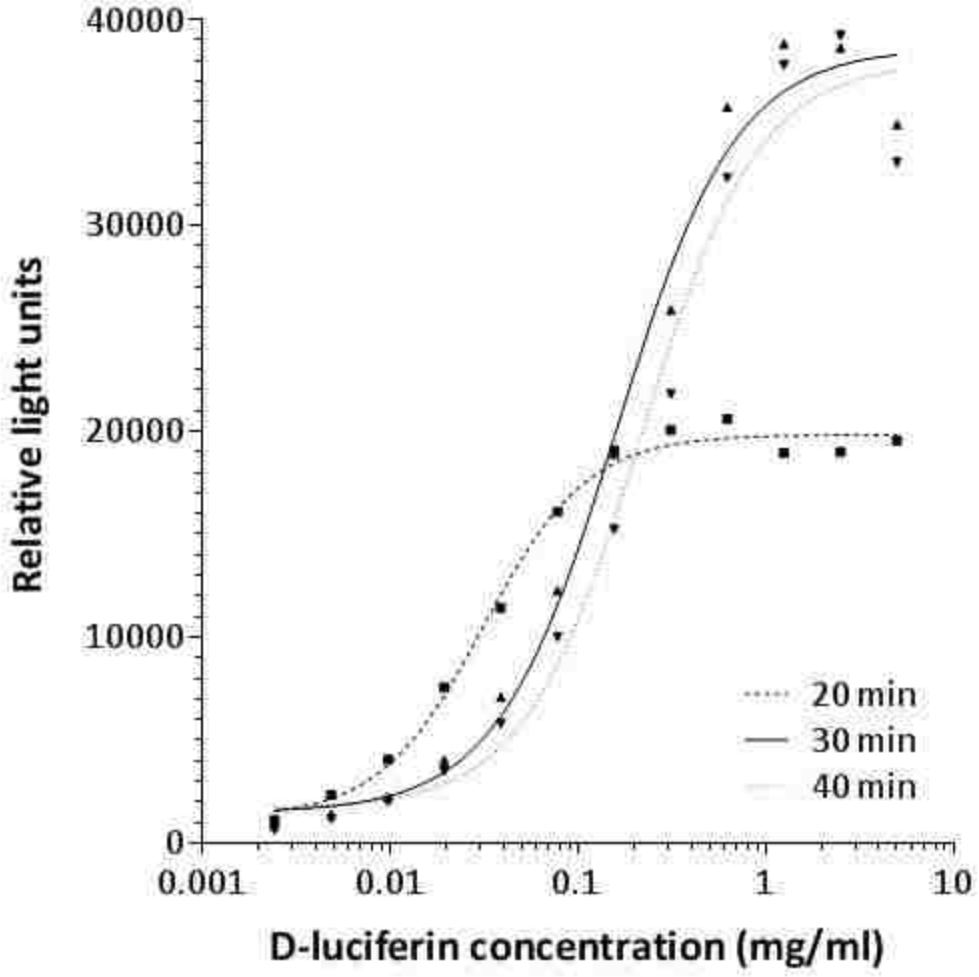
40000
30000
20000
10000
0
Relative light units
0.001
0.01
0.1
1
10
D-luciferin concentration (mg/ml)
20 min
30 min
40 min

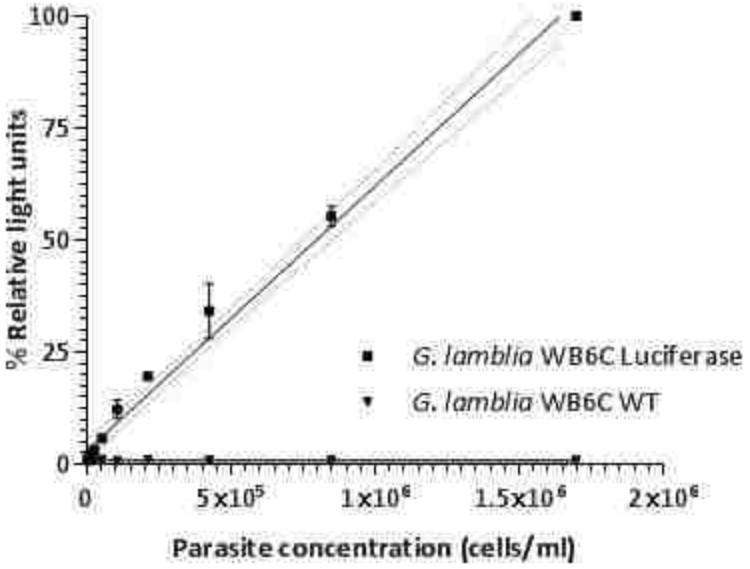
100
75
50
25
0
% Relative light units
0
5x10^5
1x10^6
1.5x10^6
2x10^6
Parasite concentration (cells/ml)
G. lamblia WB6C Luciferase
G. lamblia WB6C WT

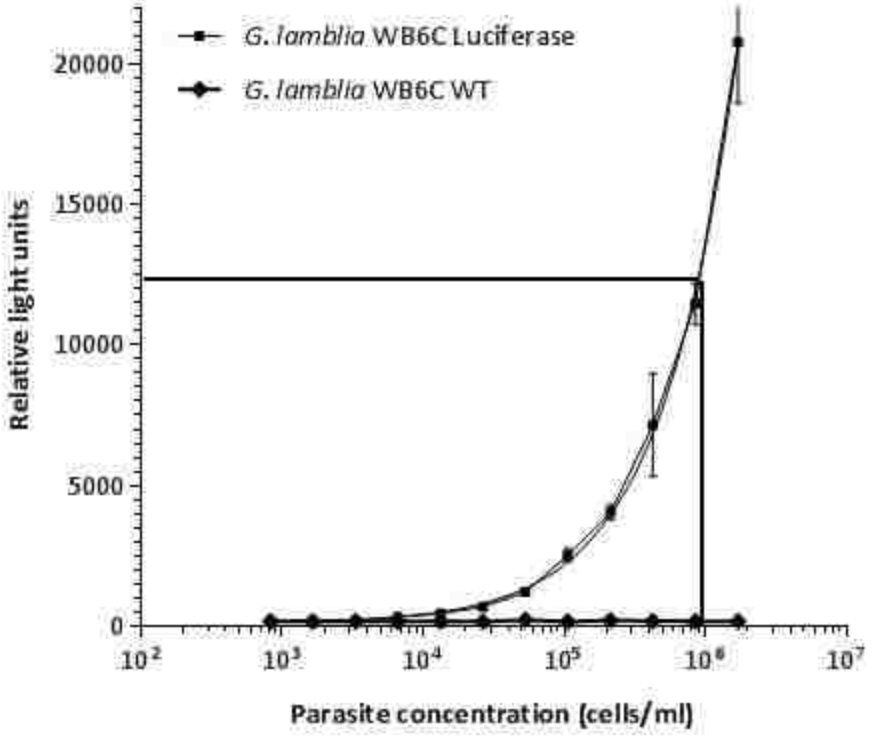
G. lamblia WB6C Luciferase
G. lamblia WB6C WT
Relative light units
20000
15000
10000
5000
0
10²
10³
10⁴
10⁵
10⁶
10⁷
Parasite concentration (cells/ml)

CHAPTER 5: Validation of prolyl-tRNA synthetase as a drug target in *Giardia lamblia* and *Trichomonas vaginalis*

Validation of prolyl-tRNA synthetase as a drug target in *Giardia lamblia* and *Trichomonas vaginalis*

Kelly M Hennessey[2], Alexander R Paredez[2], and Ethan A Merritt[1]

[1]*Department of Biochemistry, University of Washington, Seattle, Washington, USA*
[2]*Department of Biology, University of Washington, Seattle, Washington, USA*
[*]*Address correspondence to merritt@u.washington.edu*

Abstract

The human pathogen *Giardia lamblia* imposes a substantial health burden worldwide. Many gene products in this basal protist exhibit significant divergence from homologs in other eukaryotes, providing a basis for the design of new drugs badly needed to treat giardiasis. In particular the essential enzyme prolyl-tRNA synthetase from *G. lamblia* diverges significantly in both sequence and structure from homologs in higher eukaryotes. This divergence is shared by the ProRS homolog from a second pathogenic protist, *Trichomonas vaginalis*. Despite these differences, we find that the known eukaryotic prolyl-tRNA synthetase inhibitor halofuginone is active against *Giardia* and *Trichomonas* trophozoites with potency comparable to that of the current front line antigiardiasis drug metronidazole. Structural differences at the enzyme active site indicate opportunities to increase both potency and specificity for inhibition of the parasite enzymes relative to the human homolog.

Introduction

The eukaryotic pathogen *Giardia lamblia* causes giardiasis, a gastrointestinal disease characterized by diarrhea and malabsorption. Chronic infections can lead to long term growth retardation and even death. Worldwide incidence is estimated to be 200-800 symptomatic cases annually per 100,000 population[1]. Severe consequences from infection are mostly associated with developing regions lacking adequate water treatment, but *Giardia* is also the most prevalent intestinal parasite in the United States[2]. Annual incidence in the United States is more than one million[3]. Up to 20% of giardiasis cases are resistant to the front line clinical treatments metronidazole and tinidazole[4]. These and second line chemically related drugs act intracellularly via non-specific modification of cysteine residues. The mechanism of a less effective fallback drug, quinacrine, is not known. All of these drugs have serious side effects. Therefore, it is desirable to identify new therapeutics, ideally with molecular targets distinct from existing drugs so that cross-resistance is less likely.

One attractive set of molecular targets in pathogenic protozoa consists of the aminoacyl-tRNA synthetases (aaRS). Because the individual aaRS are absolutely required for protein synthesis, they are essential to normal cell function. Their active sites offer multiple opportunities for inhibitor binding because they necessarily carry out multiple reactions on multiple substrates (a specific amino acid, ATP, a cognate of tRNA).

Because they are ancient enzymes, there is often substantial sequence divergence between human and microbial homologs despite conservation of their core function. Many eukaryotic genomes code for separate cytosolic and mitochondrial aaRS orthologs.

However, *G. lamblia* is notable both for the small size of its genome and for its lack of mitochondria, so unsurprisingly it contains only a single set of aaRS genes, one for each amino

acid. We have determined crystal structures for two of these, tryptophanyl-tRNA synthetase (TrpRS) and prolyl-tRNA synthetase (ProRS), both of which show notable divergence from their respective human homologs[5,6]. We show here that the observed structural difference between human and *Giardia* ProRS offers an opportunity to develop inhibitors that are specific to the parasite enzyme and may lead to new therapeutic options for treating giardiasis. Furthermore, sequence comparison indicates that the structural divergence between *Giardia* ProRS and human ProRS homologs is shared by the ProRS of a second human pathogen *Trichomonas vaginalis.* This suggests that development of new drugs based on ProRS inhibition to treat giardiasis may also benefit treatment of trichomoniasis.

Inhibitors of individual aaRS have been discovered and evaluated in the search for new therapeutics for bacterial[7–9], fungal[10], protozoan[11,12], and nematode induced[13] infectious disease. Notably, the anti-malarial activity of traditional Chinese medicines prepared from roots of the flowering hydrangea *Dichroa febrifuga* arises from a natural product febrifugine[14] shown recently to act through the specific inhibition of ProRS[15]. A less toxic derivative, halofuginone (Figure 2), is a potent inhibitor both of the cytosolic ProRS from the malarial parasite *Plasmodium falciparum* and of the human cytosolic ProRS homolog EPRS[15,16]. Prior to discovery of its molecular target, halofuginone had been used for decades in veterinary medicine as an anticoccidial targeting cryptosporidiosis in livestock[17]and *Eimeria* infection in poultry[18].

Halofuginone inhibition of the *P. falciparum* enzyme in vitro exhibits an IC50 of 9 nM[16] . Halofuginone inhibition of the human cytosolic enzyme has an IC50 of 18 nM[15]. Toxicity limits acceptable dosing in humans. Nevertheless, anti-malarial and anticoccidial use of halofuginone is possible despite a relatively modest structural divergence between ProRS homologs in the

respective target apicomplexan parasites and the homologous cytosolic enzyme in the mammalian host. In contrast to this the sequence and structural divergence between all of these homologs and the *Giardia* ProRS is much greater. On the one hand, this raises the question of whether the *Giardia* enzyme is so different from previously characterized ProRS homologs that halofuginone and related compounds are not effective inhibitors and thus of limited interest in the treatment of giardiasis. One the other hand, the clear structural differences at the active sites of the *Giardia* and host enzymes may allow further modification of the febrifugine scaffold to produce compounds that selectively inhibit the parasite enzyme in preference to the host enzyme. We report here genetic and chemical validation of *Giardia* ProRS as a drug target and begin to address both of these questions. We find that halofuginone is active against trophozoites of both *G. lamblia* and *T. vaginalis*.

Results and Discussion

Genetic validation of ProRS as an essential gene in *Giardia*

Knockdown/knockout genetic manipulation in *Giardia* is complicated by its inherent tetraploidy. Nevertheless, targeted knockdown of *Giardia* protein expression can be achieved by using anti-sense morpholinos (nucleic acid analogs) that bind at the 5´start of a gene transcript thus blocking recruitment of the translation initiation machinery. Levels of the target protein in *Giardia* are typically reduced by 40-80% 24 hours after treatment[19,20]. The effect of morpholino knockdown on two aaRS, ProRS and TrpRS, is shown in Figure 2. Growth was reduced by >40% after knockdown of ProRS. This reduction is significant considering that morpholino knockdown is incapable of completely depleting the targeted protein. In other eukaryotes, the immediate effect of ProRS inhibition is mediated by the accumulation of un-charged tRNAPro

molecules, which triggers an amino acid starvation response pathway[21], but the precise course of action in *Giardia* has not been investigated.

Inhibition of ProRS prevents growth of trophozoites

Giardia is an extracellular parasite. Growth and replication of trophozoites necessarily occurs anaerobically while the individual parasites are attached to the surface of intestinal microvilli. To maintain colonization of the intestine, parasites must resist peristalsis and the flow of chyme through the intestine. Natural infection can be mimicked by culturing trophozoites in a tube or multi-well plate. Attachment is assayed by monitoring the ratio of cells that are free swimming to those attached to the culture tube or plate.

To evaluate the ability of halofuginone to block growth of *Giardia* trophozoites, we assayed growth of strain WBC6 in the presence of serial dilutions of halofuginone·HBr (Calbiochem). The EC50 value (with standard error) found for halofuginone inhibition based on cell counts after 48 hrs of growth was 2.4(3) μM (Figure 3a). Note that halofuginone was presented as a racemic mixture, although only the 2R,3S -(+) enantiomer is recognized by ProRS[17,22,23]. The EC50 value found for halofuginone inhibition of *T. vaginalis* trophozoites after 48 hrs of growth was 2.6(3) μM (Figure 3b).

Mechanism of action is distinct from that of existing drugs

The intracellular activity of metronidazole and related compounds in anaerobes is mediated by low-redox-potential electron transfer reactions that produce nitros and other reactive metabolites.

Resistance in *Giardia* and *Trichomonas* has been traced to selective down-regulation of pyruvate:ferredoxin oxidoreductase (PFOR) and its redox partners in the anaerobic glycolytic pathway[24]. Resistance may also develop through down-regulation of protein disulfide isomerase [25]. These mechanisms are not expected to confer cross-resistance to inhibition of ProRS. To

confirm this, we compared the efficacy of halofuginone and metronidazole against matched wild-type and resistant strains of *Giardia* (Figure 4). The EC50 found for metronidazole in blocking growth of wild-type *G. lamblia* strain 713 was 2.8(7) μM, somewhat better than the literature value 4.6 μM[26]. The observed EC50 for halofuginone inhibition of trophozoite growth for the same wild-type strain 713 was 3.0(1) μM. Assays were repeated using a laboratory-selected metronidazole resistant daughter strain 713-M3[27]. We observed halofuginone to have an EC50 of 2.7(1) μM against the resistant strain (Figure 4d), confirming the lack of cross-resistance.

The *Giardia* ProRS sequence is significantly divergent from homologs in higher eukaryotes

The ProRS gene in diplomonads apparently originated through lateral gene transfer from an archaeote[28]. It is thus highly divergent both from bacterial sequences and from other eukaryotic cytosolic and mitochondrial homologs. ProRS from the pathogenic parabasalid *Trichomonas vaginalis* also belongs to this divergent archaeote-like sequence group, but the divergent clade does not extend to less basal protozoa such as kinetoplastida or apicomplexa (Figures 5, S1).

In comparing ProRS sequences from organisms previously reported to be sensitive to halofuginone it is noteworthy that all 13 amino acid residues contributing to the binding site of halofuginone as seen in the human and *P. falciparum* crystal structures are strictly conserved. This strict conservation extends to the ProRS homologs from apicomplexan pathogens *E. tenella*, *T. gondii*, and *C. parvum* (sequence not shown). Similarly, 8 of 11 residues contributing to the adenosine binding surface of the active site are fully conserved and the remaining 3 exhibit minimal changes (alanine/glycine, leucine/isoleucine). It is thus not surprising that the affinity for halofuginone is consistent for the human and apicomplexan homologs. By contrast, two residues contributing to the halofuginone binding surface diverge from this consensus in both the *Giardia* and *Trichomonas* ProRS sequences. These positions correspond to Cys126 and Gly264

in *G. lamblia* ProRS. The *Giardia* and *Trichomonas* sequences also differ from the human sequence at five of the residue positions contributing to the adenosine binding surface. Additional differences are found for residues lining the proline-binding pocket, but these do not directly contribute to the observed binding pose of halofuginone.

Structural consequence of sequence divergence

We explored the relevance of sequence differences between the *Giardia* and human ProRS homologs to their respective recognition of inhibitors by comparing crystal structures of the parasite and human enzymes. The structure of *Giardia* ProRS with the intermediate reaction product Prolyl-AMP in the active site is directly comparable to human EPRS structures, showing minimal changes to the active site conformation observed in the apo state (no substrates present) and in the presence of proline and adenosine[29,30]. The conformation of the protein backbone in the catalytic region core is consistent even where there are differences in the amino acid sequence. Over the region shown in Figure 5, the root-mean-square deviation (rmsd) for 195 aligned Cα atoms is 1.1 Å (*Giardia* residues 115-311 PDB 3ial; human residues 1091-1289 PDB 4k87; Figure S3a).

The crystallographically observed binding pose of halofuginone occludes both the proline binding site and the presumed binding site of the tRNA acceptor stem. Halofuginone is not competitive with ATP binding. Moreover, both febrifugine and halofuginone exhibit substantially enhanced affinity in the presence of ATP[31,32]. When halofuginone is bound a conformational change is observed in the short helical region comprising residues 1091-1100 in the human enzyme, corresponding to residues 115-125 in *Giardia* ProRS[30]. This change affects the binding surface seen by the Cl and Br atoms of halofuginone, but the overall con-

formational agreement between the *Giardia*ProRS+PAMP and EPRS+halofuginone+ATP catalytic core structures (PDB entries 3ial and 4hvc respectively) is reduced on slightly to 1.3 Å rmsd for 191 alignable Cα atoms. Thus, it is plausible to infer that the *Giardia* enzyme will undergo a parallel conformational shift when binding halofuginone, and that crystal structures of halofuginone bound to the human enzyme can be used to derive a model for the binding surface it sees when binding to the *Giardia* enzyme.

To model the effect of sequence differences between the *Giardia* and human enzymes on the binding surface, we mutated in silico two key residues that differ between them by starting with crystallographic coordinates for the human structure (4hvc) and substituting glycine for residue Thr1240, substituting cysteine for Val1101, and recalculating the binding surface of the protein (Figure 6). As expected the Thr→Gly change opens up a substantial pocket adjacent to the halofuginone piperidine ring (left side of Figure 6). The Val→Cys change slightly increases the volume of the binding pocket, but also changes the chemical nature of the surface and places a reactive group, the cysteine thiol, adjacent to the halofuginone Br (right side of Figure 6).

Prospects for drug design

While the low micromolar EC50 observed for halofuginone is promising, it may be contrasted with the low nanomolar IC50s in vitro reported for various febrifugine analogs against *P. falciparum* isolates[31], and the 10-20 nM EC50 reported for halofuginone in reducing *P. berghei* parasite load in liver cells[33]. As is evident in Figure 6, halofuginone is less perfectly complementary to the *Giardia* ProRS active site than it is to the analogous site in the human and *Plasmodium* ProRS homologs. However**,** by mapping the sequence differences distinguishing the parasite and human enzymes onto the binding surface, observed crystallographically we find

graphically we find opportunities at both ends of the halofuginone scaffold to improve this complementarity. Substituents extending from the piperidine ring at one end of the molecule may fill a pocket formed by the presence of glycine rather than threonine in the active site of the *Giardia* enzyme while at the same time sterically interfering with off-target binding to human EPRS. Similarly, the presence of cysteine rather than valine confers a different environment adjacent to the halofuginone Cl atom at the other end of the molecule, possibly favoring replacement of Cl with a different substituent. Given that the potency of the starting compound halofuginone is on par with that of the current front line anti-giardiasis therapeutic metronidazole, this is a promising starting point for the design of compounds with increased potency against *Giardia* and decreased likelihood of undesirable side effects produced by inhibition of EPRS. Furthermore, there is a reasonable expectation that any such compounds would also be worth investigating for the treatment of trichomoniasis.

Methods & Materials

Parasite growth in culture

Cultures of *G. lamblia* strains WBC6 (ATCC 50803), 713 and 713-M3[27]were grown in TYI-S-33 medium supplemented with 10% bovine serum and 0.05 mg/ml bovine bile, henceforth referred to as *Giardia* growth medium[34]. Cells were cultured at 37° under hypoxic conditions using 15 mL screw-cap tubes (Corning Life Sciences DL).

Metronidazole-resistant lines were routinely maintained in 50 µM metronidazole but were grown without the drug for 5-7 days prior to experiments. Cells used for growth assays were grown in 15-ml tubes to ~80% confluency. The media and any unattached cells were discarded and replaced with 13 ml ice-cold, fresh media. Tubes were placed on ice for 30

minutes to release attached parasites. Well-suspended cells were counted using a MoxiZ coulter counter (Orflo Technologies). Based on these counts, the concentration of cells was diluted with Giardia growth medium to 20,000 cells/mL. Cells were kept on ice up to an hour until use. *T. vaginalis* strain PRA-98 was obtained from ATCC. Cultures were grown in modified TYM basal medium with pH adjusted to 6.2 and 10% heat-inactivated horse serum per culture method at ATCC. Cells were cultured at 37º under anaerobic conditions using 15 mL polystyrene screw-cap tubes.

Morpholino knockdown

G. lamblia trophozoites were cultured to confluency, placed on ice for 30 minutes to detach, spun down at 500x G for 5 minutes, and resuspended in 1.0 mL fresh *Giardia* growth medium. Cells and cuvettes were chilled on ice. Morpholinos were obtained from Gene Tools LLC (Philomath, OR).

Lyophilized morpholinos listed in Table S1 were resuspended in sterile water and 30 µL of a 100 mM morpholino stock was added to 300 µL of cells in a 4 mm cuvette. A non-targeted morpholino provided by the supplier was used as a negative control. Tubes were flicked to resuspend, and were chilled on ice for 15 minutes. Cuvettes were flicked before and after electroporation (375 V, 1000 µF, 750 Ohms, GenePulser Xcell, BioRad, Hercules, CA) to resuspend DNA/cells, then placed on ice for 15 minutes. Cells were transferred to fresh media and incubated 4 hours at 37° to allow cells to recover. Cells were then iced for 30 minutes, counted and diluted to 20,000 cells/mL. Aliquots were incubated at 37° and counted at 12, 24, 36, and 48 hours using a MoxiZ Coulter counter (Orflo Technologies, Hailey, ID). Six samples of each cell line and control were analyzed at each time point.

Structural analysis

Structure comparison, superposition, surface calculation and mutational modeling were performed in Coot[35,36]and Molecular operating environment (Chemical Computing Group Inc. Momtreal, QC, Canada).

Acknowledgments

Wild-type *G. lamblia* strain 713 and a daughter strain 713-M3 selected in the laboratory for resistance to metronidazole were kindly provided by the lab of Dr. Lars Eckmann (UCSD) We thank the lab of Patricia Johnson (UCLA) for generously providing techniques and assistance for the culture of T. vaginalis. This work is supported by NIH award R21AI119715.

References

1. Torgerson PR, Devleesschauwer B, Praet N, Speybroeck N, Willingham AL, Kasuga F, Rokni MB, Zhou XN, F??vre EM, Sripa B, et al. World Health Organization Estimates of the Global and Regional Disease Burden of 11 Foodborne Parasitic Diseases, 2010: A Data Synthesis. PLoS Medicine. 2015;12(12).

2. Huang DB, White AC. An Updated Review on Cryptosporidium and Giardia. Gastroenterology Clinics of North America. 2006;35(2):291–314.

3. Czinn S. Long-Term Consequences of Parasitic-Induced Diarrhea: A Critical Review of Issues. Current Tropical Medicine Reports. 2016;3(3):87–88.

4. Lalle M. Giardiasis in the post genomic era: treatment, drug resistance and novel therapeutic perspectives. Infectious disorders drug targets. 2010;10(4):283–94.

5. Arakaki TL, Carter M, Napuli AJ, Verlinde CLMJ, Fan E, Zucker F, Buckner FS, Van Voorhis WC, Hol WGJ, Merritt EA. The structure of tryptophanyl-tRNA synthetase from Giardia lamblia reveals divergence from eukaryotic homologs. Journal of Structural Biology. 2010;171(2):238–243.

6. Larson ET, Kim JE, Napuli AJ, Verlinde CLMJ, Fan E, Zucker FH, Van Voorhis WC, Buckner FS, Hol WGJ, Merritt E a. Structure of the prolyl-tRNA synthetase from the eukaryotic pathogen Giardia lamblia. Acta Crystallographica Section D: Biological Crystallography.

2012;68(9):1194–1200.

7. Hurdle JG, O'Neill AJ, Chopra I. Prospects for Aminoacyl-tRNA Synthetase Inhibitors as New Antimicrobial Agents. Antimicrobial Agents and Chemotherapy. 2005:0.

8. Lv P-C, Zhu H-L. Aminoacyl-tRNA synthetase inhibitors as potent antibacterials. Current medicinal chemistry. 2012;19(21):3550–63.

9. Palencia A, Li X, Bu W, Choi W, Ding CZ, Easom EE, Feng L, Hernandez V, Houston P, Liu L, et al. Discovery of novel oral protein synthesis inhibitors of mycobacterium tuberculosis that target leucyl-tRNA synthetase. Antimicrobial Agents and Chemotherapy. 2016;60(10):6271–6280.

10. Hasenoehrl A, Galić T, Ergović G, Maršić N, Skerlev M, Mittendorf J, Geschke U, Schmidt A, Schoenfeld W. In vitro activity and in vivo efficacy of icofungipen (PLD-118), a novel oral antifungal agent, against the pathogenic yeast Candida albicans. Antimicrobial Agents and Chemotherapy. 2006;50(9):3011–3018.

11. Shibata S, Gillespie JR, Kelley AM, Napuli AJ, Zhang Z, Kovzun K V., Pefley RM, Lam J, Zucker FH, Van Voorhis WC, et al. Selective inhibitors of methionyl-tRNA synthetase have potent activity against Trypanosoma brucei infection in mice. Antimicrobial Agents and Chemotherapy. 2011;55(5):1982–1989.

12. Pham JS, Dawson KL, Jackson KE, Lim EE, Pasaje CFA, Turner KEC, Ralph SA. Aminoacyl-tRNA synthetases as drug targets in eukaryotic parasites. International Journal for Parasitology: Drugs and Drug Resistance. 2014;4(1):1–13.

13. Yu Z, Vodanovic-Jankovic S, Kron M, Shen B. New WS9326A congeners from Streptomyces sp. 9078 inhibiting Brugia malayi asparaginyl-tRNA synthetase. Organic Letters. 2012;14(18):4946–4949.

14. Coatney GR, Cooper WC, Culwell WB, White WC and IC. Studies in human malaria: Trial of febrifugine, an alakaloid obtained from Dichroa febrifugalour, against the Chesson strain of Plasmodium vivax. J Natural Malaria. 1950;(9):183–186.

15. Keller TL, Zocco D, Sundrud MS, Hendrick M, Edenius M, Yum J, Kim Y-J, Lee H-K, Cortese JF, Wirth DF, et al. Halofuginone and other febrifugine derivatives inhibit prolyl-tRNA synthetase. Nature Chemical Biology. 2012;8(3):311–317.

16. Jain V, Yogavel M, Oshima Y, Kikuchi H, Touquet B, Hakimi MA, Sharma A. Structure of prolyl-tRNA synthetase-halofuginone complex provides basis for development of drugs against malaria and toxoplasmosis. Structure. 2015;23(5):819–829.

17. Linder MR, Heckeroth AR, Najdrowski M, Daugschies A, Schollmeyer D and M, C. (2R,3S)-(+)- and (2S,3R)-(-)-Halofuginone lactate: synthesis, absolute con- figuration, and activity against Cryptosporidium parvum. Bioorganic and Medicinal Chemistry Letters. 2007;17:4140–4143.

18. Ryley JF, Wilson RG. Laboratory studies with some recent anticoccidials. Parasitology. 1975;70(2):203–22.

19. Carpenter ML, Cande WZ. Using morpholinos for gene knockdown in Giardia intestinalis. Eukaryotic Cell. 2009;8(6):916–919.

20. Paredez AR, Assaf ZJ, Sept D, Timofejeva L, Dawson SC, Wang C-JR, Cande WZ. An actin cytoskeleton with evolutionarily conserved functions in the absence of canonical actin-binding proteins. Proceedings of the National Academy of Sciences of the United States of America. 2011;108(15):6151–6156.

21. Sundrud MS, Koralov SB, Feuerer M, Calado DP, Kozhaya AE, Rhule-Smith A, Lefebvre RE, Unutmaz D, Mazitschek R, Waldner H, et al. Halofuginone inhibits TH17 cell differentiation by activating the amino acid starvation response. Science (New York, N.Y.). 2009;324(5932):1334–1338.

22. Zhou H, Sun L, Yang X-L, Schimmel P. ATP-directed capture of bioactive herbal-based medicine on human tRNA synthetase. Nature. 2013;494(7435):121–4.

23. Herman JD, Pepper LR, Cortese JF, Estiu G, Galinsky K, Zuzarte-Luis V, Derbyshire ER, Ribacke U, Lukens AK, Santos SA, et al. The cytoplasmic prolyl-tRNA synthetase of the malaria parasite is a dual-stage target of febrifugine and its analogs. Sci Transl Med. 2015;7(288):288ra77.

24. Upcroft P, Upcroft JA. Drug targets and mechanisms of resistance in the anaerobic protozoa. Clinical Microbiology Reviews. 2001;14(1):150–164.

25. Müller J, Sterk M, Hemphill A, Müller N. Characterization of Giardia lamblia WB C6 clones resistant to nitazoxanide and to metronidazole. Journal of Antimicrobial Chemotherapy. 2007;60(2):280–287.

26. LH CL and M-L. The effects of the antiprotozoal drugs metronidazole and furazolidone on trophozoites of Giardia lamblia (P1 strain). Parasitology. 2002;88:80–85.

27. Townson SM, Laqua H, Upcroft P, Boreham PF and UJ. Induction of metronidazole and furazolidone resistance in Giardia. Transactions of the Royal Society of Tropical Medicine and Hygiene. 1992;86:521–522.

28. Andersson JO, Sjögren ÅM, Davis LAM, Embley TM, Roger AJ. Phylogenetic analyses of diplomonad genes reveal frequent lateral gene transfers affecting eukaryotes. Current Biology. 2003;13(2):94–104.

29. Larson ET, Kim JE, Napuli AJ, Verlinde CLMJ, Fan E, Zucker FH, Van Voorhis WC, Buckner FS, Hol WGJ, Merritt EA. Structure of the prolyl-tRNA synthetase from the eukaryotic pathogen Giardia lamblia. Acta Crystallographica Section D: Biological Crystallography. 2012;68(9):1194–1200.

30. Son J, Lee EH, Park M, Kim JH, Kim J, Kim S, Jeon YH, Hwang KY. Conformational

changes in human prolyl-tRNA synthetase upon binding of the substrates proline and ATP and the inhibitor halofuginone. Acta Crystallographica Section D: Biological Crystallography. 2013;69(10):2136–2145.

31. Zhu S, Chandrashekar G, Meng L, Robinson K, Chatterji D. Febrifugine analogue compounds: Synthesis and antimalarial evaluation. Bioorganic and Medicinal Chemistry. 2012;20(2):927–932.

32. Jain V, Kikuchi H, Oshima Y, Sharma A, Yogavel M. Structural and functional analysis of the anti-malarial drug target prolyl-tRNA synthetase. Journal of Structural and Functional Genomics. 2014;15(4):181–190.

33. Derbyshire ER, Mazitschek R, Clardy J. Characterization of Plasmodium Liver Stage Inhibition by Halofuginone. ChemMedChem. 2012;7(5):844–849.

34. Keister D. Axenic culture of Giardia lamblia in TYI-S-33 medium supplemented with bile. Transactions of the Royal Society of Tropical Medicine and Hygiene. 1983;77(4):487–88.

35. Williams T, Kelley C et al. Gnuplot 5.0: an interactive plotting program. http://gnuplot.sourceforge.net/. 2015.

36. Emsley P, Cowtan K. Coot: Model-building tools for molecular graphics. Acta Crystallographica Section D: Biological Crystallography. 2004;60(12 I):2126–2132.

Figure 1: The natural product febrifugine **1** and its derivative halofuginone **2**.

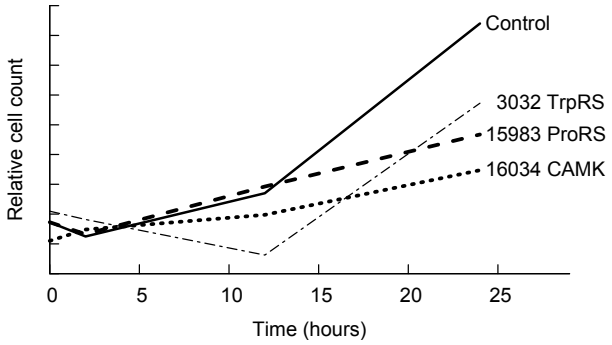

Figure 2: Giardia trophozooite growth after morpholino knockdown of the target gene at time t=0. Knockdown of a essential kinase (GL50803_16034) is included as a positive control. Each curve is an average of two replicate experiments.

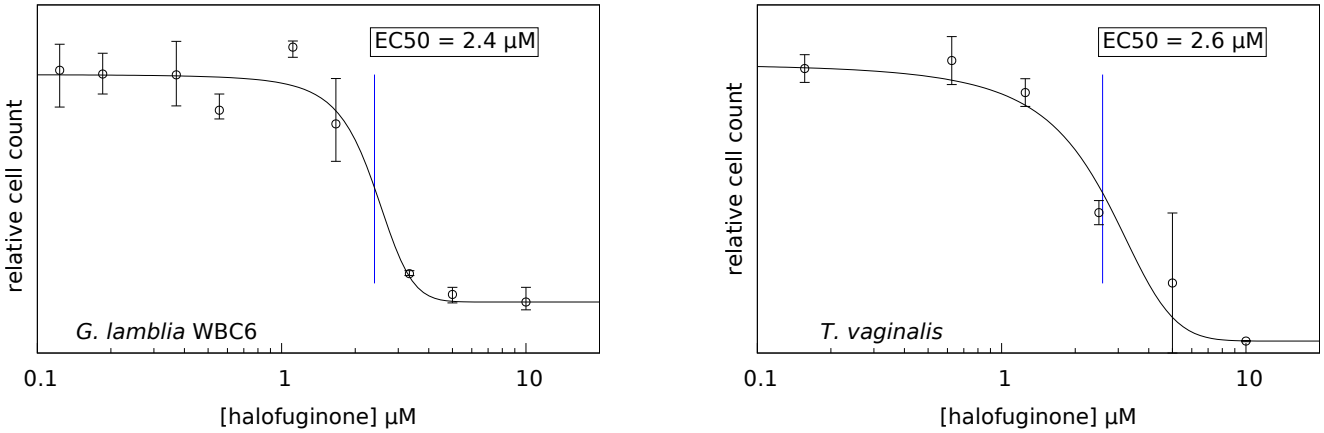

(a) (b)

Figure 3: EC50 for halofuginone inhibition of trophozoite growth in culture. **(a)** Halofuginone inhibition of *Giardia* strain WBC6 trophozoites. **(b)** Halofuginone inhibition of *Trichomonas* trophozoites.

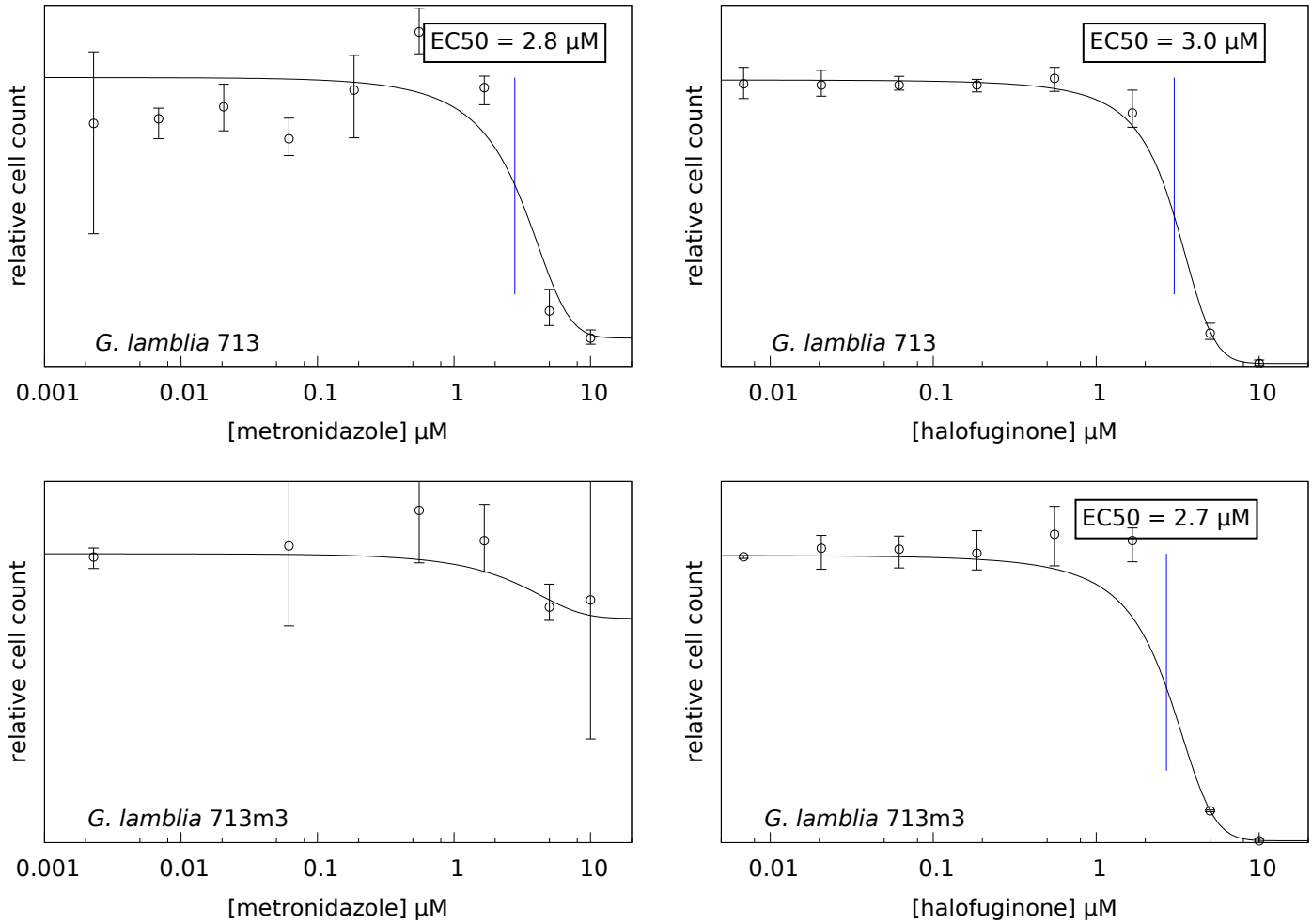

Figure 4: Metronidazole-resistant *Giardia* remain sensitive to halofuginone. Metronidazole (**a**) and halofuginone (**b**) inhibition of trophozoite growth in culture for wild-type *Giardia* strain 713. Metronidazole (**c**) and halofuginone (**d**) efficacy in inhibiting growth of the metronidazole-resistant daughter strain 713-M3. The shape of the metronidazole dose response curve in (c) suggests that a small subpopulation of the resistant strain retains some metronidazole sensitivity.

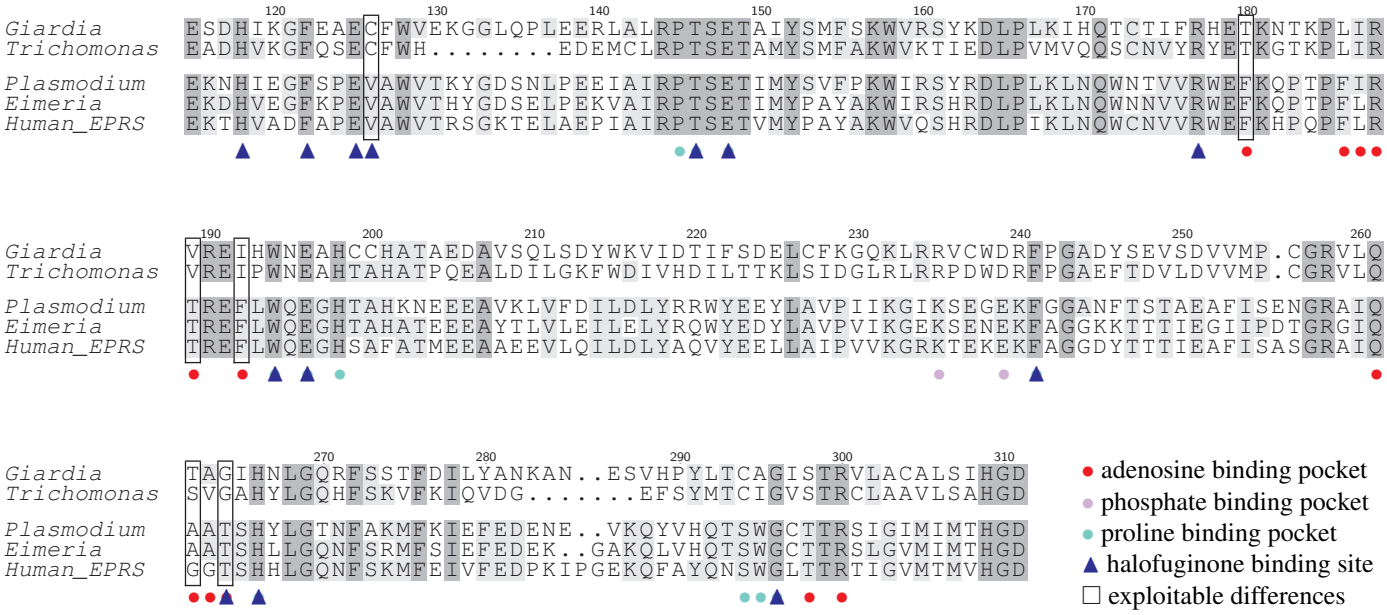

Figure 5: Structure-guided sequence alignment of the prolyl-tRNA synthetase catalytic domain core from two basal protozoan pathogens, *G. lamblia* and *T. vaginalis*, two apicomplexan pathogens *P. falciparum* and *E. tenella*, and the human cytosolic homolog EPRS. Residue positions contributing to the binding surface recognized by proline, ATP, and halofuginone are marked.

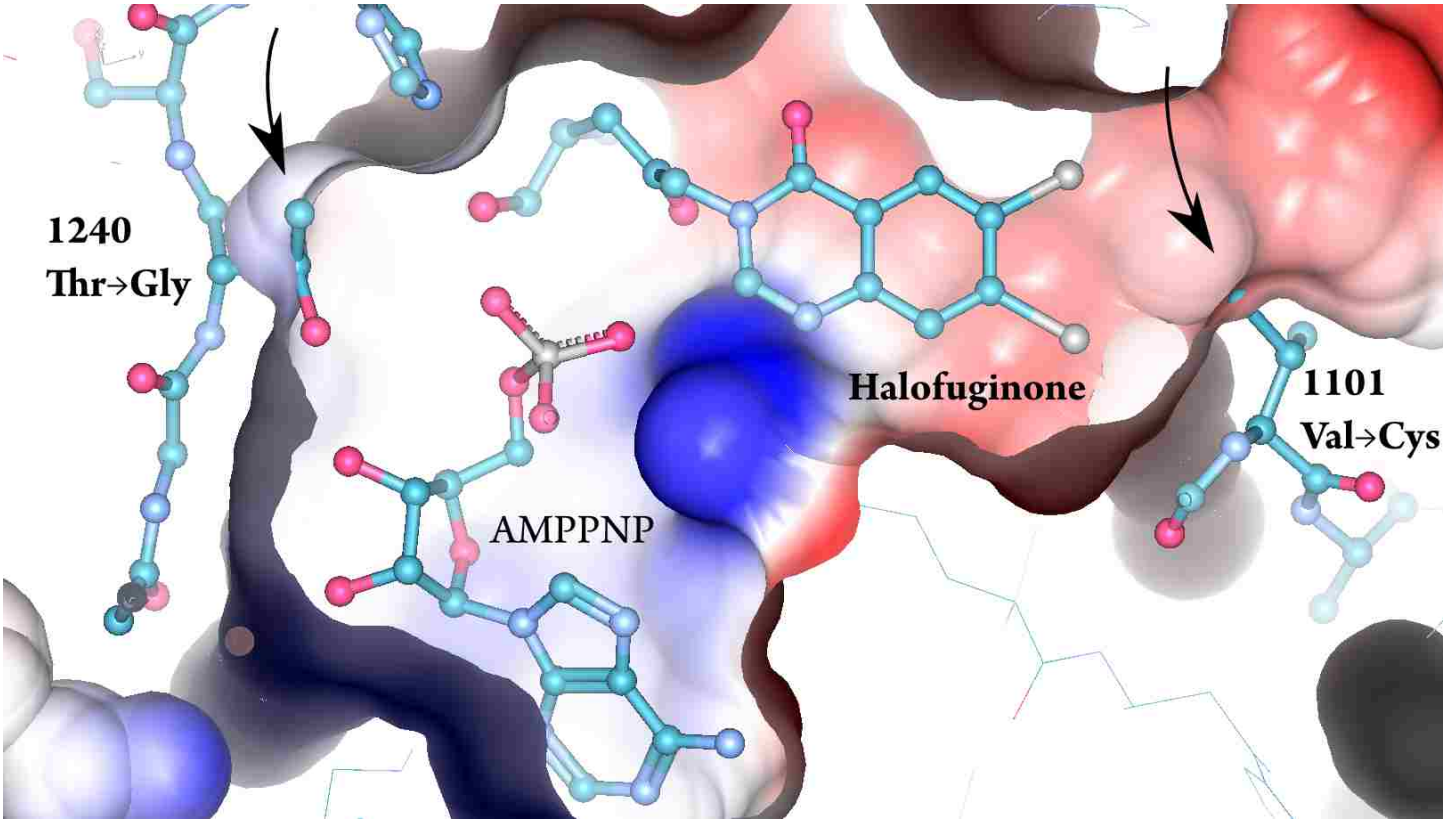

Figure 6: Human EPRS structure (PDB 4hvc) showing the protein, halofuginone, and AMPPNP as ball-and-stick. The $\beta-$ and $\gamma-$ phosphates of the AMPPNP extend directly towards the viewer but are not visible in the figure because they are clipped by the front viewing plane that also slices through the surface. The surface is shown for a modified atomic model in which two EPRS residues are replaced with the corresponding Giardia ProRS residues. In both cases the Giardia residue is smaller than the human residue it replaces, producing a larger binding pocket that can be exploited to introduce specificity for the Giardia ProRS. The human sequence residues visibly protrude into the modeled larger pocket (arrows).